THE EFFECT OF ELECTROLYTES ON THE FLOTATION OF PYRITE

by

LOUISE MADELEINE BARKER

BSc Eng (U.C.T) 1983

Submitted to the University of Cape Town in fulfilment of the requirements for the degree of Master of Science in Engineering

February 1986

ACKNOWLEDGEMENTS

I would like to thank

The Council for Mineral Technology (MINTEK) for having sponsored this project

Associate Professor O'Connor of the Department of Chemical Engineering for his supervision

Mr R. Dunne from MINTEK for his assistance and interest in the project

Dr J. P. Franzidis of the Department of Chemical Engineering for his assistance

Mr A. M. Barker of the Department of Chemical Engineering for his enthusiastic assistance with equipment

The postgraduates of the Minerals Group

Michael Bowley for assistance with the photography

ABSTRACT

In the flotation of pyrite a minimum concentration of any ions is necessary to stabilize the froth and thus produce a reasonable recovery of pyrite. In the absence of ions a "dry froth" is formed which results in a decreased mass pull and thus a low pyrite recovery.

The predominant effect of an increased concentration of univalent ions was a decrease in the formation of "dry froth" during flotation which resulted in an increase in pyrite recovery. This was due to the increase in froth stability with the addition of ions and was verified in the two and three phase froth stability tests.

The predominant effects of the divalent ions were:

(i) an increase in froth stability resulting in increased pyrite recovery

(ii) a sharp increase in grade due to a decrease in gangue recovery

(iii) a decreased rate of flotation.

The decrease in gangue recovery was possibly due to the effect of the ion on the compression of the electrical double layer resulting in coagulation of the quartz particles. The slow rate of flotation was ascribed to the slow rate of the ascent of the heavily mineralized bubbles. This increase in bubble mineralization could be due to coagulation of pyrite in the pulp phase.

The adsorption of the collector, sodium ethyl xanthate, on pyrite was not affected by the univalent or divalent cations but decreased with the addition of the nitrate anion. However these variations in xanthate adsorption did not seem to have a significant effect on the flotation of pyrite.

Flotation experiments using oxidised ore showed a reduced pyrite recovery compared with the leached ore. This was ascribed to the low xanthate adsorption and the low natural floatability of the ore.

TABLE OF CONTENTS

LIST OF TABLES

LIST OF FIGURES

1. INTRODUCTION

1.1 FLOTATION

Flotation is a concentration process based on the different physico-chemical surface properties of the mineral particles. The process involves the treatment of the ore with a collector which coats the mineral causing it to have hydrophobic properties. When air is bubbled through the pulp, the hydrophobic mineral is attached to the bubble and is carried to the surface. The addition of frother enables the mineral to be retained at the surface by a stable froth. The froth containing a much higher concentration of the mineral is then scraped off the surface leaving behind the unwanted mineral or gangue.

1.2 PYRITE FLOTATION IN SOUTH AFRICA

1.2.1 Flotation Process

There is a close association between gold, uranium and pyrite in the Witwatersand reefs. This means that the recovery of sulphides during flotation often results in high recoveries of gold and uranium (Lloyd 1981). In addition to this pyrite is primarily used for the production of sulphuric acid by the roasting of the concentrate and the catalytic oxidation of the sulphur dioxide formed.

Gold is recovered by a cyanidation process. This usually occurs before flotation due to the deleterious effects of flotation reagents on the cyanidation process (Lloyd 1981) but also takes place after the roasting of the pyrite concentrate by cyanidation of the calcine (OFS Metallurgical Scheme 1981). Therefore factors which affect the flotation of pyrite recovery will also affect the gold recovery.

The flowsheet of a typical flotation plant is shown in Figure 1.1 and dosage of reagents added in Table 1.1.

Figure 1.1 Flowsheet employed at Zandpan (Lloyd 1981)

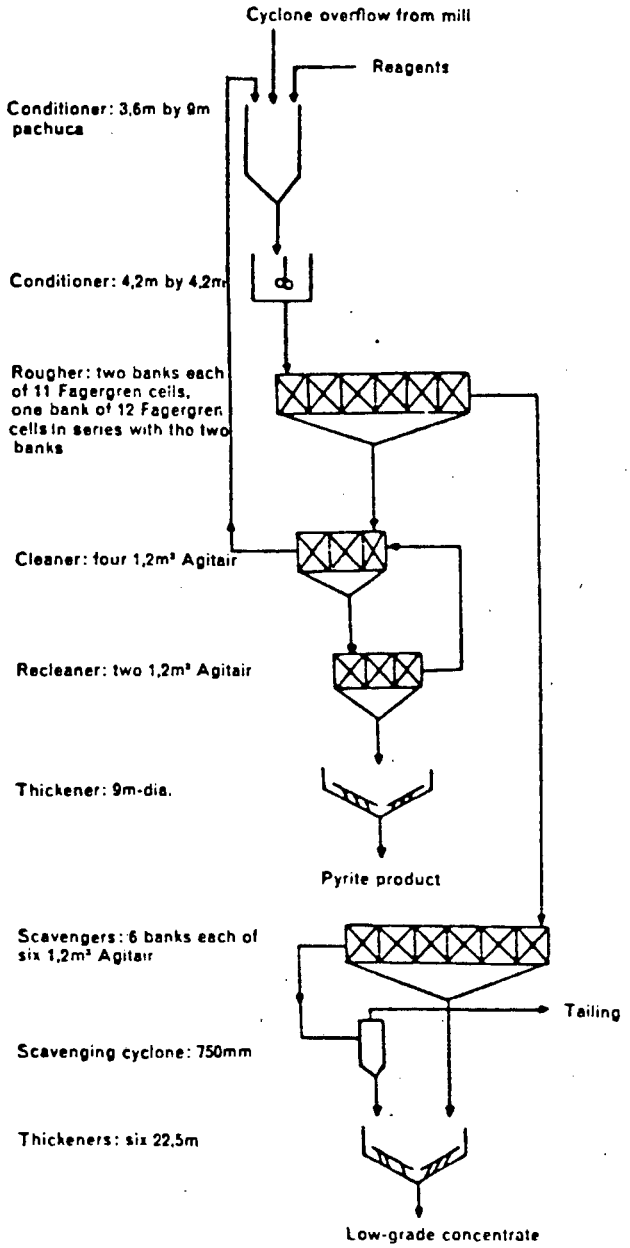

Table 1.1 Plant Dosage at Zandpan

REAGENT	ADDITION RATE kg/t
Secbutyl xanthate	.030
Aerofroth 65	.008
Aerofroth 25	.013
$CuSO_4$	.053

The pH range used at Zandpan was 10,1 but these values vary from plant to plant. For example, uranium residues from Virginia are floated at a pH of 4,9-5,7, gold residues from Merriespruit at a pH of 5,5 and coarse ore from Zandpan, Hartebeespoort and Loraine at a pH of 9,9 to 11 (Lloyd 1981).

Acid conditioning prior to flotation usually occurs in order to counteract the depressant effects of residual lime and cyanide. These reagents occur after the alkaline cyanidation process and do not only result in a high pH but also cause the activation of quartz by calcium (Lloyd 1981).

Acid conditioning is also necessary when floating residues from the slimes dams (OFS Joint Metallurgical Scheme 1981, Westwood et al 1970). These residues may be depressed by lime and cyanide or a $CaSO_4$ layer. The rapid oxidation of sulphur was also found to occur in the open face.

$CuSO_4$ was added as a complexing agent for the cyanide ion. Ferric and ferrous ions were found to be not as effective.

1.2.2 Water Quality

Water conservation has become a necessity in South Africa, especially during drought periods. As a result of this, mines in South Africa are increasing their use of recycled water. In the past however this has resulted in a decrease in sulphur and gold recovery (Westwood, Stander and Carlisle 1970). A study of the effect of a buildup of certain ions in the water could possibly determine which ions produce the most harmful effects. These ions could then be removed from the recycled water before the flotation process.

Make-up water is usually obtained from water used in other processes on the plant, for example roasting (Ross, Dunne and Burger 1984) and milling (Viviers 1979).

Ions present in this water can be divided into 3 groups:

1. Ions common to the water system, viz CO_3^{2-}, HCO_3^-, Cl^-, Ca^{2+} and Mg^{2+}.
2. Ions added during acid leaching, viz H^+, SO_4^{2-}.
3. Ions obtained during milling and roasting, viz Fe^{++} and Fe^{+++}.

Concentration levels of these ions are shown in Table 1.2.

Table 1.2 Water quality in South Africa

INORGANIC SALT	MINE WATER *		TAP WATER	
	Highest	Lowest	Rand#	Cape+
Total Dissolved Salts ppm $CaCO_3$	10380	428	300	115
Hardness ppm $CaCO_3$	3840	264	380	58
Calcium ppm $CaCO_3$	1280	51		41
Magnesium ppm $CaCO_3$	730	137	146	17
Sodium ppm	922	54	80	13
Chloride ppm	365	4	91	23
Sulphate ppm	3760	122	305	18
Total Alkalinity ppm $CaCO_3$	336	54		

* Western Plats, Phalaborwa Mining Company, Agnes, President Brandt, Sheba data (1984)

\# Rand Water Board (1983)

\+ MINTEK analysis (1985)

1.3 THE FLOTATION SYSTEM

The flotation system is an interactive system comprising mineral, reagents and ions. This is shown in Figure 1.2.

Figure 1.2 The Flotation System

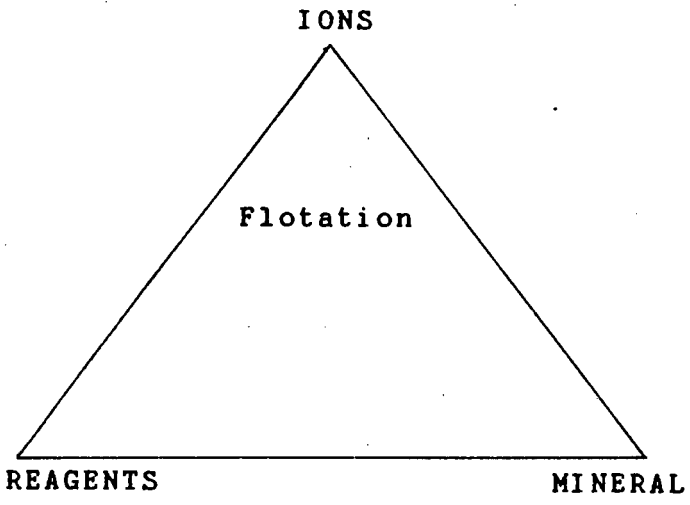

1.3.1 Minerals

1.3.1.1 Pyrite

Pyrite has a cubic crystal structure with Fe^{++} ions at the corners and sulphur ions occupying the face centres in the form of the S_2^{2-} ion. Bonding is mainly covalent.

Pyrite oxidises readily in air (Fuerstenau D.W. and Mishra R.K. 1980) with initial absorption of ionic oxygen, then covalent oxygen and resulting in the formation of oxidation products (Hoberg, Loesche and Schneider 1985) (which are possibly oxygen sulphur compounds (Majima 1971)).

In an aqueous solution different oxidation products form depending on the pH of the solution. In acidic solutions the main oxidation products are the ferrous ion Fe^{++} and sulphate ion. In the alkaline range the oxidation products are polythionates and iron oxide species (possibly FeOOH) (Goldhaber 1983).

The intermediate species of polythionates present are dependent on pH as is shown in Figure 1.3 and are also time dependent as is shown in Figure 1.4. After a long time interval all sulphur in solution is oxidised to the sulphate form (Goldhaber 1983).

More iron oxide is formed at higher pH values. It was found that approximately six times the amount of iron oxide formed at pH 6 was formed at pH 9 (Goldhaber 1983).

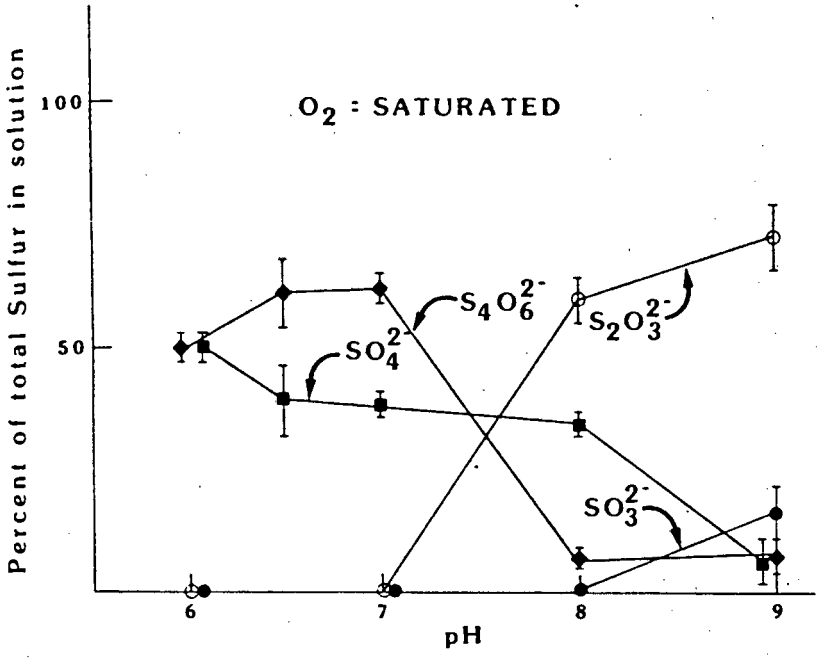

Figure 1.3 Relative Abundance of Aqueous Sulfur Species (as S) Produced during Short Term Pyrite Oxidation Experiments as a Function of pH (Goldhaber 1983)

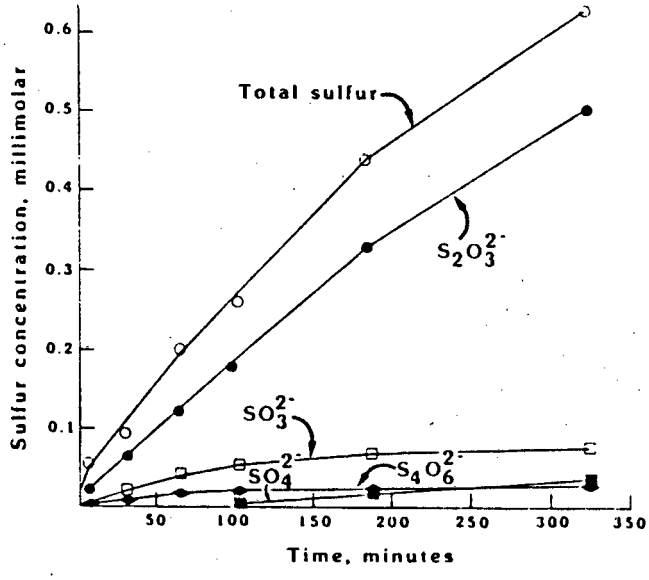

Figure 1.4 Plot of Sulfur Species in Solution Produced during Pyrite Oxidation at pH 9 versus Time. Oxygen held at Saturation. (Goldhaber 1983)

1.3.1.2 Quartz

Quartz (SiO_2) is a framework silicate made up of a three dimensional network of tetrahedra which share 4 oxygen atoms (Fuerstenau D.W. and Fuerstenau M.C. 1982). This forms an electrical neutral structure. Cleavage of the mineral particles causes Si-O bonds to break thus enabling hydration to occur. This is shown in Figure 1.5. The hydrated quartz particle has a hydrophilic character (Hoberg, Laubscher and Schneider 1985).

Figure 1.5 Surface states of SiO_2

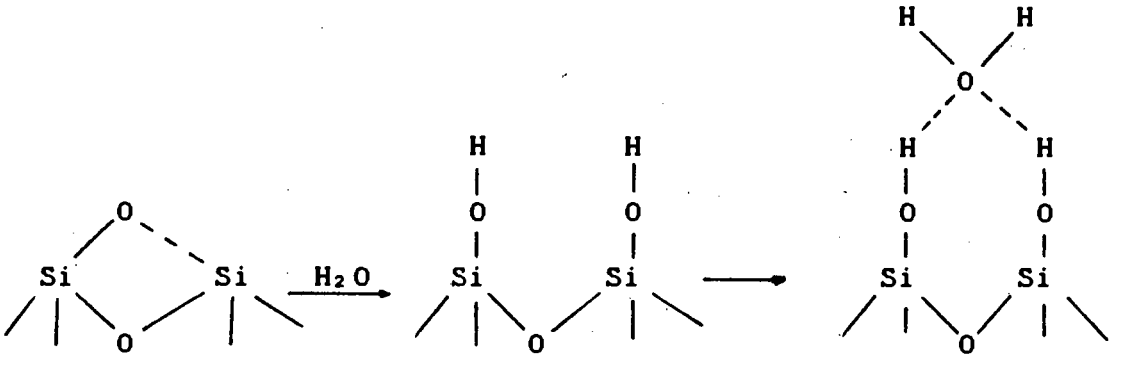

freshly fractured water adsorption formation of a hydrate layer

1.3.2 Reagents

1.3.2.1 Collectors

Collectors are complex heteropolar molecules, ie. they comprise a polar hydrophilic end and a non-polar hydrophobic hydrocarbon group. They are usually added in small quantities to form a monolayer on the particle surface.

The type of collector used is the sulphydryl anionic collector, xanthate. Xanthates are dithiocarbonates with the following structure

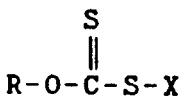

where R is an alkyl radical

X is a alkali metal e.g. Na or K

The type of xanthate used was SEX, sodium ethyl xanthate.

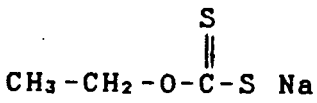

Xanthates are unstable in an acid medium. The xanthate ion decomposes to form xanthic acid which decomposes further to form carbon disulphide and alcohol. In an alkaline medium, xanthate is not rapidly decomposed. Decomposition products are carbon disulphide and monothiocarbonates (Fuerstenau D.W. and Mishra R.K. 1980).

There are two theories concerning the reaction of xanthates with pyrite

a. Dixanthogen may be the species of xanthate responsible for the flotation of pyrite. This has been concluded from spectroscopic studies (Fuerstenau M.C. 1982) and electrochemical flotation (Majima 1971).

The reactions taking place are

$2X^- \rightarrow X_2 + 2e^-$ anodic oxidation

$^1/_2O_{2(ads)} + H_2O + 2e^- \rightarrow 2OH^-$ cathodic oxidation

where X^- is the xanthate ion
X_2 is the dixanthogen molecule

Electron transfer takes place through the pyrite which has a heterogenous surface containing both cathodic and anodic sites.

The overall reaction is
$2X^- + {}^1/_2\ O_{2(ads)} + H_2O \rightarrow X_2 + 2OH^-$

The assumption that dixanthogen is the species responsible is based on the similarity of recovery with dixanthogen and recovery with xanthate ions (Fuerstenau M.C. 1982). In addition, the pH rises when pyrite is added to xanthate, showing that hydroxyl ions are formed (Fuerstenau M.C. 1982).

The recovery of pyrite with potassium ethyl xanthate and diethyl dixanthogen is shown in Figures 1.6 and 1.7. In Figure 1.6 two maxima can be seen. Depression at low pH values is due to the xanthate decomposing to form xanthic acid, depression at high pH values is due to lack of dixanthogen.

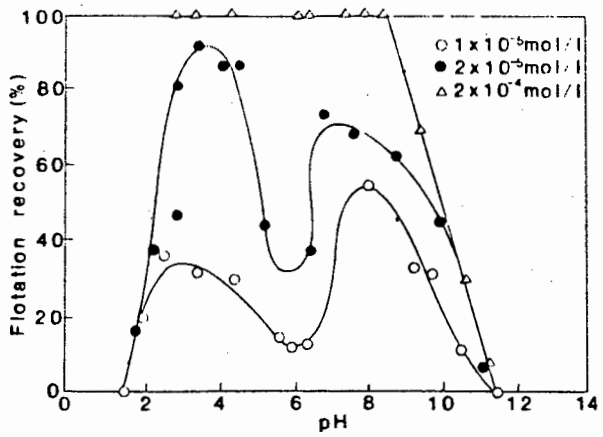

Figure 1.6 Recovery of pyrite as a function of flotation pH with various additions of potassium ethyl xanthate (Fuerstenau M.C. 1982)

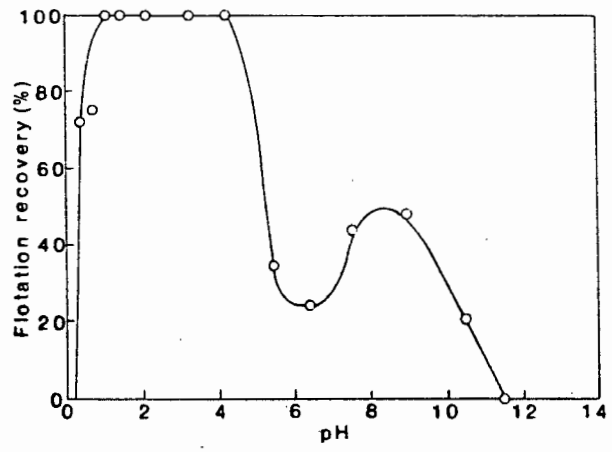

Figure 1.7 Recovery of pyrite as a function of pH with $1,3*10^{-5}$ mol/l diethyl dixanthogen (Fuerstenau M.C. 1982)

b. It is postulated by D.W. Fuerstenau and R.K. Mishra (Fuerstenau and Mishra 1980) that xanthate ions are also adsorbed onto the pyrite. This was obtained from studies of electrophoretic mobilities. It was found that the electrophoretic mobility was decreased by the addition of xanthate at pH values below the isoelectric point (at a pH of approximately 7). Dixanthogen did not affect the electrophoretic mobility at all.

The following mechanism was suggested

$$^1/_2O_{2(aq)} \rightleftharpoons {}^1/_2O_{2(ads)}$$

$$X^-_{(aq)} \rightleftharpoons X^-_{(ads)}$$

$$2X^-_{(ads)} + 2H^+ + {}^1/_2O_{2(ads)} \rightleftharpoons X_2 + 2H_2O$$

At low pH levels xanthate ions adsorb onto the positive pyrite surface. At neutral pH the xanthate ion has minimal effect on the electromobility and there is a minimal effect of xanthate on pyrite recovery. At high pH values adsorption of the xanthate is decreased and the increased recovery may be due to interaction between xanthate ions, dixanthogen, polythionate ions and iron oxide species (Fuerstenau D. W. and Mishra R. K. 1980).

1.3.2.2 Frothers

Frothers are heteropolar molecules which normally establish a position at the bubble walls with the polar end towards the water and the non-polar end towards the air.

The addition of frother causes the surface tension of the solution to decrease. This results in a fairly stable froth layer being formed by the following mechanism.

Gibbs absorption equation gives the degree of adsorption of the frother at the interface by the following equation

$$\Gamma = - a/RT \, dY/da$$

where Γ is the surface excess concentration of surface active agent

Y is the surface tension

a is the activity of the solute (which can be replaced by the concentration of a solute in a dilute solution).

Therefore, if dY/da is negative, due to the frother lowering the surface tension with increasing concentration, the excess concentration of the surfactant in the surface layer increases.

When a film of the solution containing surfactant is deformed causing local thinning, the concentration of surfactant decreases. This causes an increase in surface tension which then causes the surfactant molecules to be drawn back into the thinned section dragging underlying layers with them and restoring the flat shape. This is known as the Maragoni effect (Harris 1982, Finch 1979) and provides film stability. If the solution is too concentrated surfactant molecules diffuse from the bulk solution to the thinned section which leaves the section deformed and likely to rupture on further disturbance.

The frother used was DOWFROTH 400 which is a polypropylene glycol ether with the formula $CH_3(OC_3H_6)_7OH$. It is fairly soluble due to the hydrophilic oxygen atoms.

1.3.3 Ions and Water Chemistry

The ions to be dealt with are cations and anions. In order to determine exactly in what form the ion exists these ions are analysed by two different methods.

a. Anions are analysed in terms of the acid-base system
b. Cations are analysed in terms of complex formation.

1.3.3.1 Acid-base System

1.3.3.1.1 Algebraic Analysis

Anions in solution form part of the acid-base system where an acid is defined as being a substance which yields H^+ ions on dissociation and a base as being a substance which yields OH^- ions on dissociation.

Acids and bases which dissociate completely or almost completely are known as strong acids or bases. Examples are HCl, HNO_3 and H_2SO_4. Those that ionize only partly are weak acids or bases e.g. H_2CO_3.

There are two types of acids: monoprotic and diprotic. The equilibrium reactions and equations for the dissociation of a monoprotic acid are:

$$HA \rightleftharpoons H^+ + A^- \qquad A \text{ - anion}$$

$$\frac{[H^+][A^-]}{[HA]} = K \qquad K\text{- dissociation constant} \qquad (1)$$

For a diprotic acid the reactions and equations are as follows:

$$H_2A \rightleftharpoons H^+ + HA^-$$
$$HA^- \rightleftharpoons H^+ + A^{2-}$$
$$H_2O \rightleftharpoons H^+ + OH^-$$

$$\frac{[H^+][HA^-]}{[H_2A]} = K_1 \qquad (2)$$

$$\frac{[H^+][A^{2-}]}{[HA^-]} = K_2 \qquad (3)$$

$$[H^+][OH^-] = K_w \qquad (4)$$

A material balance can be set up for the anion of a weak diprotic acid of concentration C_t (in mol/l) (assuming a basis of 1 litre):

$$C_t = [H_2A] + [HA^-] + [A^{2-}] \qquad (5)$$

A proton balance is obtained thus:

addition of proton		H^+
zero proton condition	H_2A	H_2O
loss of one proton	HA^-	OH^-
loss of two protons	A^{2-}	

$$[H^+] = [HA^-] + 2[A^{2-}] + [OH^-] \qquad (6)$$

There are 5 equations and 5 unknowns, thus providing sufficient information to solve the equations providing C_t is known.

1.3.3.1.2 Graphical analysis

A graphical presentation of these reactions can be made and is known as the pH - log [species] diagram.

a) Monoprotic acid

From the equation

$$[HA] = [A^-][H^+] / K$$

the material balance is:

$$C_t = [HA] + [A^-]$$

$$= [A^-][H^+]/K + [A^-]$$

$$[A^-] = C_t / (1 + [H^+]/ K)$$

Let $Y = 1 + [H^+]/ K$

$$[A^-] = C_t / Y$$

$$[HA] = C_t [H^+] / (Y*K)$$

Taking logs

$$\log [A^-] = \log C_t - \log Y$$

$$\log [HA] = \log C_t - \log Y + \log [H^+]/K$$

This is then plotted in Figure 1.8.

Figure 1.8 : pH - log [species] diagram for monoprotic acids

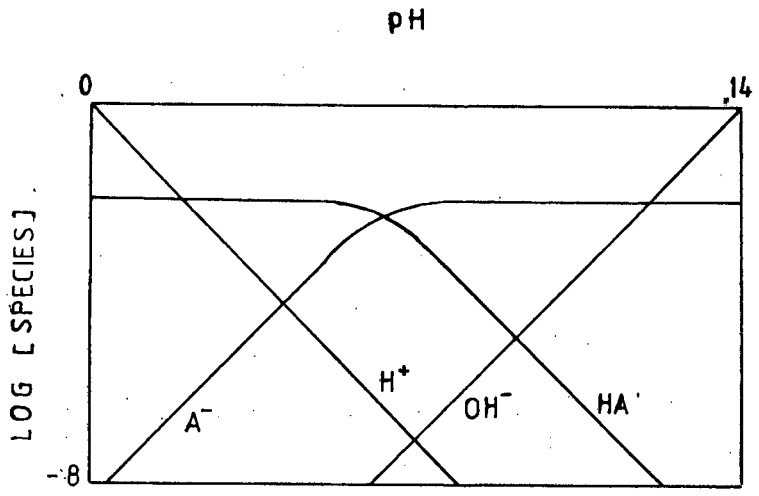

b) Polyprotic acids

From equations (2) and (3)

$$\left[H_2A\right] = \left[HA^-\right]\left[H^+\right]/K_1$$

$$\left[A^{2-}\right] = K_2\left[HA^-\right]/\left[H^+\right]$$

substituting into (5)

$$C_t = \left[HA^-\right]\left[H^+\right]/K_1 + \left[HA^-\right] + K_2\left[HA^-\right]/\left[H^+\right]$$

$$\left[HA^-\right] = C_t/(\left[H^+\right]/K_1 + 1 + K_2/\left[H^+\right])$$

Set $X = \left[H^+\right]/K_1 + 1 + K_2/\left[H^+\right]$

$$\left[HA^-\right] = C_t/X$$

$$\left[H_2A\right] = Ct\left[H^+\right]/(X*K_1)$$

$$\left[A^{2-}\right] = K_2\ C_t/(\left[H^+\right]*X)$$

$$\left[OH^-\right] = K_w/\left[H^+\right]$$

Taking logs

$$\log \left[HA^-\right] = \log C_t - \log X$$

$$\log \left[H_2A\right] = \log C_t - \log X + \log \left[H^+\right]/K_1$$

$$\log \left[A^{2-}\right] = \log C_t - \log X + \log K_2/\left[H^+\right]$$

$$\log \left[H^+\right] = -pH$$

$$\log \left[OH^-\right] = \log K_w + pH$$

This is plotted in Figure 1.9.

Figure 1.9: pH-log [species] diagram for diprotic acid

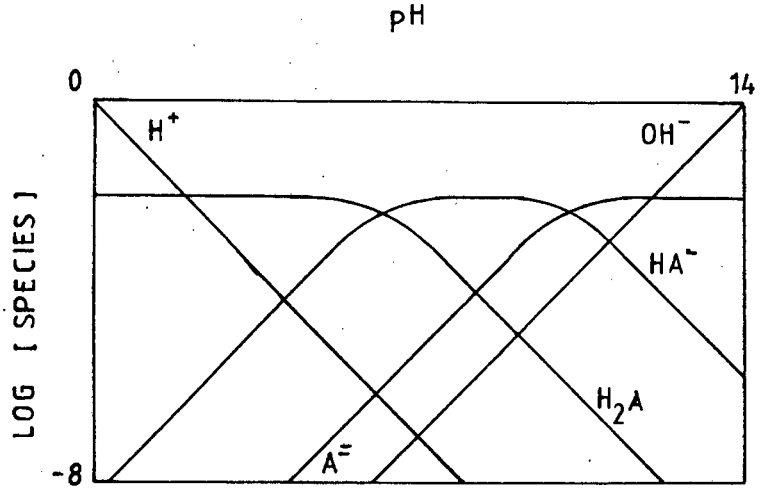

Thus knowing C_t and pH one can determine exactly what the concentrations of the ions present in solution are.

1.3.3.1.3 Analysis of anions

As previously mentioned HCl, HNO_3 and H_2SO_4 are strong acids while H_2CO_3 is a weak acid. This is shown by the pK values in Table 1.3.

Table 1.3 : pK values for certain acids

Species of Acid	pK_1	pK_2
Carbonic	6,37	10,25
Sulphuric	< 0	1,92
Nitric	< 0	
Hydrochloric	< 0	

Thus at any pH nitric and hydrochloric acid will be completely dissociated to form nitrate and chloride ions. Sulphuric acid will be mainly present as the SO_4^{2-} ion and will only be present as HSO_4^- ions at very low pH values. Carbonic acid is the only species that has a variety of ions present at various pH values. It is therefore to be analysed in greater depth.

1.3.3.1.4 The Carbonic Acid System

Dynamic equilibria present in the system are

$CO_2 + H_2O = H_2CO_3$

$H_2CO_3 = H^+ + HCO_3^-$

$HCO_3^- = H^+ + CO_3^{2-}$

$H_2O = H^+ + OH^-$

The pH-log[species] is shown in Figure 1.10 (Loewenthal and Marais 1976).

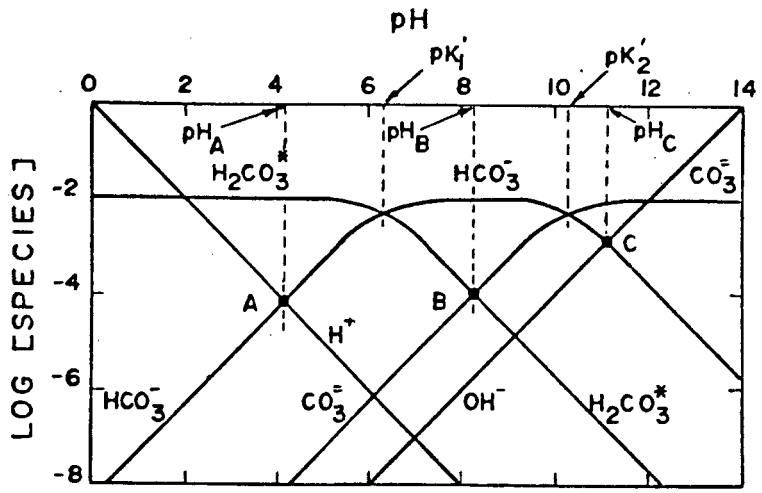

Figure 1.10 Distribution of carbonic species with pH; $C_T = 10^{-2}$ M (Loewenthal and Marais 1976)

Three points shown in Figure 1.10 can be defined as follows:

a. A is known as the total acidity equilibrium point and is obtained from the intersection of the HA^- and H^+ lines.

b. B is called the phenolpthalein alkalinity equivalence point.

c. C is called the total alkalinity equivalence point.

From proton balances these points are defined as follows:

Total alkalinity $= 2\left[CO_3^{2-}\right] + \left[HCO_3^-\right] + \left[OH^-\right] - \left[H^+\right]$

Phenolpthalein alkalinity $= \left[CO_3^{2-}\right] + \left[OH^-\right] - \left[H^+\right] - \left[H_2CO_3^*\right]$

Total acidity $= 2\left[H_2CO_3^*\right] + \left[HCO_3^-\right] + \left[H^+\right] - \left[OH^-\right]$

where $\left[H_2CO_3^*\right] = \left[CO_2 \text{ dissolved}\right] + \left[H_2CO_3\right]$

Total concentration of the carbonic species = C_t

$$C_t = \left[CO_3^{2-}\right] + \left[HCO_3^-\right] + \left[H_2CO_3^*\right]$$

with $\left[H_2CO_3^*\right] = \left[HCO_3^-\right]\left[H^+\right]/K_1$

$$\left[CO_3^{2-}\right] = K_2\left[HCO_3^-\right]/\left[H^+\right]$$

From the above equations

Total alkalinity + total acidity = $2C_t$

These equations are relevant for a one phase system i.e. only the liquid phase is present. If $CaCO_3$ starts precipitating out, the solid phase is involved. A new equation has then to be incorporated. This is

$$\left[Ca^{++}\right]\left[CO_3^{2-}\right] = K_{sp} \qquad (7)$$

The total concentration of the carbonic species now becomes

$$C_t = \left[CO_3^{2-}\right] + \left[HCO_3^-\right] + \left[H_2CO_3^*\right] + P \qquad (8)$$

where P is the concentration of precipitated CO_3^{2-}.

The total concentration of calcium is

$$C_{Ca} = \left[Ca^{++}\right] + P + \left[CaOH^+\right] \qquad (9)$$

$$= \left[Ca^{++}\right](1 + K_1K_w/[H^+]) + P$$

If equation 9 is subtracted from equation 8 and $[Ca^{++}]$ from equation 7 substituted in the resulting equation, the following equation is obtained.

$$\left[HCO_3^-\right]^2 \left((K_2/\left[H^+\right]) + 1 + (\left[H^+\right]/K_1)\right)*(K_2/\left[H^+\right])$$

$$-((K_2/\left[H^+\right])(C_t - C_{ca})) \left[HCO_3^-\right] - K_{sp}(1+K_1K_w/[H^+]) = 0$$

If the pH and values of C_t and C_{ca} are known the concentration of HCO_3^- ions can be determined. Other carbonic species and the $CaCO_3$ precipitate can then be calculated.

1.3.3.2 Formation of Complexes

The cations to be investigated are Mg^{++} and Ca^{++}. These metal ions are hydrolysed in solution to form intermediate species which may be unstable. The hydroxide formed are relatively insoluble and precipitate out in alkaline solutions.

The formation of the hydroxides is regarded as being the addition of ligands, viz the OH^- ions, to a central metal ion, the cation, to form a complex.

There are two types of complexes

1. Mononuclear - Only one metal cation is present in the complex e.g. hydroxides of Ca^{++}, Mg^{++} and Fe^{++}.
2. Polynuclear - Several hydroxide complexes are formed which may contain several metal atoms e.g. hydroxides of Fe^{+++}.

1. Mononuclear Complexes

The following reactions occur in solution

$$Ca^{++} + OH^- \rightleftharpoons Ca(OH)^+$$

$$Ca(OH)^+ + OH^- \rightleftharpoons Ca(OH)_{2(s)}$$

Similar reactions occur for Mg^{++} and Fe^{++} except that $Fe(OH)_{2(aq)}$ forms and there is an additional equation.

$$Fe(OH)_{2(aq)} \rightleftharpoons Fe(OH)_{2(s)}$$

The equilibria equations are

$$\left[Ca(OH)^+\right] = K_1\left[Ca^{++}\right]\left[OH^-\right]$$

$$\left[Ca(OH)_2\right] = K_2\left[CaOH^+\right]\left[OH^-\right]$$

Precipitation occurs if

$$\left[Ca(OH)^+\right] > K_{s1}/\left[OH^-\right]$$

or $$\left[Ca(OH)_2\right] > K_{s2}$$

There are 2 cases to be studied: the one phase system which is an unsaturated solution with no precipitation occurring and the two phase system which is a saturated solution with precipitation of solids.

a. One phase system

Material balance for calcium:

$$\left[Ca^{++}\right] + \left[CaOH^{+}\right] = C_{Ca}$$ where C_{Ca} is the total calcium concentration

Equilibria equation:

$$K_1 = \left[CaOH^{+}\right] / \left[Ca^{++}\right]\left[OH^{-}\right]$$

From these two equations

$$\left[CaOH^{+}\right] = C_{Ca}\ (K_1 K_W / (\left[H^{+}\right] + K_1 K_W))$$

Let $X = K_1 K_W / (\left[H^{+}\right] + K_1 K_W)$

therefore

$$\left[CaOH^{+}\right] = C_{Ca} X$$

$$\left[Ca^{++}\right] = C_{Ca}(1-X)$$

b. Two phase system

Material balance for the calcium component:

$$\left[Ca^{++}\right] + \left[CaOH^{+}\right] + \left[Ca(OH)_{2s}\right] = C_{Ca}$$

Equilibria equations:

$$\left[Ca^{++}\right] = K_{s0}/\left[OH^{-}\right] = K_{s0}\left[H^{+}\right]^{2}/K_{w}^{2}$$

$$\left[CaOH^{+}\right] = K_{s1}/\left[OH^{-}\right] = K_{s1}\left[H^{+}\right]/K_{w}$$

therefore

$$\frac{K_{s0}}{K_{w}^{2}}\left[H^{+}\right]^{2} + \frac{K_{s1}}{K_{w}}\left[H^{+}\right] + \left[Ca(OH)_{2s}\right] = C_{Ca}$$

$$\left[Ca(OH)_{2s}\right] = C_{Ca} - \frac{K_{s0}}{K_{w}^{2}}\left[H^{+}\right]^{2} - \frac{K_{s1}}{K_{w}}\left[H^{+}\right]$$

From the two phases log[species]-pH diagrams can be plotted as is shown in Figures 1.11, 1.12 and 1.13.

Figure 1.11 Logarithmic concentration diagram for $1*10^{-3}$ mol/l Ca^{++}. Equilibrium data from Butler(1964), p287

(Fuerstenau D.W and Fuerstenau M.C. 1982)

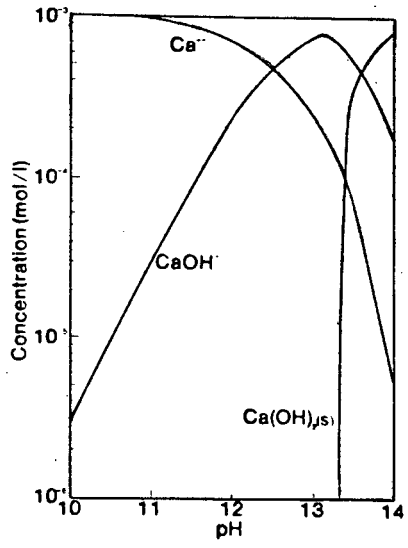

Figure 1.12 Logarithmic concentration diagram for $1*10^{-4}$ mol/l Mg^{++}. Equilibrium data from Butler (1964).

(Fuerstenau D. W. and Fuerstenau M. C. 1982)

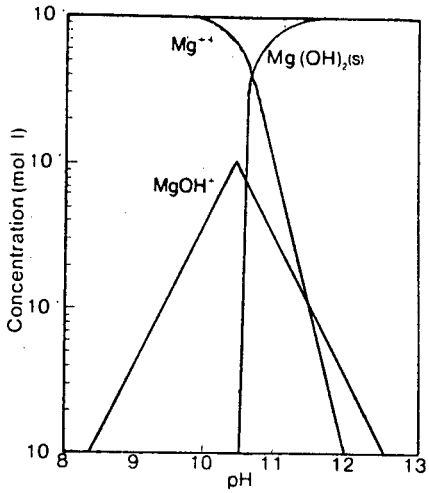

Figure 1.13 Logarthmic concentration diagram for $1*10^{-4}$ mol/l Fe^{++}.

(Fuerstenau D. W. and Fuerstenau M. C. 1982)

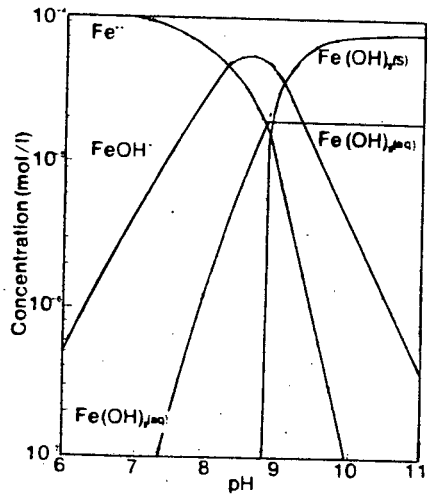

2. Polynuclear complexes

Hydrolysis of the ferric ion results in the formation of $FeOH^{++}$, $Fe(OH)_2^{+}$, $Fe_2(OH)_2^{4+}$ and $Fe(OH)_3(s)$ at different pH values. Mass balances are set up as for the mononuclear system and a log [species]-pH diagram can be drawn as shown in Figure 1.14 (Butler 1964). Equilibrium constants for all the above systems are given in Table 1.4.

Table 1.4 : Equilibrium Constants

ION	CO-ION	pK_1	pK_{s0}	pK_{s1}
Ca^{++}	OH^-	-1,51	5,26	3,75
Ca^{++}	CO_3^{2-}		8,06	
Mg^{++}	OH^-	-2,58	10,74	8,16
Fe^{++}	OH^-	-5,7	15,1	9,4

(Butler 1964, CRC Handbook 1980)

Figure 1.14 Logarthmic concentration diagram for $1*10^{-4}$ mol/l $FeCl_3$. Equilibrium data from Butler(1964) p394

(Fuerstenau D.W. and Fuerstenau M.C. 1982)

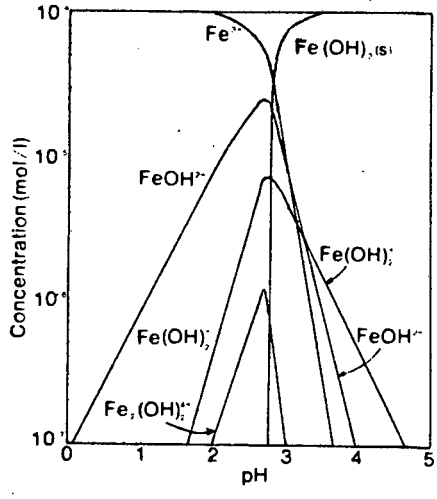

1.4 EFFECT OF IONS ON THE FLOTATION SYSTEM

1.4.1 The Pulp Phase

1.4.1.1 Theory

Two processes occur in the pulp phase. Firstly the mineral reacts with the collector in order to become hydrophobic. As a result of this hydrophobicity it then becomes attached to a bubble of air rising through the pulp.

The first process is dependent on the surface properties of the mineral. Two factors affect these properties: the electrical double layer at the mineral-water interface and the interaction of water molecules with the surface.

When the mineral surface is brought into contact with a polar medium like water, several ions from the mineral surface are transferred into solution (Klaasen and Mokrousov). This causes the surface to become electrically charged. Ions of the opposite charge (counter-ions) in the water are attracted towards the surface, whereas ions of the same charge (co-ions) are repelled from the surface. This produces a double electrical layer comprising a bound layer known as the Stern layer which moves with the solid mineral and a diffuse region in which ions are affected by electrostatic forces and random thermal motion. There is a distribution of electrical potential across this layer which is shown in Figure 1.15.

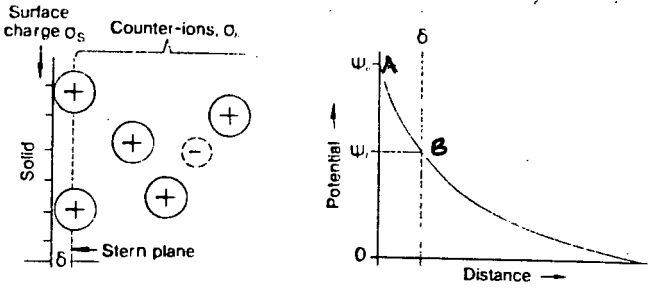

Figure 1.15 Schematic representation of the electrical double layer and the potential drop across the double layer at a solid-water interface

(Fuerstenau D.W 1982)

Two points on this diagram are important. The electrochemical potential or surface potential shown by point A and the electrokinetic or zeta potential approximated by point B. The zeta potential arises when the mineral particle moves and the two layers are separated thus disturbing the electroneutrality of the system.

Changes in zeta potentials can show the effects of the absorption of ions whether by electrostatic attraction, chemisorption or chemical reaction.

The second process i.e. the attachment of the mineral to the bubble, consists of the following steps: the approach of the bubble to the solid, the formation of the thin water film between bubbles and the solid, the rupture of this film due to thinning, the retreat of the water and the establishment of a contact angle. The induction time is defined as the time taken from the deformation of the bubble to the rupture of the film (Finch 1979).

The contact angle is determined from the following equation

$$\gamma_{sa} = \gamma_{wa} \cos\theta + \gamma_{sw}$$

where γ_{sa} γ_{wa} and γ_{sw} are surface energies between air-solid, water-air and solid-water interfaces
and θ is the contact angle

The contact angle is shown in Figure 1.16. The greater the contact angle the greater is the work of adhesion between particle and bubble and the greater the floatability of the mineral.

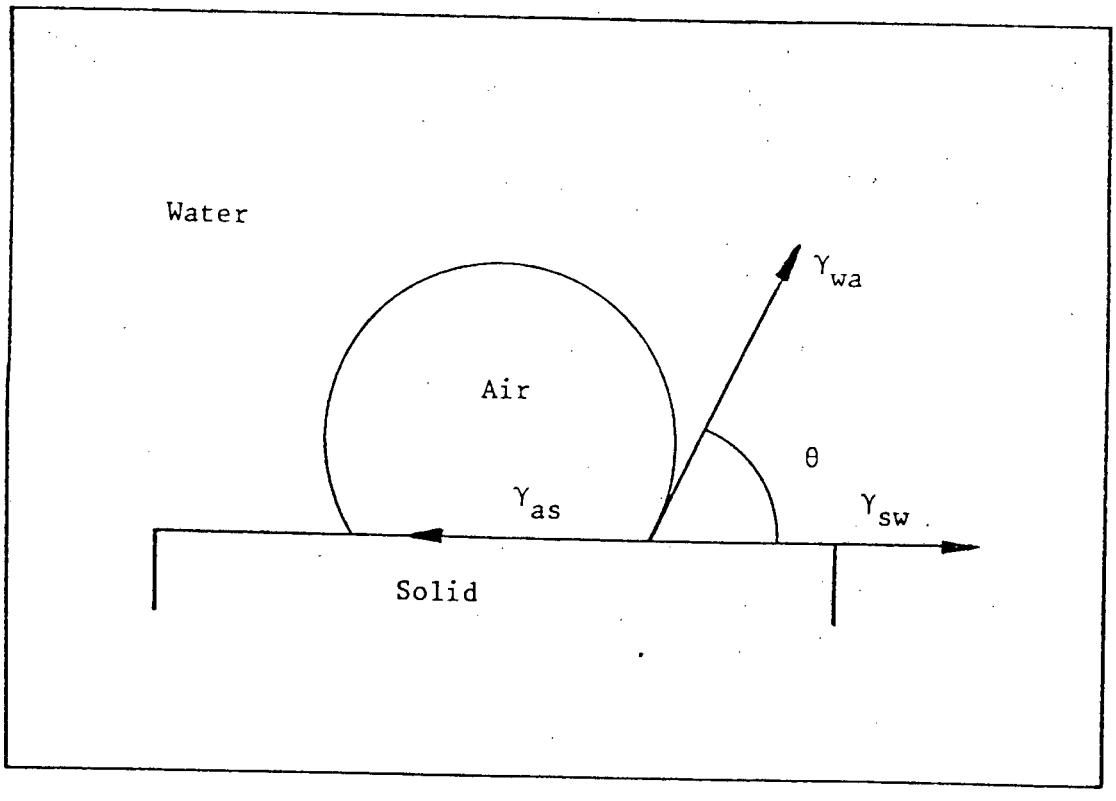

Figure 1.16 Contact between air-bubble and mineral particle in aqueous medium

1.4.1.2. The Effect of Ions on Quartz

a. Indifferent electrolytes (NaCl, KCl)

The addition of inorganic salts was found to cause compression of the double layer and thus a reduction of the film thickness. This is shown by the effect of ionic strength on alumina (Fuerstenau D.W. 1982) and the effect of KCl and $BaCl_2$ on polished vitreous silica (Read and Kitchener 1969). The thickness was found to decrease with an increase in salt concentration and with an increase in the valency of the cation. Figure 1.17 shows the effect of electrolyte on the electrokinetic potential (Klaasen and Mokrousov 1963).

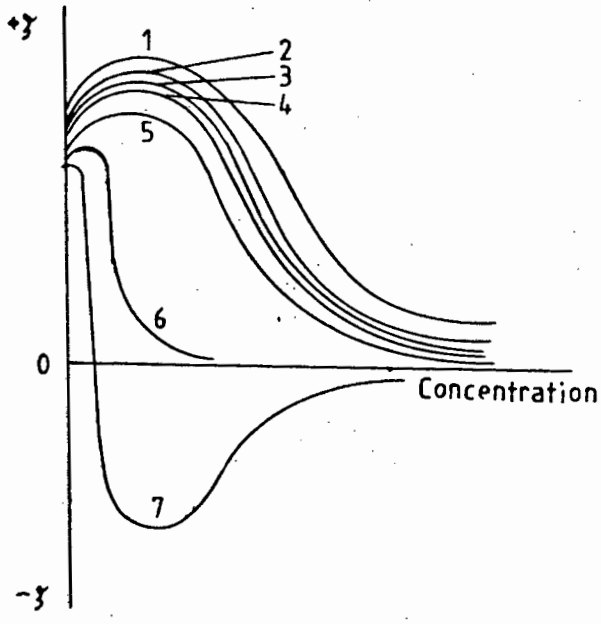

Figure 1.17 The influence of the concentration of various inorganic electrolytes on the electrokinetic potential: 1. Na_2SO_4: 2. LiCl: 3. NaBr: 4. NaCl: 5. KCl: 6. $BaCl_2$: 7. $FeCl_3$
(Klaasen and Mokrousov 1963)

KCl was added to a solution in contact with methylated quartz (with a hydrophobic surface). The contact angle remained constant with an increase in concentration but the induction time decreased and the recovery increased (Laskowski and Iskra 1970).

The addition of inorganic salts with surfactant could possibly increase the absorption of the surfactant at the interfacial surfaces (Finch 1979).

Ba^{++} and Na^{+} were found to depress quartz flotation with a cationic collector with the effect being greater with the divalent salt (Fuerstenau D.W. and Fuerstenau M.C. 1982).

The addition of NaCl decreased the electrostatic repulsion between particles and caused coagulation of particles (size -37µm)(Yarar and Kitchener 1970). The coagulation increased with pH and NaCl addition (0-800 meq/l). The salts of divalent ions (Ca++) were found to coagulate silica more readily. Coagulation of quartz was also found to occur at addition rates of more than 50 meq/l (Read and Hollick 1976).

b. Calcium and Magnesium Ions

The effect of increased concentration of $MgCl_2$ and $CaCl_2$ on the zeta potential of quartz is shown in Figure 1.18, on flocculation in Figure 1.19 and on flotation with a cationic collector in Figure 1.20 The effect of pH on abstraction of calcium and magnesium by quartz is shown in Figure 1.21 (Iwasaki et al 1980).

Figure 1.18 Zeta potentials of quartz and goethite as functions of calcium and magnesium chloride concentrations at pH 7 and 11

(Iwasaki et al 1980)

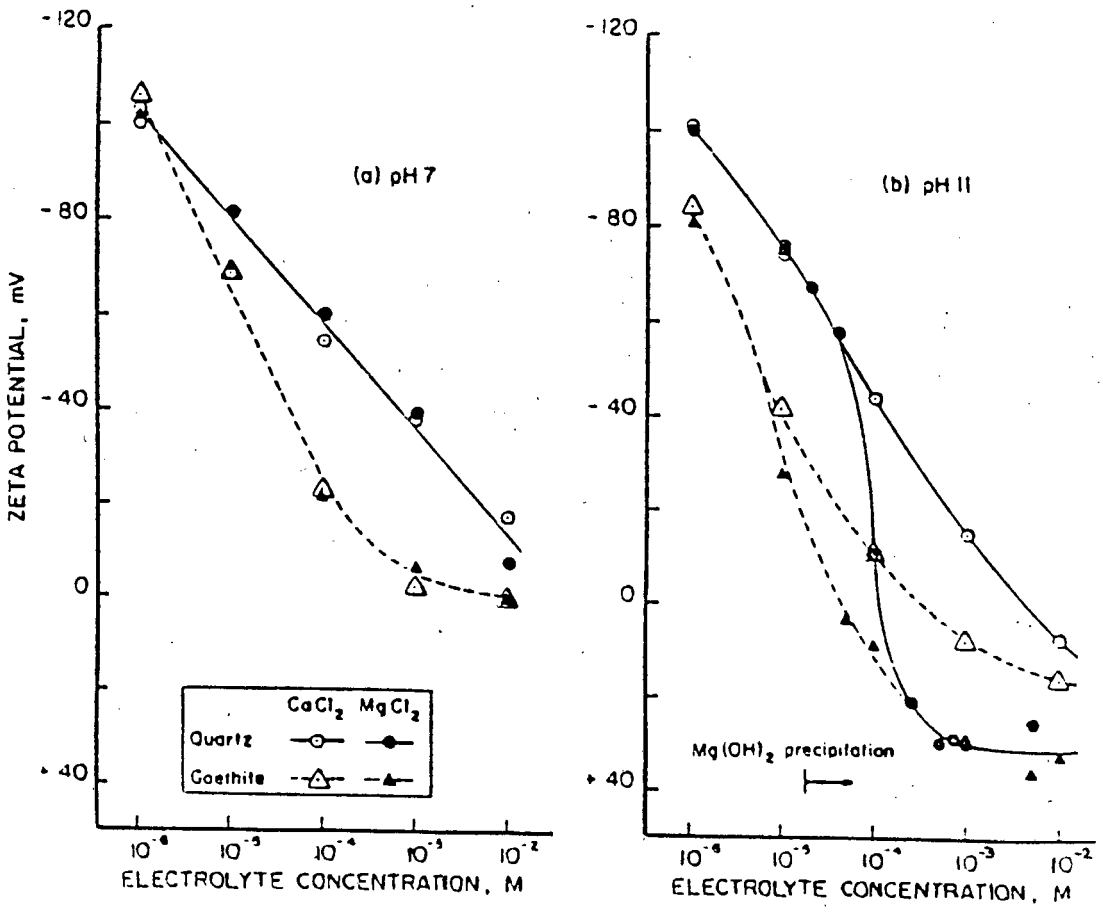

Figure 1.19 Flocculation test results on quartz as functions of calcium and magnesium chloride concentrations at pH 7 and 11

(Iwasaki et al 1980)

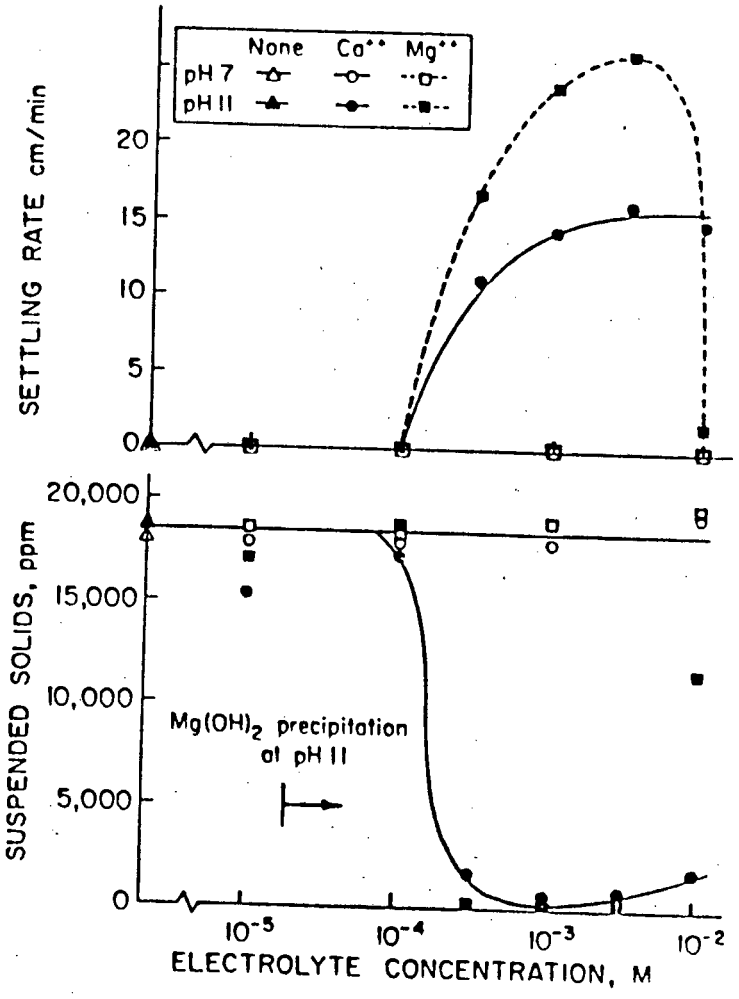

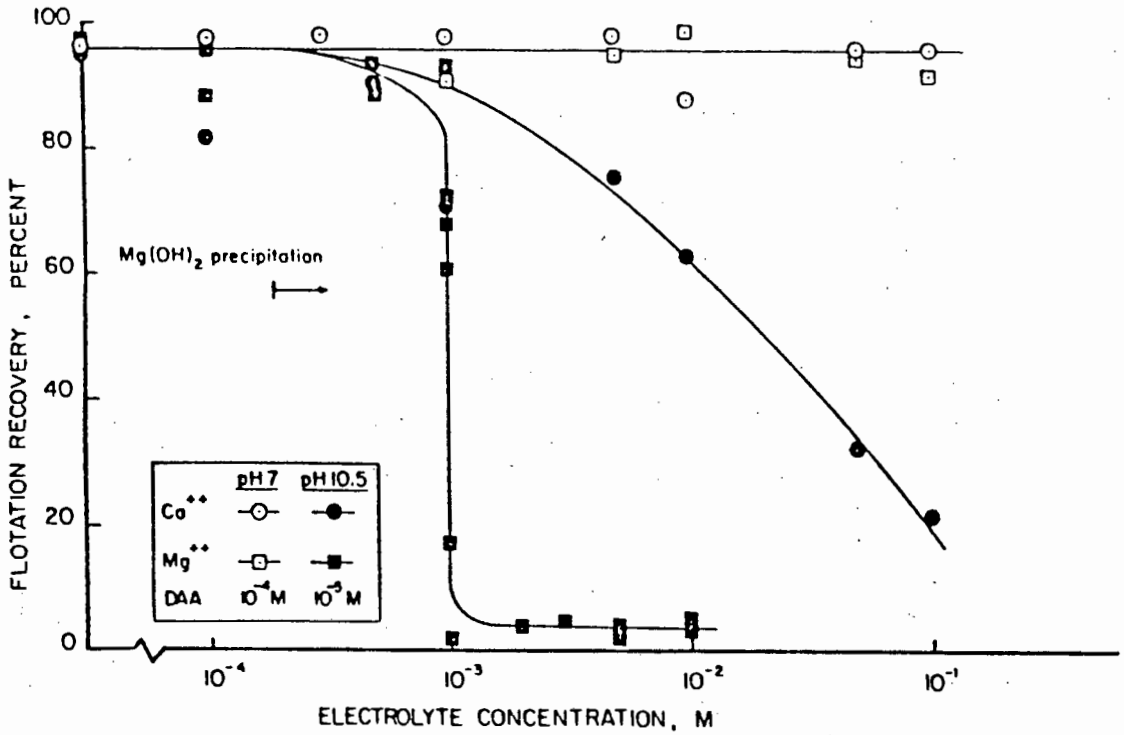

Figure 1.20 Flotation recovery of quartz as functions of calcium and magnesium chloride concentrations at pH 7 and 10,5 (Iwasaki et al 1980)

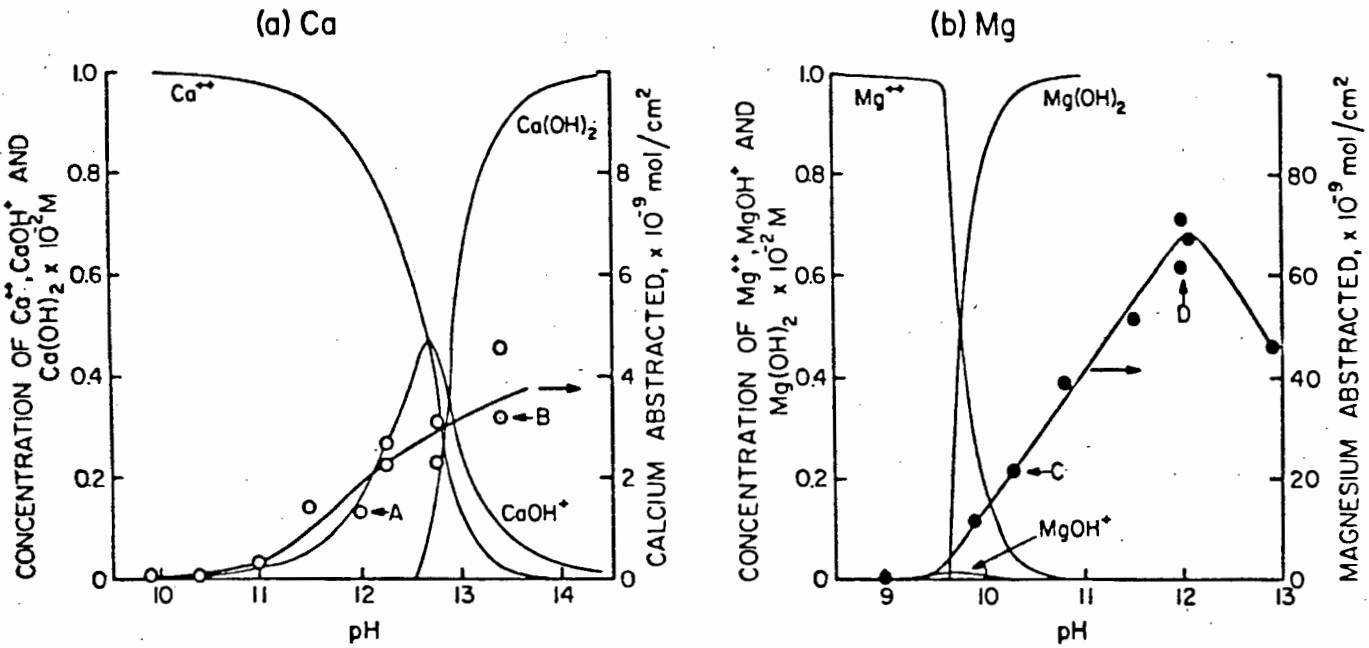

Figure 1.21 Relationship of hydrolysis and precipitation of calcium and magnesium to their abstractions by quartz at a total concentration of 10^{-2} M (Iwasaki et al 1980)

From the above it is concluded that calcium is adsorbed as $CaOH^+$ and magnesium as $Mg(OH)_2$ precipitate and that these ions were responsible for the flocculation of quartz suspension and the depression in cationic flotation of silica in an alkaline pulp solution (Iwasaki et al 1980).

Calcium has been thought to activate quartz in anionic flotation (Lloyd 1981).

The mechanism of the absorption of these cations is said to be due to hydrogen bonding between an adsorbed hydrogen ion and the MOH^+ complex (M being the calcium or magnesium ion) or the splitting out of water molecules from the complex of

$$-Si-O-H \cdots\cdots H-O-M^+ \quad \text{to form} \quad -Si-O-M^+$$

This results in the decrease in the negative charge of the quartz surface (Fuerstenau et al 1970, Palmer et al 1975). Adsorption of hydrolyzed cation followed by condensation to metal hydroxide resulting in coating is also said to occur (James and Healy 1972).

Activation by MOH^+ ions in flotation is said to be due to the dehydration of the surface allowing the air-solid interface to hold little or no water. However the metal ions M^{++} are adsorbed as hydrated ions. A layer of water molecules then separates the bubble from the solid thus depressing the quartz (Fuerstenau M.C. et al 1970).

c. Carbonates

Na_2CO_3 and NaOH are used to disperse gangue slimes (Lovell 1982).

The addition of Na_2CO_3 to a solution of quartz and calcium chloride leads to adsorption of calcium carbonate on the quartz (Figure 1.22). This resulted in reduction in recovery in cationic flotation (Heerema and Iwasaki 1980).

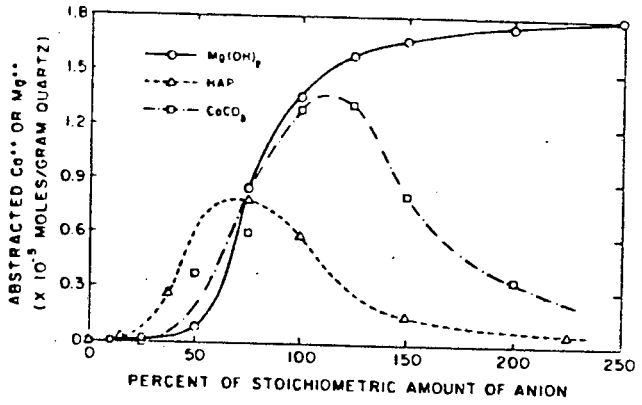

Figure 1.22 Abstraction of precipitate by quartz as a function of the stoichiometric fraction of anion with calcium and magnesium (HAP refers to hydroxyapatite). (Heerema and Iwasaki 1980)

1.4.1.3 The Effect of Ions on Pyrite

a. $NaNO_3$

The increased addition of $NaNO_3$ caused a decrease in the negative charge of the pyrite surface. This is shown in Figure 1.23.

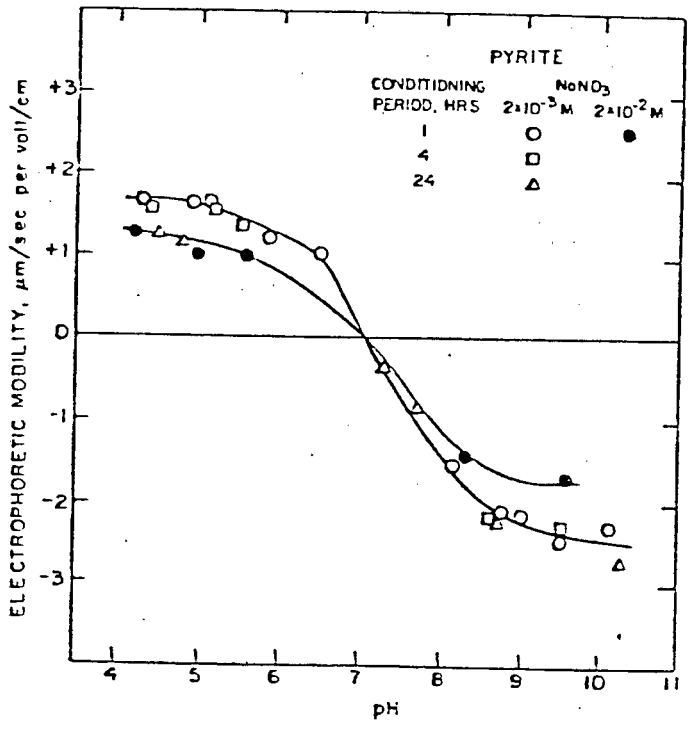

Figure 1.23 Effect of conditioning period and concentration of $NaNO_3$ on electrophoretic mobility versus pH behaviour of pyrite

(Fuerstenau D.W. and Mishra R.K. 1980)

b. Calcium

Calcium adsorption on pyrite increases with increasing pH and calcium concentration (Gaudin and Charles 1953). Ca^{++} adsorbs by electrostatic attraction above pH 6,9 onto negatively charged pyrite thus hindering the oxidation of xanthate (Fuerstenau M.C. 1982). This results in a decreased recovery of pyrite as is shown in Figure 1.24.

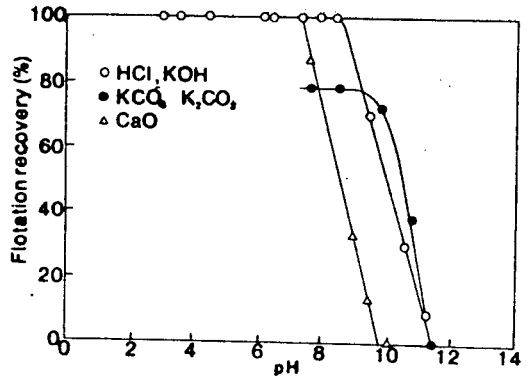

Figure 1.24 Flotation of pyrite with $2*10^{-4}$ mol/l KEX (Fuerstenau M.C. 1982)

In an alkaline medium calcium reacts with products of sulphur oxidation and atmospheric carbon dioxide to form calcium sulphate and calcium carbonate films. These films usually increase the hydration of pyrite which results in depression of the pyrite (Glembotski et al 1972, Klaasen and Mokrousov 1963).

c. Carbonate

From Figure 1.24 it can be seen that potassium hydrogen carbonate and K_2CO_3 reduce the recovery of pyrite (Fuerstenau M.C. 1982).

The addition of sodium bicarbonate precipitates calcium reducing the plating action of $CaSO_4$ and $CaCO_3$ film (Pryor 1965).

d. Sulphate

An increase in concentration of $MgSO_4$ and $CaSO_4$ initially reduces the recovery and grade of pyrite but further increases have no effect (Ross, Dunne and Burger 1984).

1.4.1.4 The Effect of Ions on Other Minerals

Molybdenite (MoS_2) is a sulphide often found with copper sulphides. It has a rest potential of 0,16V (pyrite has a rest potential of 0,22V) and therefore reacts with xanthate to form dixanthogen at the surface in the same way as pyrite (Allison et al 1972).

It was found that the use of sewerage water resulted in a decrease in recovery of 16,2% MoS_2 as opposed to demineralized water. The removal of cations provided a slight increase but removal of anions provided the greatest increase.

The zeta potential of molybdenite becomes less negative with the addition of $CaCl_2$ and KCl. However the zeta potential produced by $CaCl_2$ is less negative (sign reversal occurs) than that of KCl. Similarly the addition of $Ca(OH)_2$ produces a less negative zeta potential than NaOH and Na_2CO_3.

The adsorbance of calcium increases with an increase in pH and increase in free $Ca(OH)_2$ in the system. It also increases with the addition of Fe^{3+} ions.

The recovery of molybdenite initially increases with calcium addition (possibly due to the compression of the double layer) then decreases (possibly due to the increased adsorption of Ca^{++} causing the faces to become hydrophilic).

Al^{3+}, Fe^{3+} and Fe^{++} depress molybdenite at the pH values at which the metal hydroxide precipitate forms (7,5, 7,5 to 11,3 and 11,3 respectively). Na^{+} has no effect on the recovery.

The addition of Fe^{3+} causes more iron adsorption onto MoS_2 in the presence of $Ca(OH)_2$ than NaOH and a greater depressive action. Different types of precipitate are formed: with $Ca(OH)_2$ a finely dispersed slowly

precipitating iron hydroxide with a substantial amount of $CaCO_3$ is formed; whereas with NaOH a gel-like precipitate forms which coagulates rapidly (Hoover 1980).

1.4.2 The Froth Phase

1.4.2.1 Theory

The froth layer consists of bubbles coated with mineral particles. As these bubbles rise to the surface, water in the bubble walls and suspended solids drain downwards. The bubble walls become thinner until adjacent bubble walls contact at one point. The bubbles are spherical but as the pulp drains further the bubbles become polygonal in shape. If the bubble walls become too thin coalescence of the bubbles takes place (Gaudin 1953).

The drainage of a single vertical film was given the equation

$$\delta^2 = \frac{4\eta}{\rho g}\frac{z}{t}$$

where δ is the film thickness
η is the viscosity of the solution
ρ is the density of the solution
z is the distance down the film
t is the time (Harris 1982).

It is proposed that the following model also fits a three phase froth system. When the froth contains solid particles, a proportion will float in the interfaces of the films. If the particles are hydrophobic enough, coalescence will occur when the films have thinned sufficiently to allow the parts of particles extending into the liquid film to bridge the films. After coalescence the particle remains in the interface surrrounding the bigger bubble and causes repeated coalescence. This increased rate of destruction of films causes a smaller equilibrium volume of froth for a constant production rate of froth (Dippenaar and Harris 1978).

Contact angles of approximately 90° induce coalescence whereas smaller contact angles tend to stabilze the bubbles.

Particle sizes of approximately 10 µm tend to destabilize froth. Smaller particles coagulate and therefore do not have the same effect. These highly flocculated particles tend to produce an overstable froth with thick walls of interlocking particles. The bubbles may be denser than the pulp and result in loss of mineral by non-levitation and difficulty in froth removal (Gaudin 1932). Smaller particles also tend to be entrained by ascending streams. The hydrophobic particle then either adhere to the bubbles or larger hydrophobic grains only in the froth phase.

1.4.2.2 Effect of Ions of the Froth Phase

The addition of ions such as $NaNO_3$, NaCl, $NaHCO_3$, $MgCl_2$, $CaCl_2$ and Na_2SO_4 causes the surface tension to increase (i.e. dY/da increases)(CRC Handbook). Therefore from Gibbs equation ($\Gamma = -(a/RT)dY/da$) there is a negative adsorption of ions which tend to move into the bulk solution as opposed to the positive adsorption of organic surfactants. An increase in surface tension leads to an increase in bubble size and therefore a decrease in froth stability (Perry 1973).

The addition of ions causes the kinematic viscosity (η/ρ) to increase from 1,0038 cS (pure water) to 1,04 cS (100 eq/l $MgCl_2$)(CRC Handbook). Therefore the film thickness will increase, slower drainage occurs and the froth will be more stable (Harris 1982). This slower drainage occurs over addition rates of 0 to 100 meq/l for both NaCl and KCl but the film drainage time then increases over addition rates of 100 to 200 meq/l for NaCl while decreasing for KCl(Parekh et al 1983).

However increased ionic strength was found to decrease the volume of froth (Shaw 1983). Divalent and trivalent ions were more effective in destabilising the froth than the univalent sodium ion (Wark and Sutherland 1955).

The addition of certain ions to a mixture of frother and xanthate collector can cause precipitation of the hydrophobic metal xanthate which destabilizes the froth

(Harris 1982). Substances like copper sulphate and lead acetate were found to increase the bubble size and reduce the froth volume due to the formation of insoluble metal precipitates, however zinc sulphate, which is soluble, had little effect on the size of the bubbles or froth stability(Dudenkov and Livshits 1959). Alkali metal xanthates (e.g. Na^{+}) and alkaline earth metals (e.g. Ca^{++}) are soluble in water and therefore xanthate precipitates will not be formed with the addition of these ions. Ferric xanthate is an unstable species and is not found as a precipitate in the iron-xanthate system at high pH levels as ferric hydroxide forms preferentially (Fuerstenau M.C. 1982).

2. OBJECTIVES OF RESEARCH

The aim of this research was to determine the effect of various ions on the flotation of pyrite using a xanthate collector in an alkaline medium. The ions that were studied were sodium, magnesium, calcium, sulphate, hydrogen carbonate and chloride.

These ions were considered to be typical of those present in most samples of flotation plant process water. The investigation involved a study of the effect these ions had on the recoveries of pyrite and gangue in a flotation cell, on the stability of both two and three phase froths and on the adsorption of the collector on pyrite.

3. EXPERIMENTAL METHODS

3.1 FLOTATION

Different ions were added to a synthetic mixture of pyrite and quartz in a flotation cell to observe their effect on the grade and recovery of the pyrite in the concentrates collected.

3.1.1 Conditions

3.1.1.1 Apparatus

A 3l modified Leeds cell was used. This is shown in Figure 3.1 and Figure 3.2. Modifications that were made included the installation of:

a. An impingement plate which lies at an angle of 45 degrees instead of 60 degrees to the cell walls;

b. A head tank level control device was installed. This device maintained a constant froth height of 2,5 cm.

Figure 3.1 Modified Leeds Cell

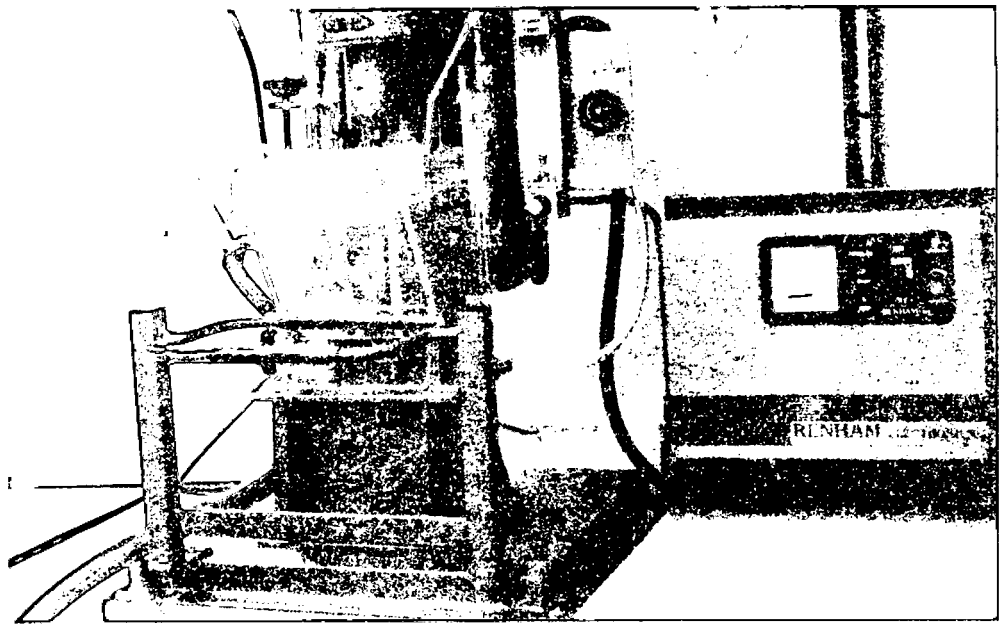

Figure 3.2 View of Level Control Device and Impingement Plate

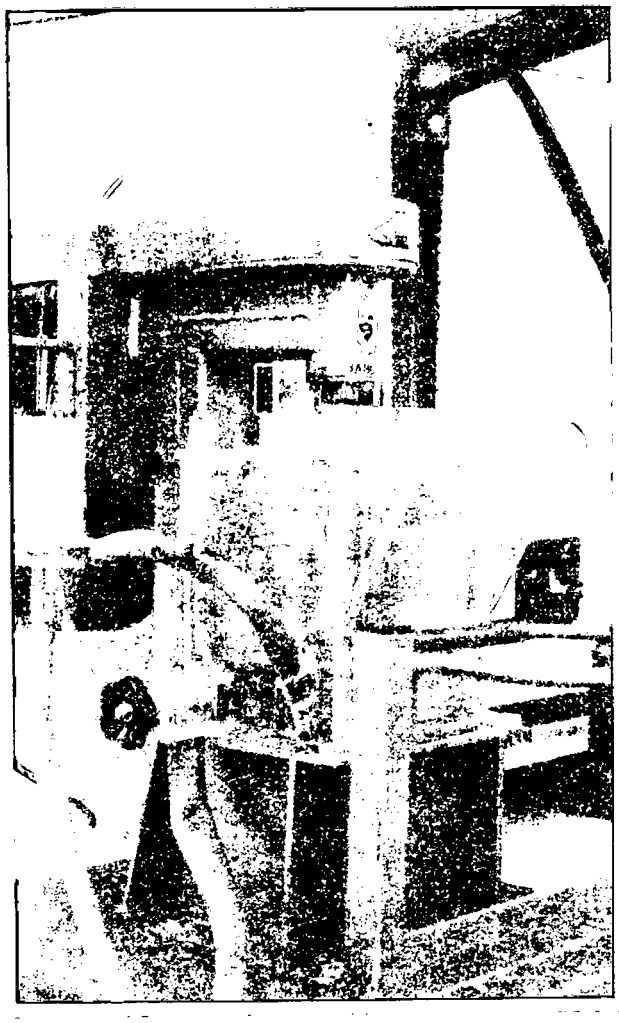

Two froth removal methods were used: scraping with a scraper every 5 seconds or using a porous ceramic plate. The dimensions of the scraper are shown in Figure 3.3. The horizontal projections rest on the side walls ensuring that scraping is always at a constant level. The porous ceramic plate placed on top of the cell forces the rising froth to flow over the lip of the cell. A constant flow of water through the plate prevents the adhesion of froth.

The impeller speed was 1300 rpm and the aeration rate was 5l/min.

Figure 3.3 Full Width Scraper to Ensure Consistent Froth Removal

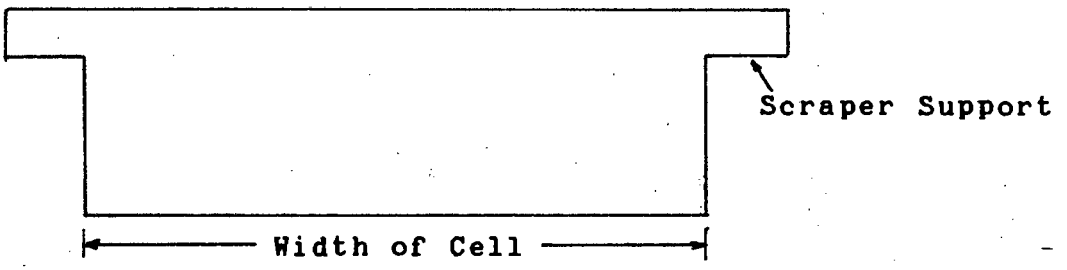

3.1.1.2 Reagents

The collector used was sodium ethyl xanthate at an addition rate of 60g/t. The xanthate was added to the pulp as 12g/l solution which was prepared daily to avoid the problem of xanthate decomposition.

The frother used was Dowfroth 400 at an addition rate of 26,05g/t. It was added as 10% (v/v) solution using a micropipette.

Sodium isobutyl xanthate and Dowfroth 250 were also used in initial reproducibility runs at different addition rates.

The collectors were purified by dissolving the xanthates in acetone, filtering the solution to remove impurities, precipitating the xanthate from the ice-cooled acetone solution with benzene and evaporating any residual benzene in a vacuum oven. This process was repeated twice.

3.1.1.3 Ore

Initially pyrite from Ergo was to be used. However after washing the ore in de-ionised water and then in 0,1M HCl, it was found that the ore contained fairly high levels of adsorbed calcium (23 mmol/kg ore) and magnesium (4 mmol/kg ore). The presence of these ions might have disguised any effect of ions added to the pulp during the experiments and therefore it was decided to use a synthetic pyrite-quartz mixture.

This synthetic mixture consisted of:
15g pyrite from Durban Roodepoort Deep ~~Sands~~ Gold Mine (the size was 96% less than 38 µm)
and
985g quartz from Delmas (the size was 70% less than 75 µm).

Although the pyrite was stored in sealed plastic packets and stored under nitrogen upon opening the packets, oxidation occurred over the period of a year. The pyrite was therefore leached in a solution consisting of 50%

concentrated HCl. However mass loss occurred during leaching. This was quantified by leaching and drying one sample of ore from each 100g packet. It was then assumed that the mass of ore obtained from leaching for each run was identical to the mass of this leached and dried sample. The sulphur content was assumed to be unchanged.

3.1.1.4 Water

De-ionized water with a conductivity of approximately 3µS was used.

3.1.1.5 Inorganic Salts

The following salts were added to the floats: $NaNO_3$, $Ca(NO_3)_2 \cdot 4H_2O$, $Mg(NO_3)_2 \cdot 6H_2O$, NaCl, $NaHCO_3$ and Na_2SO_4.

The addition rates were 0, 25, 50, 75 and 100 meq/l of each salt.

The pH regulator for $NaNO_3$ addition was NaOH, for $Mg(NO_3)_2 \cdot 6H_2O$ addition was $Mg(OH)_2$ and for the addition of $Ca(NO_3)_2 \cdot 4H_2O$, NaCl, $NaHCO_3$ and Na_2SO_4 was $Ca(OH)_2$.

3.1.2 Experimental Procedure

3.1.2.1 Leaching

17 g of dry pyrite was leached for 1 hour in a solution consisting of 150 ml of concentrated HCl and 150 ml of de-ionized water in a beaker on a magnetic stirrer. It was then washed four times with de-ionized water until the pH of the solution containing the ore was approximately 7.

3.1.2.2 Float Procedure

i. The pulp comprising the leached ore, the quartz and the inorganic salt was added to the cell and the water level was kept constant. The pulp density was 30% solids by mass.

ii. The pH of the pulp was controlled for 30 minutes at a pH of 9 using either NaOH, $Ca(OH)_2$ or $Mg(OH)_2$ as described above.

iii. 5 ml of collector was added and a conditioning time of 5 minutes allowed.

iv. The frother conditioning time was 1 minute.

v. Air was connected and a 2,5 cm froth was formed.

vi. Concentrates were collected at time intervals of 5, 5, 10, 10, 30, 60, 180 and 300 seconds thus yielding a cumulative recovery time of 10 minutes.

vii. When using the porous plate the flowrate of water was maintained at approximately 50 cm^3/min.

3.1.2.3 Sample Preparation

The concentrates were filtered using a Buchner funnel and the tailings using a pressure filter. The samples were dried overnight at a temperature of 90 to 100°C and then crushed using a pestle and mortar and stored in plastic bottles for sulphur analysis.

3.1.3 Sulphur Analysis

The sulphur content of the pyrite samples was determined by burning the pyrite in oxygen at a high temperature in a Leco induction furnace. Combustion products obtained were SO_2 and SO_3. The SO_2 produced was then analysed using the iodate titration method. Details of this procedure are given in Appendix A.

3.1.4 Calculation of Results

Results are described in terms of grade and recovery of pyrite in the concentrates.

The grade of the total concentrate is the cumulative mass of sulphur in the concentrates divided by the cumulative mass of concentrate.

The recovery of pyrite in the concentrate is defined as the cumulative mass of sulphur in the concentrates divided by the total mass of sulphur in the feed.

The recovery of gangue can be similarly defined.

The calculations of grade and recovery using values of sulphur assays and concentrate masses are shown in Appendix B.

3.2 FROTH TESTS

Different ions were added to two and three phase systems to observe their effect on the froth height and the breakdown rate of the froth phase.

3.2.1 Apparatus

The apparatus consisted of a long graduated cylinder containing a porous disc through which air was dispersed. The cylinder was placed on a magnetic stirrer.

The apparatus is shown in Figure 3.4.

Two sizes of cylinders were used for the tests: the smaller one made of glass and the larger of perspex. The glass cylinder contained a sintered glass disc of porosity 2 (40-90μm) while the perspex cylinder contained one of porosity 3 (15-40μm).

The air flow used with the glass cylinder was 900 ml/min and with the perspex cylinder 1382 ml/min. The rate was measured with an air flow meter.

3.2.2 Experimental Procedure

Tests were done on the following systems:

3.2.2.1. Using the glass cylinder at pH 10

a. Frother, de-ionized water and various addition rates of $NaNO_3$, $Ca(NO_3)_2 \cdot 4H_2O$ or $Mg(NO_3) \cdot 6H_2O$.
b. Frother, tap water and the same ions as above.
c. Frother, de-ionized water, 9,85 g quartz and the same ions.
d. Frother, tap water, 9,85 g quartz and the same ions.

3.2.2.2. Using the perspex cylinder at pH 9

Frother, de-ionized water, 98,5 g quartz, 1,5 g pyrite and various addition rates of $NaNO_3$, $Ca(NO_3)_2 \cdot 4H_2O$ or NaCl.

The method used was as follows:

a. 26 ml water (glass cylinder) or 260 ml water (perspex cylinder) was conditioned for 5 minutes with the respective mass of leached ore and quartz, pH regulator and inorganic ions. The pH regulator was either NaOH, $Ca(OH)_2$ or $Mg(OH)_2$. The stirrer speed was 500 rpm.

b. 36,5 g/t Dowfroth 400 was conditioned for 1 minute. The stirrer speed was decreased to 200 rpm.

c. The air was connected and the froth height was measured over a period of 5 minutes.

d. The air was disconnected and the time taken for the froth to break down over a distance of one quarter of the froth height obtained at 5 minutes was recorded. This determined the breakdown rate in cms^{-1}.

FIGURE 3.4 APPARATUS USED FOR FROTH STABILITY TESTS

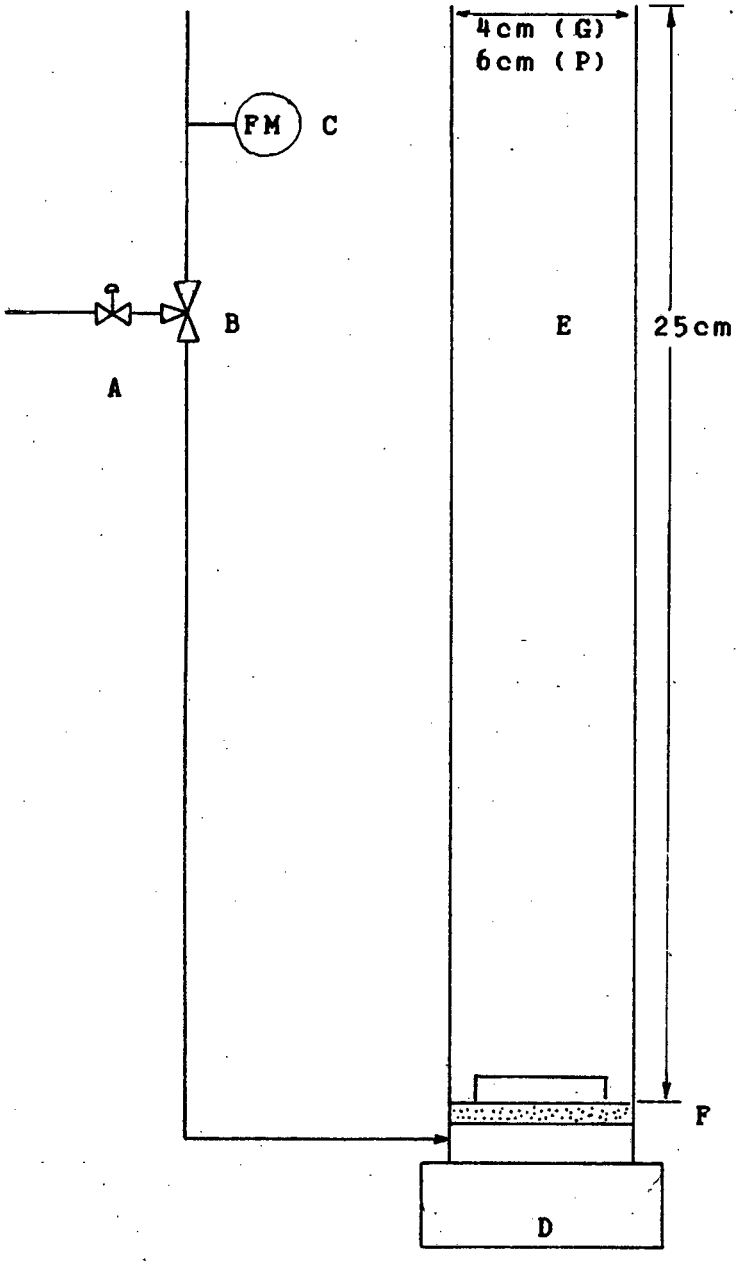

A Vernier control valve
B Three way valve
C Flow meter
D Magnetic stirrer
E Cylinder (G=Glass, P=Perspex)
F Sintered Glass Disc

3.3 ADSORPTION TESTS

The effect of different ions on the adsorption rates of xanthate on pyrite was studied by sampling at regular intervals from a continuous reacting system of sodium ethyl xanthate and pyrite and analysing the results by measuring the change in the adsorbance of the xanthate solution in a UV spectrophotometer.

3.3.1 Apparatus

The apparatus consisted of a round glass vessel (with a capacity of approximately 1 litre) covered by a 5 port glass lid. The vessel was suspended in a water bath at a controlled temperature of 25°C. A metal stirrer driven by an electric motor was inserted through a side port at a slight angle. Other ports contained the pH probe and the exit tube through which the solution was extracted from the pulp via a glass frit. This tube was connected to a peristaltic pump which delivered the solution to an automatic sampling device in which samples were collected in small plastic containers every 5 seconds. The pumping rate was 47,4 ml/min.

The glass frit was required to separate xanthate solution from the pyrite. The fineness of the ore used initially caused blockage of the glass pores in the filter. The ensuing layer of pyrite coating the filter resulted in many smaller fine bubbles being liberated into the sampling line.

To prevent this problem, two factors had to be taken into account: the porosity of the filtering medium and the shape of the filter. The best porosity to be used for ore (90% less than 38 µm) is either, using glass, a porosity of 4 (5-15 µm) or, using Millipore membranes, either 8 or 0,8 µm. The best shape was found to be a large flat disc with the maximum area possible. The glass disc and membrane worked equally well but it was decided to use the 0,8 µm disposable membranes instead as these could be discarded at the end of each run thus reducing the possibility of sample contamination from run to run.

The samples were analysed in a UV spectrophotometer at a wavelength of 300 nm.

The apparatus is shown in Figure 3.5.

3.3.2 Experimental Procedure

1. The pyrite was leached, filtered and washed.
2. 5g of moist pyrite (4 ±0,1 g dry ore) (moisture content 20 ± 1 %) was added to 300ml of de-ionized water and the appropiate inorganic salt and dispersed for 3 minutes in an ultrasonic bath.
3. The solution was placed in the glass vessel and a further 700ml of de-ionized water added.
4. The sample tubing was washed out with de-ionised water.
5. The solution was stirred for half an hour at 733 rpm. $Ca(OH)_2$ was added to maintain a pH of 9.
6. 5ml of 4 g/l solution of sodium ethyl xanthate was added (equivalent to approximately 500g/ton of pyrite which is equivalent to 75 g/ton ore).
7. 50 samples were taken over 5 second intervals and a further sample 9 minutes after the starting time.
8. The adsorbance of each aliquot was measured in the UV spectrophotometer at a wave length of 300nm. The zero was set using de-ionized water.
9. As the xanthate is absorbed very rapidly the maximum reading at t=0 is not obtained experimentally. To obtain this result 1 litre xanthate solution was made up and the adsorbance tested. The nitrate ion also shows a small peak at 300nm. Therefore to obtain the maximum reading for the nitrate systems the appropriate concentration of nitrate was added to 200 ml of the xanthate solution and the adsorbance measured.

Figure 3.5 EQUIPMENT USED IN ADSORPTION STUDIES

KEY

A: Timer
B: Automatic Sampler
C: Peristaltic Pump
D: Glass Frit
E: Metal Stirrer
F: pH Probe
G: Glass Reactor
H: Water Bath
I: Temperature Controller
J: pH Meter

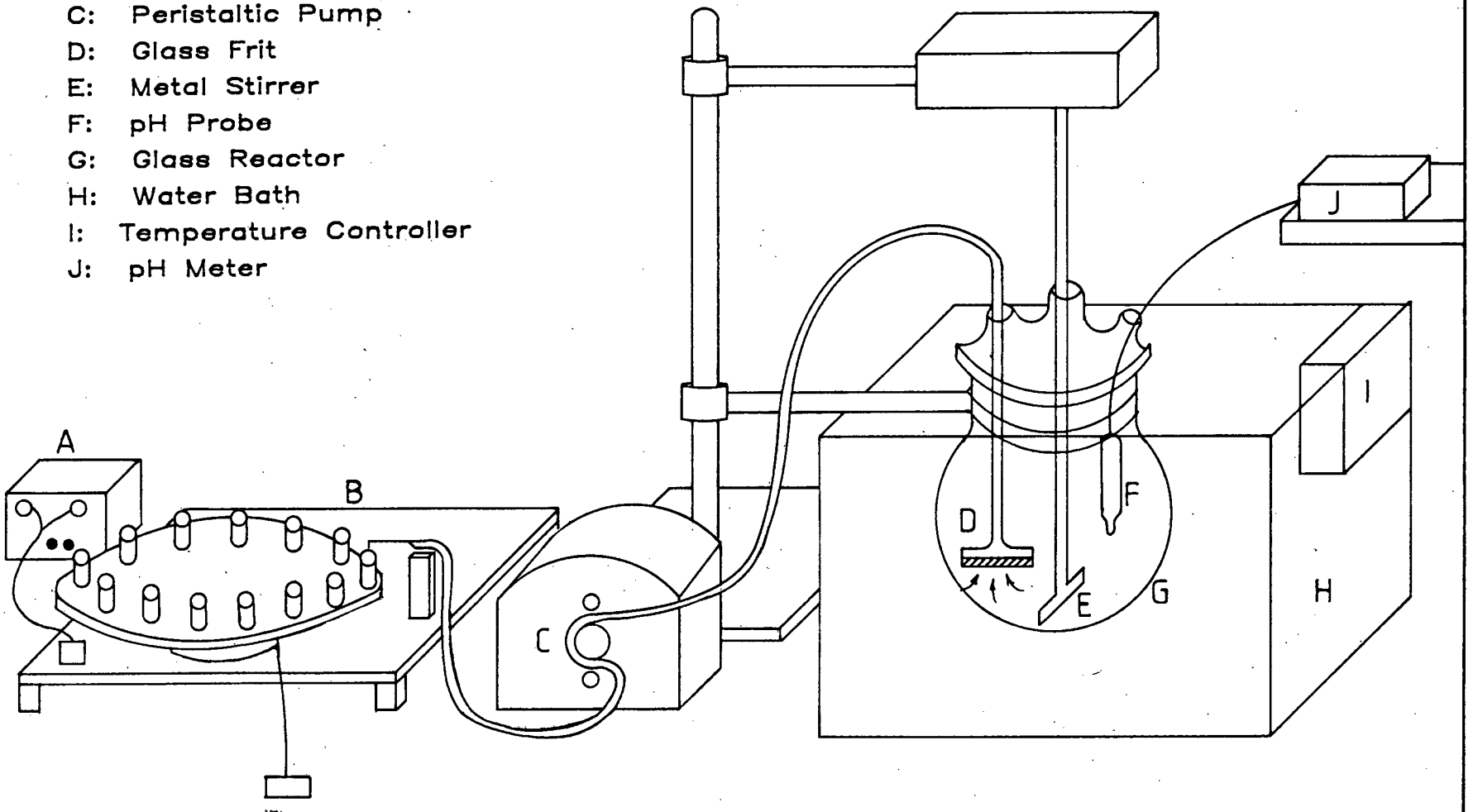

4. RESULTS

4.1 FLOTATION

4.1.1 Reproducibility

The reproducibility of the modified Leeds cell using the scraping technique to remove the froth was tested using 60g/t of two collectors, sodium isobutyl xanthate SIBX and sodium normal butyl xanthate SNBX and ore obtained from Ergo. The frother addition rate was 24,3 g/t DF250 and the pH regulator used was NaOH maintaining a pH of 8.

The recovery-time graphs for both systems are shown in Figures 4.1 and 4.2 with standard deviations for each concentrate listed in Table 4.1. Recovery-time data were analysed using the Klimpel model described in Appendix C. The rate constant k and the ultimate equilibrium recovery R obtained from this model are also listed in Table 4.1.

Table 4.1 Reproducibility of the Modified Leeds Cell

TIME	SIBX		SNBX	
	Mean Recovery	Standard Deviation	Mean Recovery	Standard Deviation
15	43,20	1,135	32,39	5,296
30	54,82	0,701	45,33	4,337
60	62,60	0,560	59,49	0,982
120	67,36	0,503	65,32	0,115
240	69,83	0,411	68,13	0,229
420	70,95	0,479	69,25	0,234
k	0,146	0,0074	0,092	0,0232
R	71,51	0,552	71,82	1,356

These results show good reproducibility particularly when using SIBX.

FIGURE 4.1 : RECOVERY vs TIME

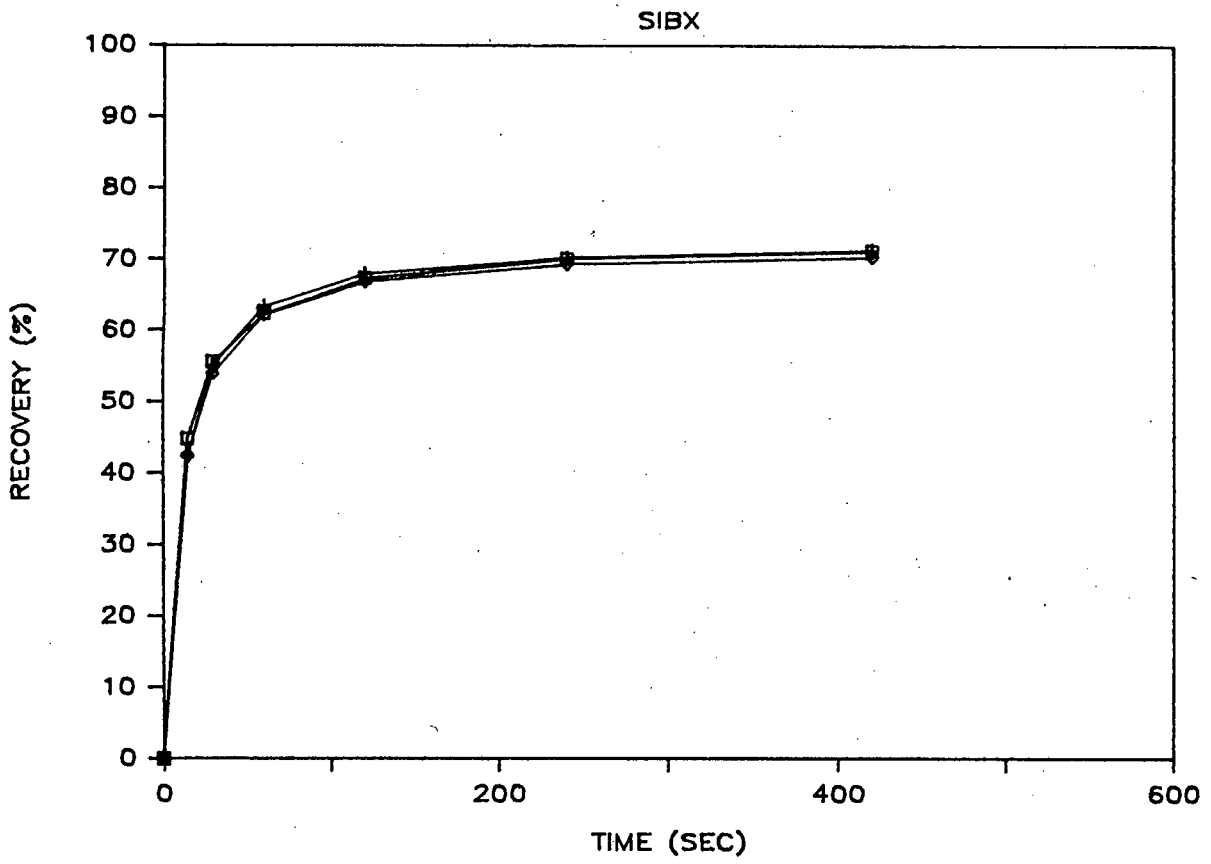

FIGURE 4.2: RECOVERY vs TIME

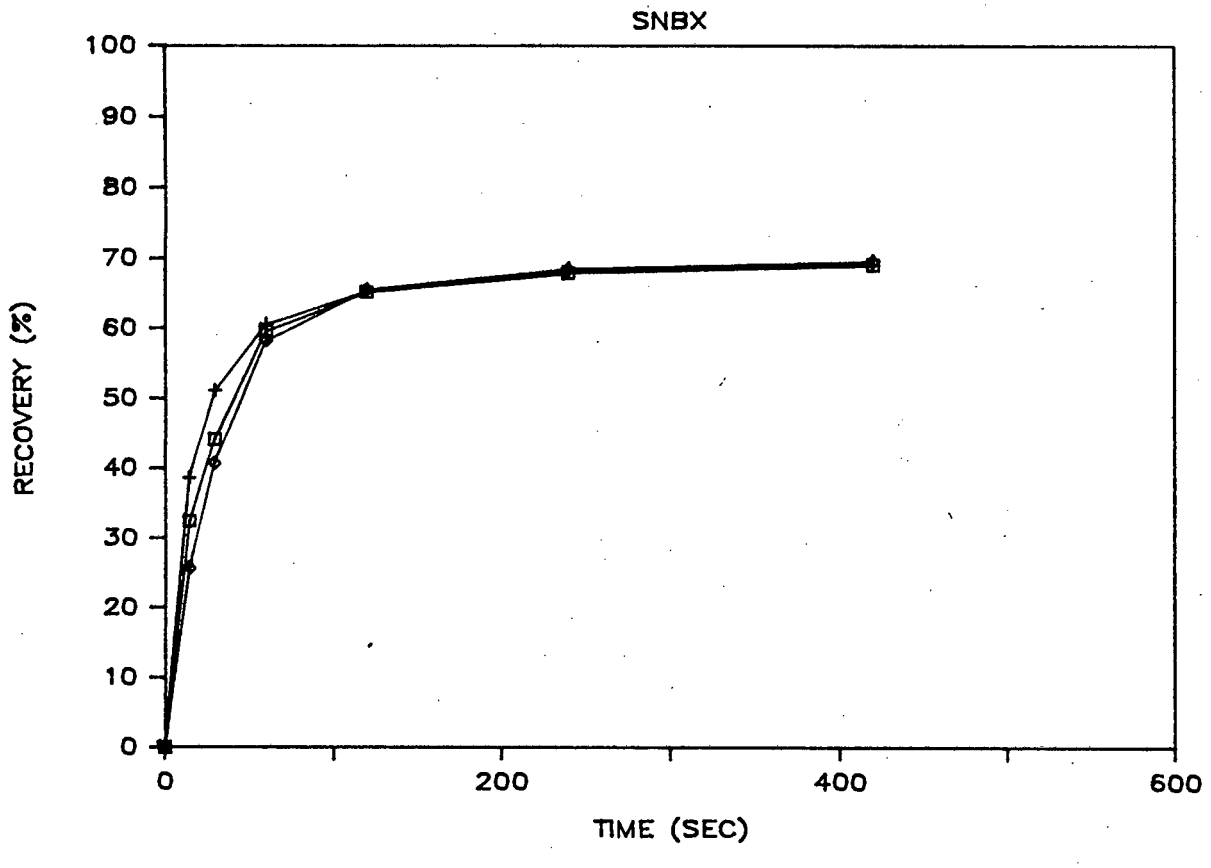

4.1.2 Effect of Leaching the Ore

Figures 4.3 and 4.4 show the recovery-time and grade-recovery graphs for the synthetic unleached pyrite-quartz system using a paddle to scrape the froth. Standard deviations are listed in Table 4.2 with values of k and R.

Table 4.2 Standard Deviation of the Pyrite-Quartz System

TIME	MEAN RECOVERY	STANDARD DEVIATION
5	22,55	1,395
10	32,55	1,522
20	44,92	2,272
30	51,80	2,251
60	59,92	2,435
120	64,17	2,499
300	66,69	2,565
600	67,12	2,611
k	0,135	0,0036
R	68,43	2,578

FIGURE 4.3: RECOVERY vs TIME

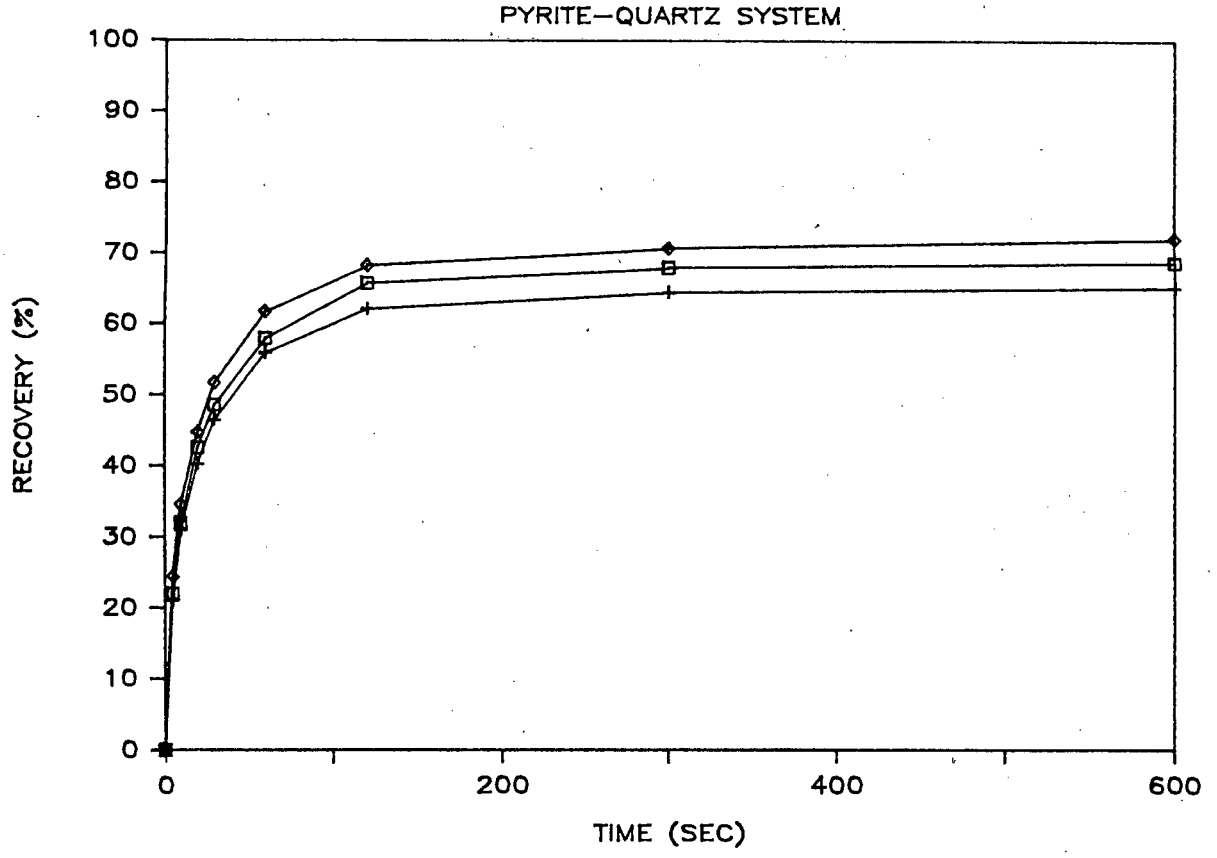

FIGURE 4.4: GRADE vs RECOVERY

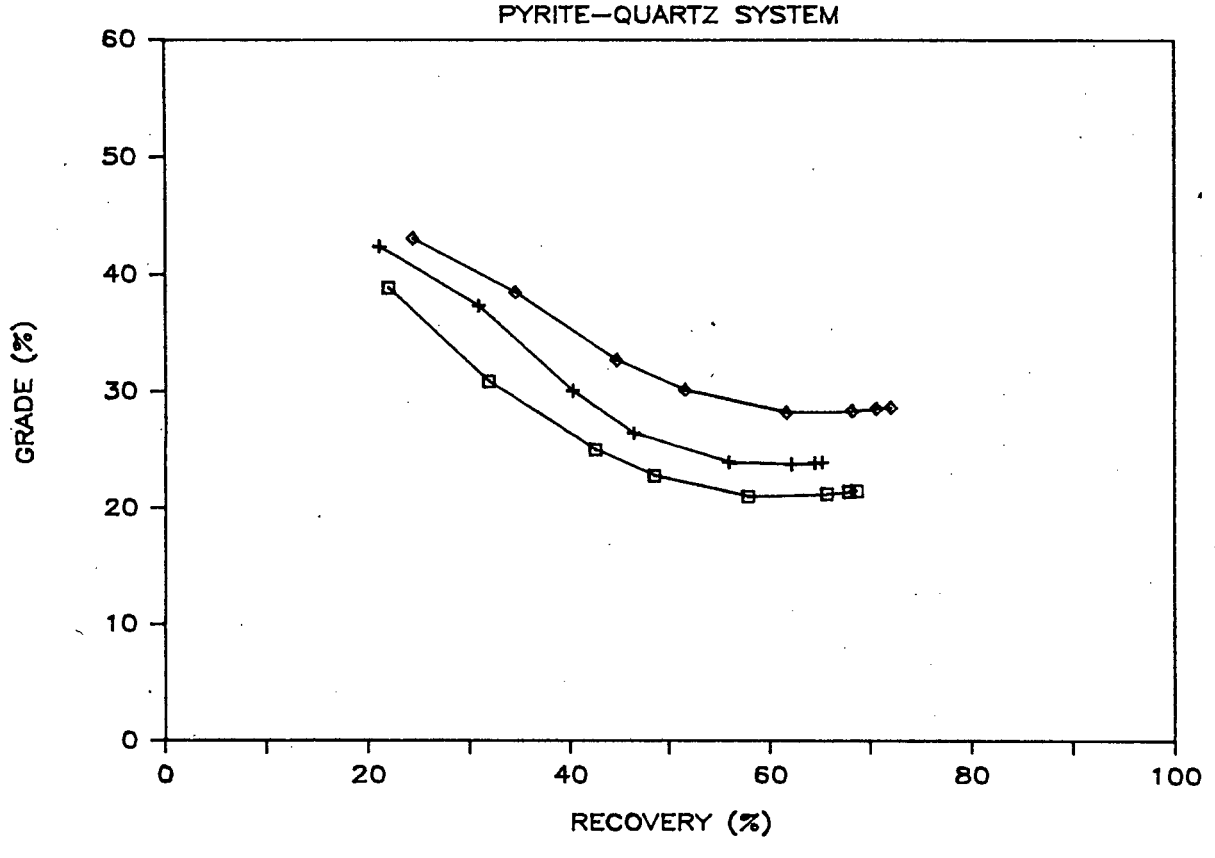

The froth initially formed was stable but after two minutes a layer of small pyrite-rich bubbles formed. This layer prevented the movement of bubbles from the lower layers of the froth to the upper surface of the froth phase. The thickness of the froth layer decreased after two minutes. As a result of this reduction in thickness of the froth layer, froth could not be removed.

An analysis based on the mass balance of the froth obtained in the sixth concentrate is shown below in Table 4.3. It is compared to runs using Ergo ore and SIBX and runs done by A. Dimou (Dimou 1986) using the same quartz-pyrite mixture but using tap water instead of de-ionised water.

Table 4.3 Analysis of Froth

SYSTEM	AVERAGE WATER %	AVERAGE PYRITE %	GANGUE %
Pyrite-quartz & de-ionised water	82,9	4,8	12,3
Pyrite-quartz & tap water *	92,2	1,5	6,3
Ergo	92,4	1,0	6,6

* (Dimou A. 1986)

The reproducibility of the pyrite-quartz system is poor and therefore various aspects of the flotation system were investigated.

The pyrite was leached with HCl to remove any oxidation products. The results of two runs, each using either NaOH and 25 meq/l $NaNO_3$ or $Ca(OH)_2$ and 50 meq/l $Ca(NO_3)_2 \cdot 4H_2O$ are shown in Table 4.4. 60g/t SEX was added. The runs using NaOH and 25 meq/l $NaNO_3$ are shown in Figure 4.5 and 4.6.

FIGURE 4.5 RECOVERY vs TIME

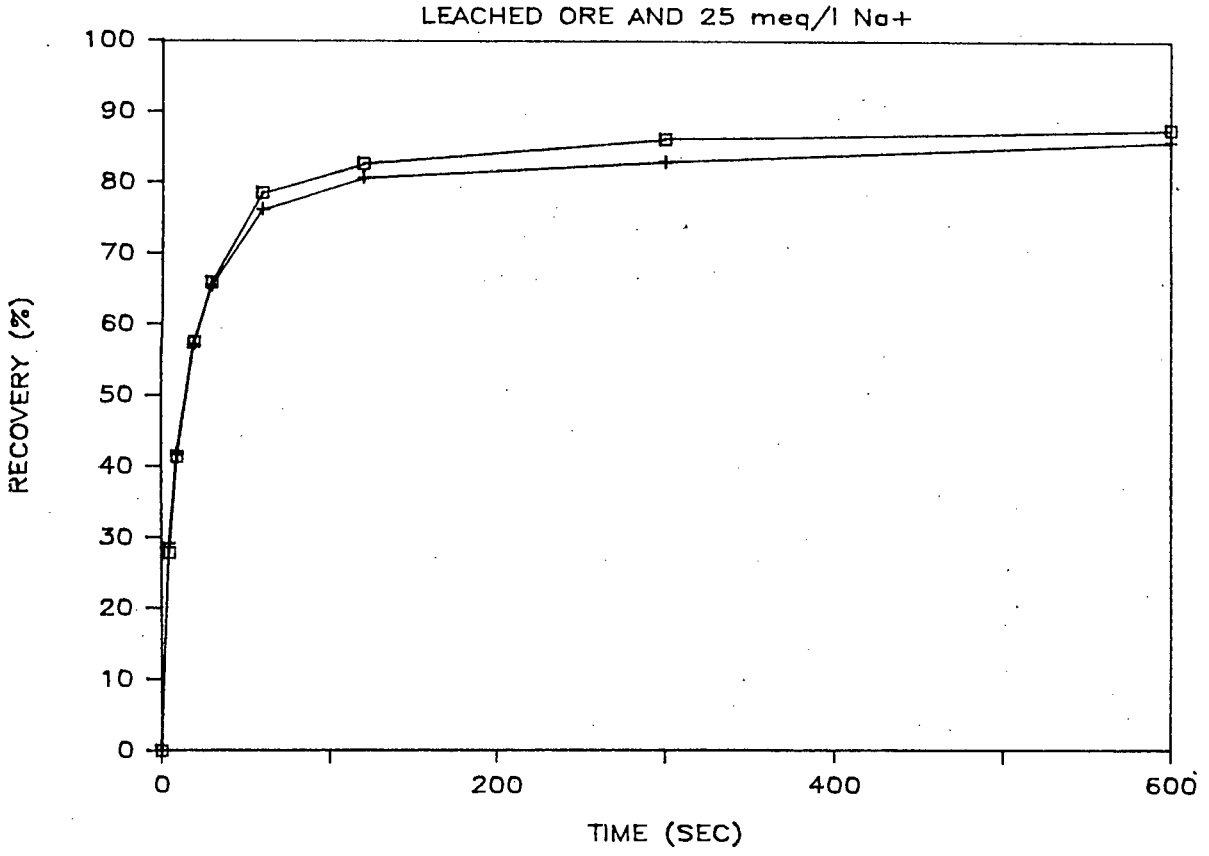

FIGURE 4.6 GRADE vs RECOVERY

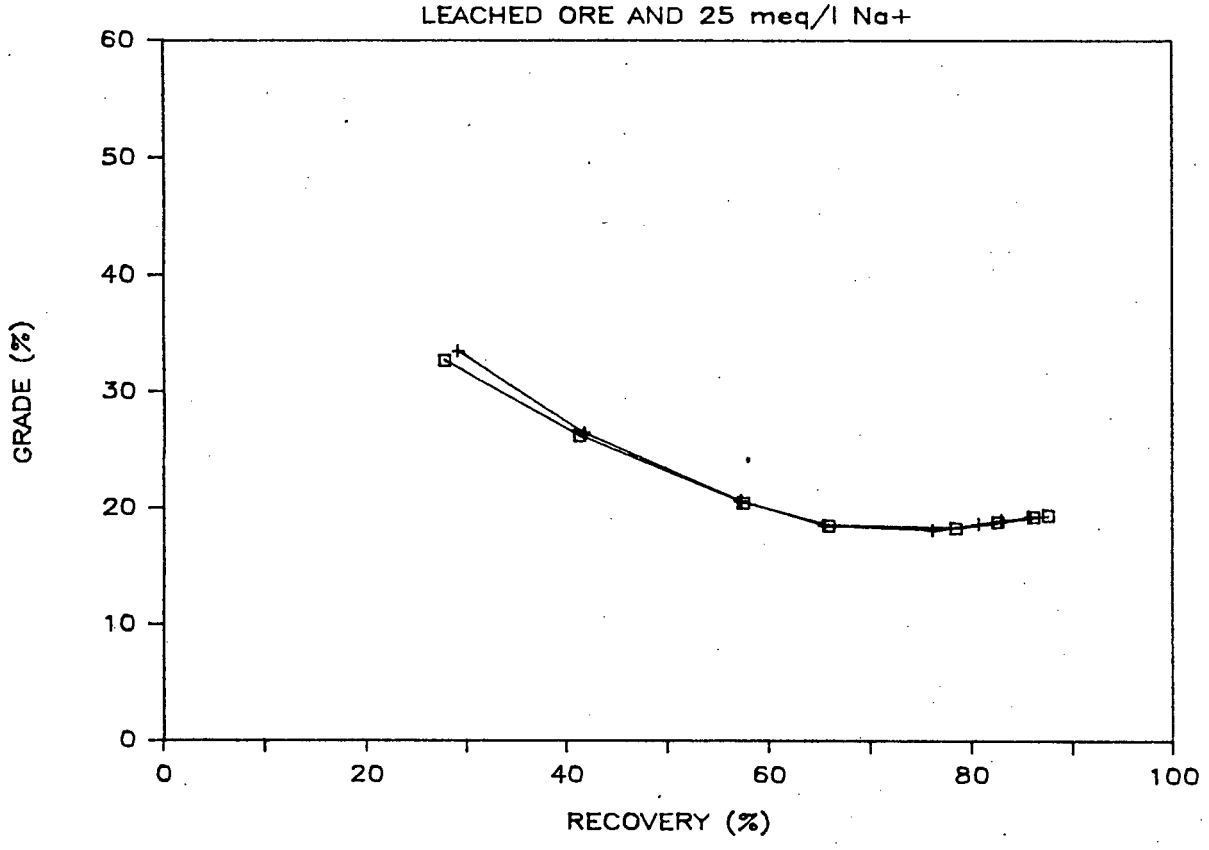

Table 4.4 Effect of Leaching

TIME	$NaOH + NaNO_3$		$Ca(OH)_2 + Ca(NO_3)\cdot 4H_2O$	
sec	mean	σ_{n-1}	mean	σ_{n-1}
5	28,55	0,665	6,24	2,565
10	41,60	0,200	12,61	2,760
20	57,40	0,130	22,59	3,465
30	65,70	0,210	31,49	4,310
60	77,33	1,170	52,51	4,700
120	81,67	0,990	77,20	0,835
300	84,58	1,580	91,05	0,650
600	86,71	0,900	95,66	0,900
k	0,149	0,0062	0,028	0,0051
R	86,55	1,402	103,73	3,04

From Table 4.4 it can be seen that leaching the pyrite provides a considerable increase in recovery (80 to 90%) as opposed to previous runs (60 to 70%). The standard deviation also decreases to values between 1,6 to 2,9% of the total recovery.

4.1.3 Effect of scraping methods

Two scraping methods were used: scraping with a paddle and using a ceramic porous plate. A comparison of R and k values and recoveries for the two methods are shown in Table 4.5.

Table 4.5 Comparison of Different Scraping Methods

CELL	LEEDS		MODIFIED LEEDS	
pH	8		10	
pH Regulator	NaOH		NaOH	
Collector	60g/t SIBX		60g/t SEX	
Frother	36,5g/t DF400		36,5G/T DF400	
Scraping Method	Paddle	Plate	Paddle	Plate
k mean	0,135	0,068	0,169	0,158
σ_{n-1}	0,0036	0,0035	0,0090	0,0081
R mean	68,43	71,21	60,42	63,49
σ_{n-1}	2,578	2,677	1,200	1,833
Time (sec)	Recovery			
5 mean	22,55	11,62	22,08	20,82
σ_{n-1}	1,395	0,033	1,461	1,339
10 mean	32,55	21,04	31,90	33,00
σ_{n-1}	1,522	0,452	1,434	1,633
20 mean	44,92	33,15	41,58	43,83
σ_{n-1}	2,272	0,472	1,662	2,212
30 mean	51,80	40,39	47,05	49,37
σ_{n-1}	2,251	0,711	1,432	1,998
60 mean	59,92	52,06	56,20	56,41
σ_{n-1}	2,435	1,437	1,352	1,834
120 mean	64,17	60,39	58,66	58,92
σ_{n-1}	2,499	2,223	1,232	1,820
300 mean	66,69	67,80	58,96	61,43
σ_{n-1}	2,565	2,569	1,336	2,206
600 mean	67,12	71,90	59,27	65,46
σ_{n-1}	2,611	2,111	1,401	1,963

It can be seen that the reproducibility does not improve when using the ceramic plate. However the equilibrium recovery does increase by approximately 3%. This is caused by the increase of 300 to 400% in the mass of the last two concentrates (at 300 and 600 seconds). This is possibly due to the water which flows through the ceramic plate

overcoming the effects of "dry froth" phenomena referred to in Section 4.1.2.

4.1.4 Effect of pH regulators

A comparison of R and k values and recoveries obtained when using sodium hydroxide, calcium hydroxide and magnesium hydroxide at a pH of 8 is shown in Table 4.6. 60g/t SIBX and 36,5 g/t DF400 were added. The ceramic plate was used for froth removal.

Table 4.6 Comparison of pH Regulators

pH REGULATOR	NaOH		$Ca(OH)_2$		$Mg(OH)_2$	
Concentration meq/l	7,7		8,4		9,3	
Time seconds	Recovery		Recovery		Recovery	
	Mean	σ_{n-1}	Mean	σ_{n-1}	Mean	σ_{n-1}
5	11,62	3,12	11,43	0,11	9,61	1,23
10	20,24	3,94	19,90	0,32	20,91	2,17
20	33,27	5,56	32,26	1,21	35,72	0,68
30	40,87	5,51	38,98	2,18	43,90	0,03
60	53,28	5,79	50,80	3,06	57,99	1,28
120	62,98	3,57	59,64	3,17	69,18	3,12
300	71,20	3,14	67,91	3,56	77,23	3,39
600	75,70	2,84	70,45	3,58	80,65	2,82
k	0,063	0,0145	0,061	0,0033	0,055	0,0050
R	75,53	2,457	70,78	3,375	81,68	4,160

The reproducibility as determined by the standard deviation of the final recovery did not improve with the use of $Ca(OH)_2$ or $Mg(OH)_2$.

4.1.5 Effect of Varying pH

A comparison of R and k values and recoveries using two pH values, 8 and 10 is shown in Table 4.7. The ceramic plate was used and 36,5g/t DF400 added.

Table 4.7 Effect of pH

pH	8		10	
Collector	60g/t SIBX		71g/t SIBX	
Time	Recovery			
	Mean	σ_{n-1}	Mean	σ_{n-1}
5	11,62	0,033	18,29	2,386
10	21,04	0,452	28,85	2,232
20	33,15	0,472	40,49	2,909
30	40,39	0,711	46,05	3,907
60	52,06	1,437	53,62	3,549
120	60,39	2,223	56,75	3,878
300	67,80	2,569	60,18	2,983
600	71,90	2,111	64,22	2,688
k	0,068	0,0035	0,134	0,0074
R	71,21	2,677	62,15	3,037

An increase in pH produced a decrease in recovery as well as reproducibility.

4.1.6 Effect of Collector

The effect of equimolar addition of sodium ethyl xanthate (SEX) and sodium isobutyl xanthate (SIBX) was investigated. NaOH was added to maintain a pH of 10. 36,5g/t DF400 was also added. The values of R and k and recoveries obtained are shown in Table 4.8. The ceramic plate was used.

Table 4.8 Comparison of Collectors

COLLECTOR	30g/t SIBX		71g/t SIBX		60 g/t SEX	
Time	Recovery					
	Mean	σ_{n-1}	Mean	σ_{n-1}	Mean	σ_{n-1}
5	22,48	1,575	18,29	2,386	20,82	1,339
10	32,31	2,029	28,85	2,232	33,00	1,633
20	42,75	3,018	40,49	2,909	43,83	2,212
30	47,58	3,463	46,05	3,907	49,37	1,998
60	53,55	3,757	53,62	3,549	56,41	1,834
120	55,58	3,973	56,75	3,878	58,92	1,820
300	58,30	3,686	60,18	2,983	61,43	2,206
600	61,00	3,686	64,22	2,688	65,46	1,963
k	0,186	0,0112	0,134	0,0074	0,158	0,0081
R	59,30	3,745	62,15	3,037	63,49	1,833

The reproducibility decreased slightly with a lower addition of SIBX but increased quite considerably when using SEX with the standard deviation of the ultimate equilibrium recovery decreasing from 5% to 2,9% of the total recovery. From Table 4.5 (SEX data) it can also be seen that the use of the paddle decreases this standard deviation to 2% of the total equilibrium recovery.

4.1.7 Effect of Purity of the Water

The water used in previous experiments was purified using the ion exchange method. The conductivity was 3µS. However organics could be present in this water. To test whether these organics affect the system, water purified by a reverse osmosis membrane was used. The conductivity of the water for the 2 runs was 2,4 and 4,2 µS respectively. The values for k and R were:

$k = 0,214 \pm 0,0254$

$R = 63,86 \pm 1,460$

The reproducibility in the absence of organics improved slightly.

4.1.8 Effect of ions on leached ore

The effect of five addition rates from 0 to 100 meq/l of 6 inorganic salts was investigated. The salts were magnesium nitrate, calcium nitrate, sodium nitrate, sodium chloride, sodium sulphate and sodium hydrogen carbonate.

The recovery-time, recovery-grade, gangue recovery-time and gangue recovery-water recovery graphs for each salt are shown in Figures 4.7 to 4.30.

The recovery-time curves were fitted using the Klimpel model. However at high addition rates of calcium nitrate and magnesium nitrate this model did not fit the experimental curves well. As a result of this, the rate constant k used by Klimpel is approximated by R_{30} which is the recovery after 30 seconds and the ultimate equilibrium recovery R by R_{600}, the recovery after 600 seconds. The variation of R_{600}, R_{30}, R_{6600} (the gangue recovery at 600 seconds) and $G_{70\%}$ (the grade at 70% recovery) with the concentration of ions added is shown in Figures 4.31 to 4.34 and in Table 4.9.

Table 4.9 Variation of R_{600}, R_{30}, R_{6600} and G_{70x} with concentration using leached pyrite

CONCENTRATION meq/l	meq/l	ppm	R_{600}	R_{30}	R_{6600}	G_{70x}
$Mg(OH)_2$	Magnesium Nitrate					
1,7	0	0	73,24	55,94	2,198	15,92
2,7	25	300	89,53	37,13	0,286	44,84
4,1	50	600	92,30	27,09	0,291	45,77
3,9	75	900	97,24	11,90	0,244	47,40
4,2	100	1200	92,32	4,80	0,209	47,84
$Ca(OH)_2$	Calcium nitrate					
0,7	0	0	85,28	66,27	1,945	19,86
1,2	25	500	100,16	59,66	0,396	43,68
0,9	50	1000	94,76	35,80	0,349	45,00
1,1	75	1500	93,13	33,90	0,262	46.75
1,3	100	2000	93,74	18,05	0,319	45,22
NaOH	Sodium nitrate					
1,8	0	0	79,91	59,53	1,580	20,83
0,5	25	575	87,61	65,91	2,091	18,44
0,6	50	1150	94,79	67,31	1,839	20,21
0,8	75	1725	90,33	68,25	2,306	17,97
0,7	100	2300	95,92	69,20	1,433	24,37
$Ca(OH)_2$	Sodium chloride					
0,7	0	0	85,28	66,27	1,945	19,86
1,2	25	888	81,08	66,25	2,589	15,16
0,9	50	1775	83,02	64,48	2,040	18,09
0,9	75	2663	92,83	71,68	1,646	21,60
0,9	100	3550	95,80	68,86	1,101	27,36
$Ca(OH)_2$	Na_2SO_4					
0,7	0	0	85,28	66,27	1,945	19,86
0,9	25	1200	79,22	63,53	2,620	15,41
0,8	50	2400	85,87	65,06	1,712	21,20
0,7	75	3600	88,45	65,27	1,214	26,24
0,9	100	4800	93,22	68,24	1,112	28,28
$Ca(OH)_2$	$NaHCO_3$					
0,7	0	0	85,28	66,27	1,945	19,86
7,4	25	1525	84,51	66,37	1,516	23,13
13,8	50	3050	86,09	63,42	1,431	22,98
19,7	75	4575	88,81	66,79	1,284	25,02
26,1	100	6100	90,45	67,30	1,220	26,77

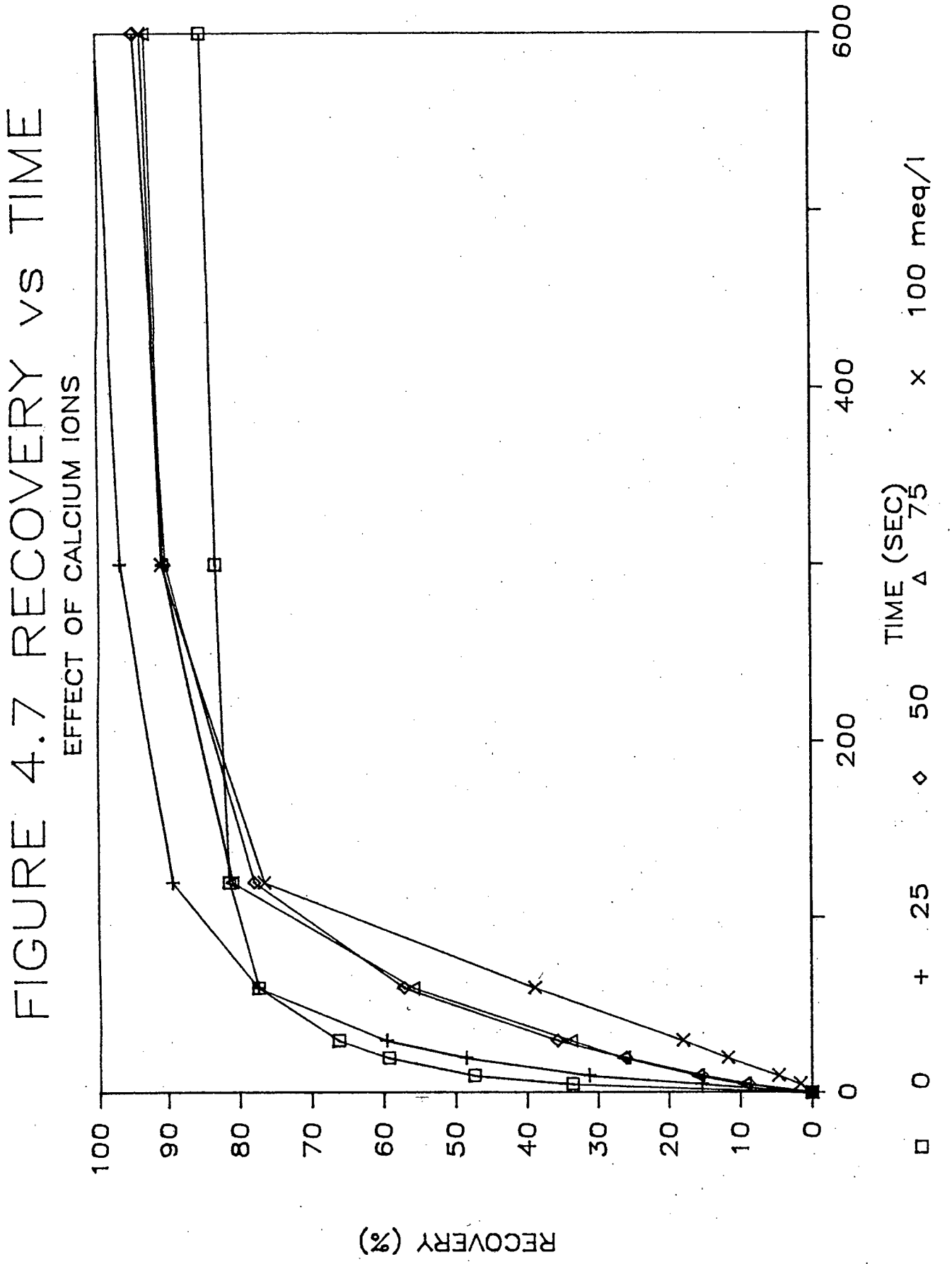
FIGURE 4.7 RECOVERY vs TIME
EFFECT OF CALCIUM IONS
RECOVERY (%)
TIME (SEC)
0
10
20
30
40
50
60
70
80
90
100
200
400
600
□ 0
+ 25
◇ 50
△ 75
× 100 meq/l

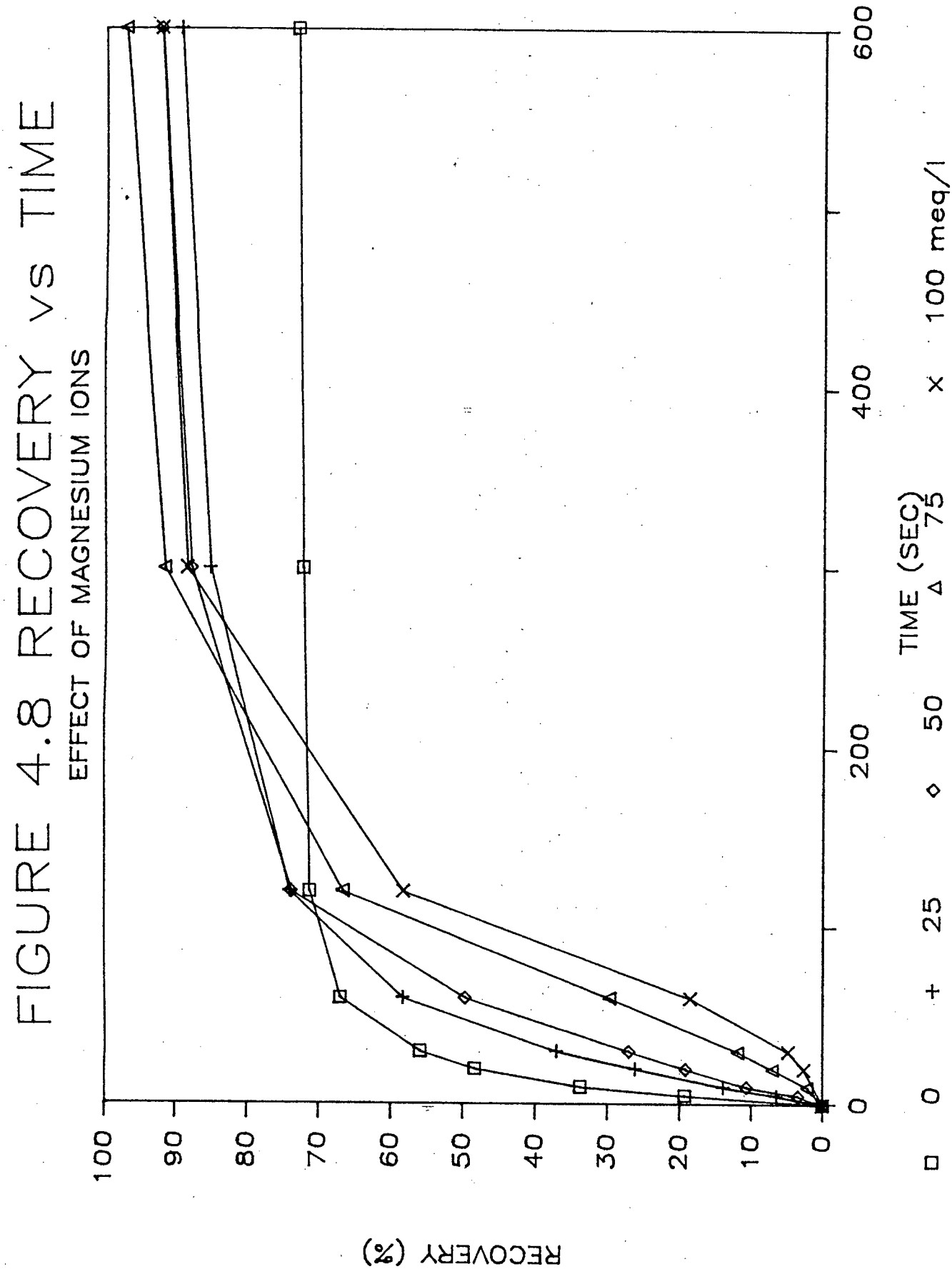
FIGURE 4.8 RECOVERY vs TIME
EFFECT OF MAGNESIUM IONS
RECOVERY (%)
100
90
80
70
60
50
40
30
20
10
0
0
200
400
600
TIME (SEC)
□ 0
+ 25
◇ 50
△ 75
× 100 meq/l

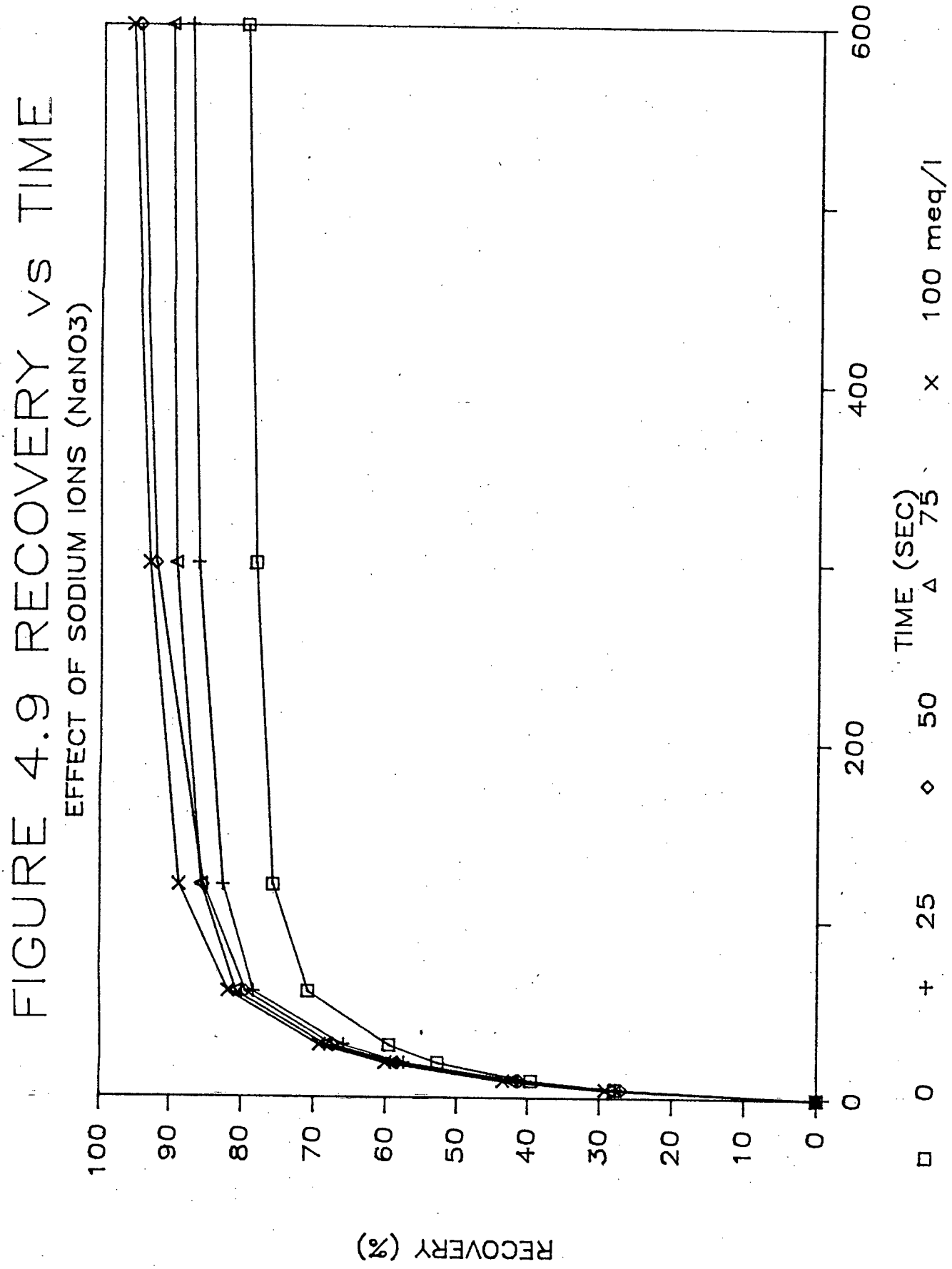
FIGURE 4.9 RECOVERY vs TIME
EFFECT OF SODIUM IONS (NaNO3)
RECOVERY (%)
100
90
80
70
60
50
40
30
20
10
0
0
200
400
600
TIME (SEC)
□ 0
+ 25
◇ 50
△ 75
× 100 meq/l

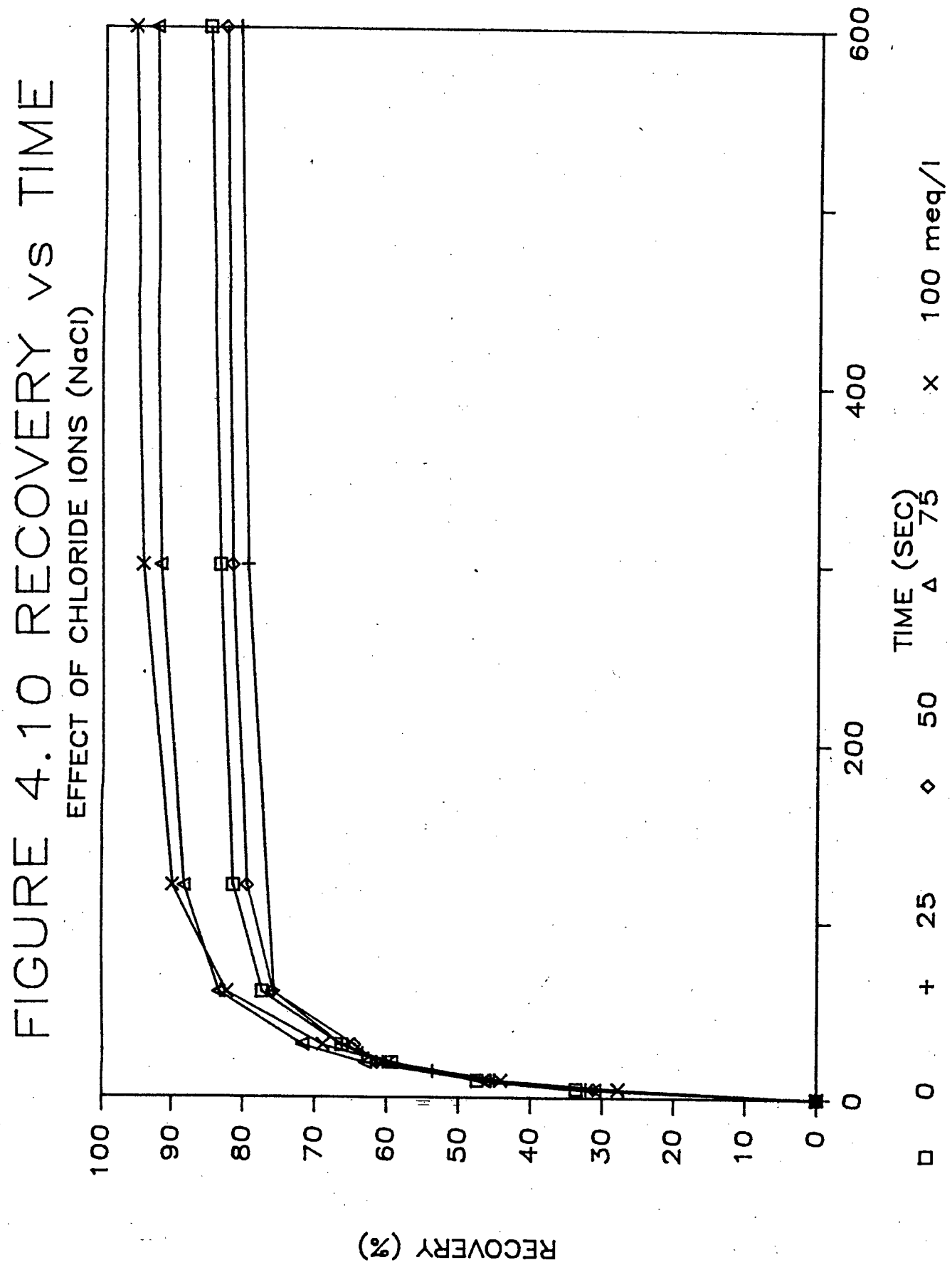
FIGURE 4.10 RECOVERY vs TIME
EFFECT OF CHLORIDE IONS (NaCl)
RECOVERY (%)
100
90
80
70
60
50
40
30
20
10
0
0
200
400
600
TIME (SEC)
□ 0
+ 25
◇ 50
△ 75
× 100 meq/l

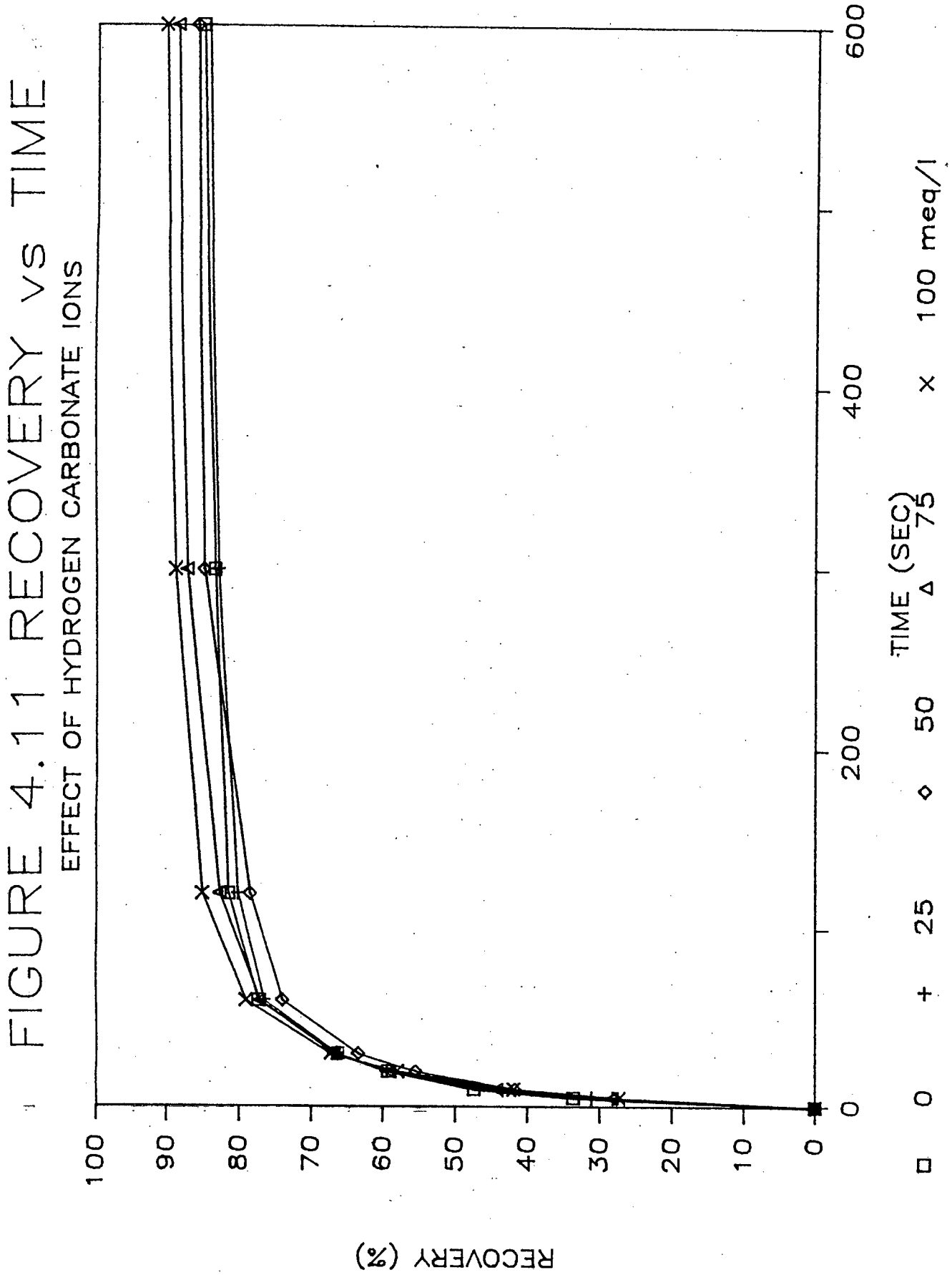
FIGURE 4.11 RECOVERY vs TIME
EFFECT OF HYDROGEN CARBONATE IONS
RECOVERY (%)
100
90
80
70
60
50
40
30
20
10
0
TIME (SEC)
0
200
400
600
□ 0
+ 25
◇ 50
△ 75
× 100 meq/l

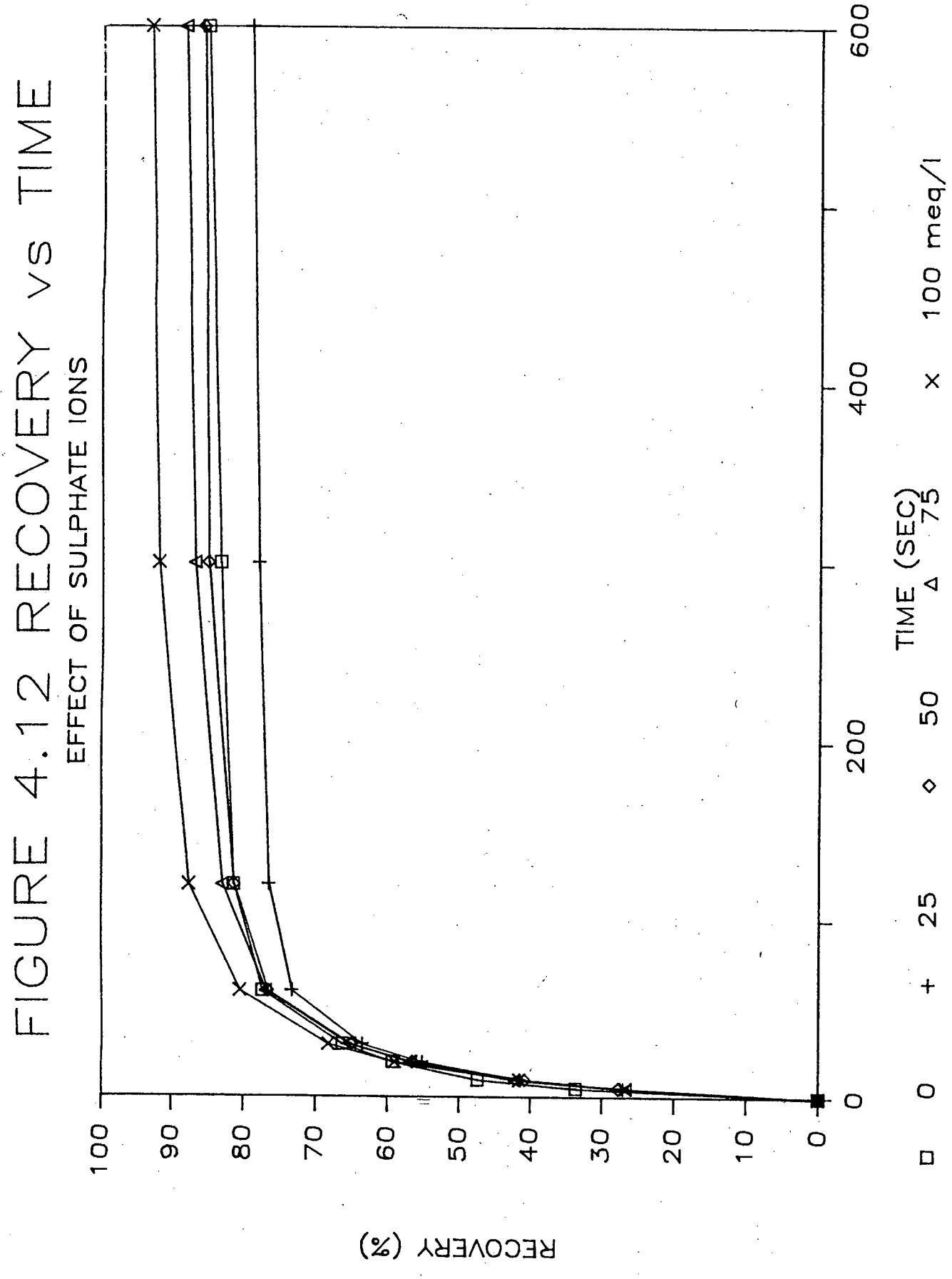
FIGURE 4.12 RECOVERY vs TIME
EFFECT OF SULPHATE IONS
RECOVERY (%)
100
90
80
70
60
50
40
30
20
10
0
0
200
400
600
TIME (SEC)
□ 0
+ 25
◇ 50
△ 75
× 100 meq/l

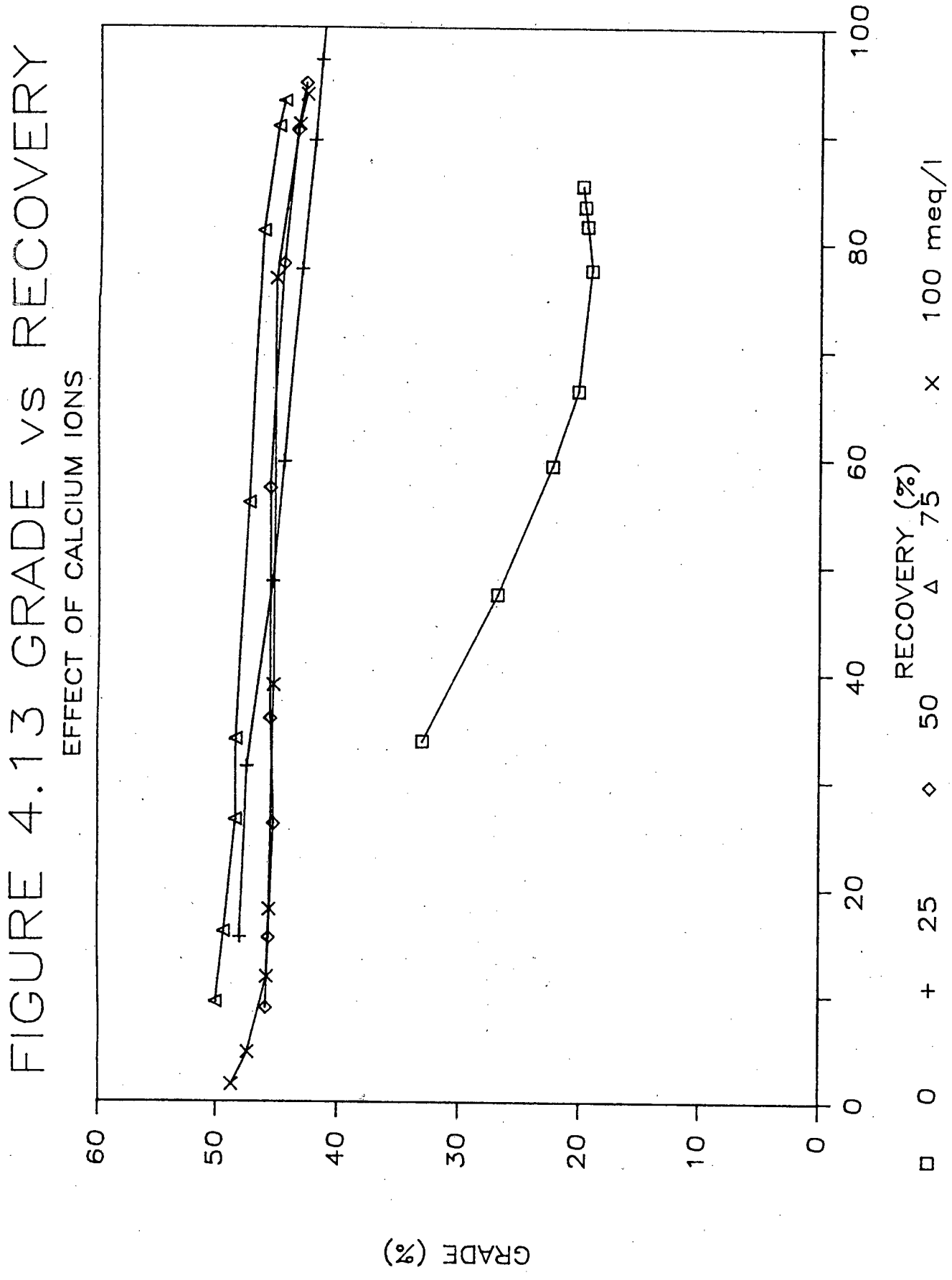
FIGURE 4.13 GRADE vs RECOVERY
EFFECT OF CALCIUM IONS
GRADE (%)
RECOVERY (%)
0
10
20
30
40
50
60
0
20
40
60
80
100
□ 0
+ 25
◇ 50
△ 75
× 100 meq/l

FIGURE 4.14 GRADE vs RECOVERY

EFFECT OF MAGNESIUM IONS

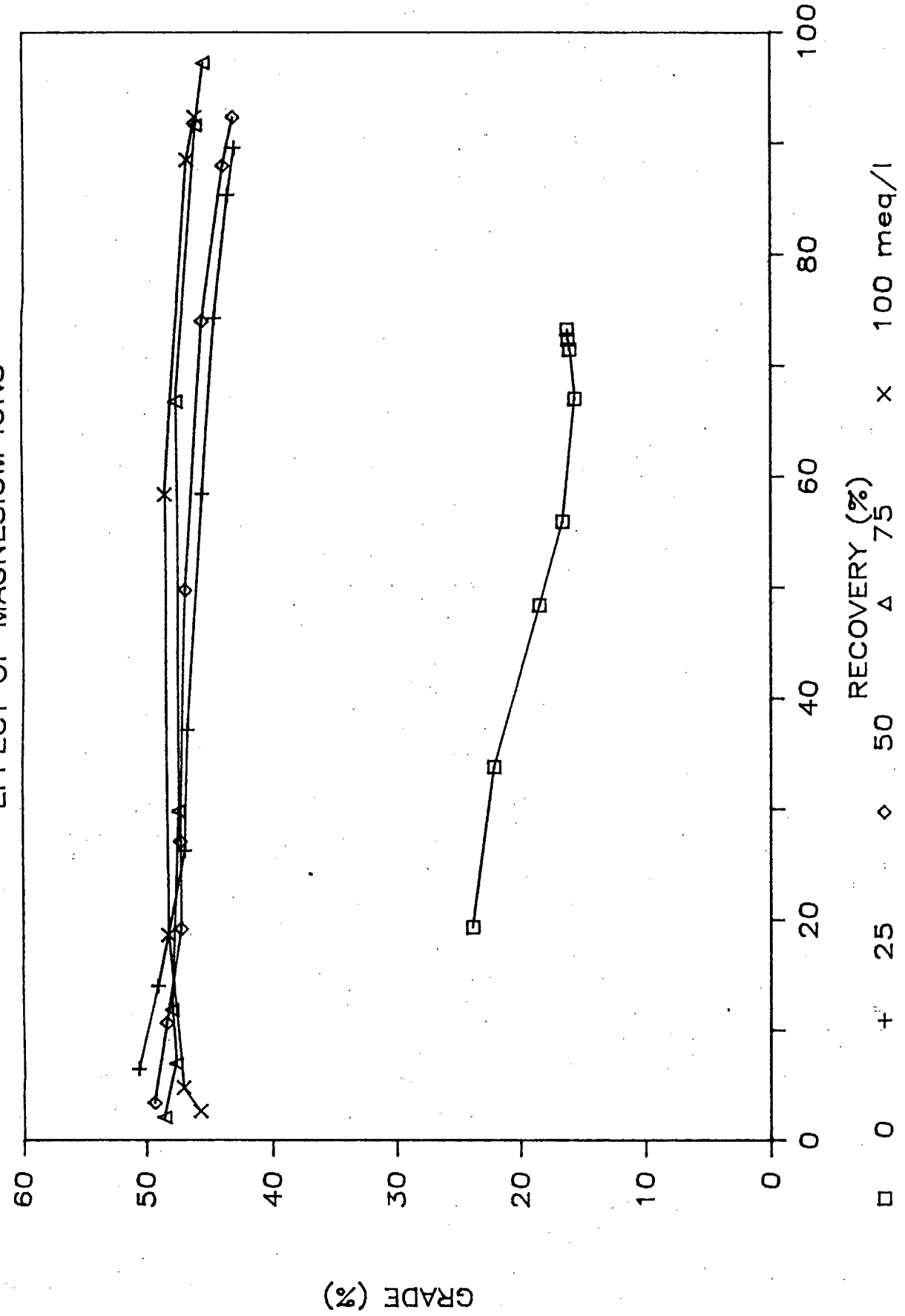

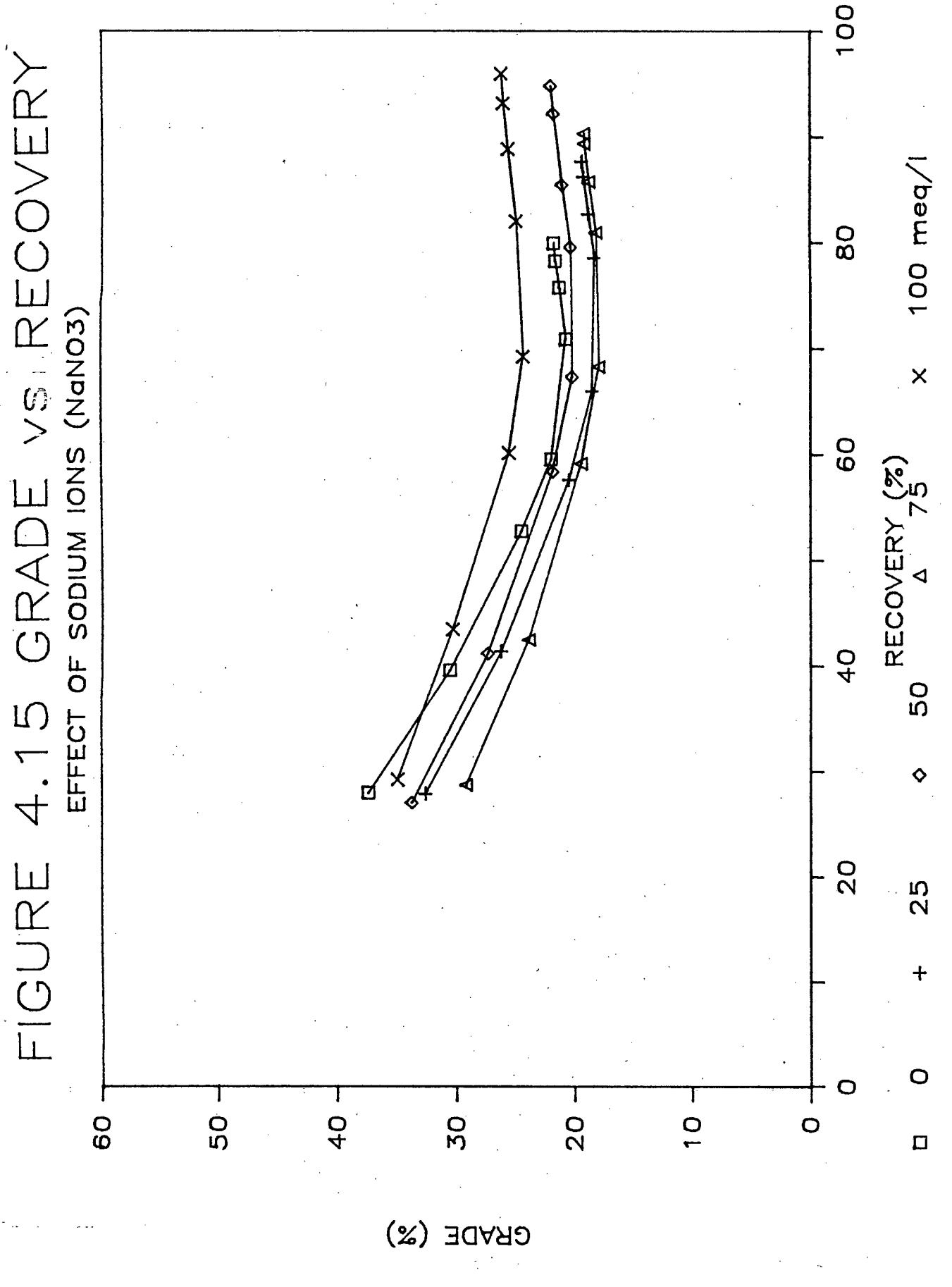
FIGURE 4.15 GRADE VS RECOVERY
EFFECT OF SODIUM IONS (NaNO3)
GRADE (%)
60
50
40
30
20
10
0
0
20
40
60
80
100
RECOVERY (%)
□ 0
+ 25
◇ 50
△ 75
× 100 meq/l

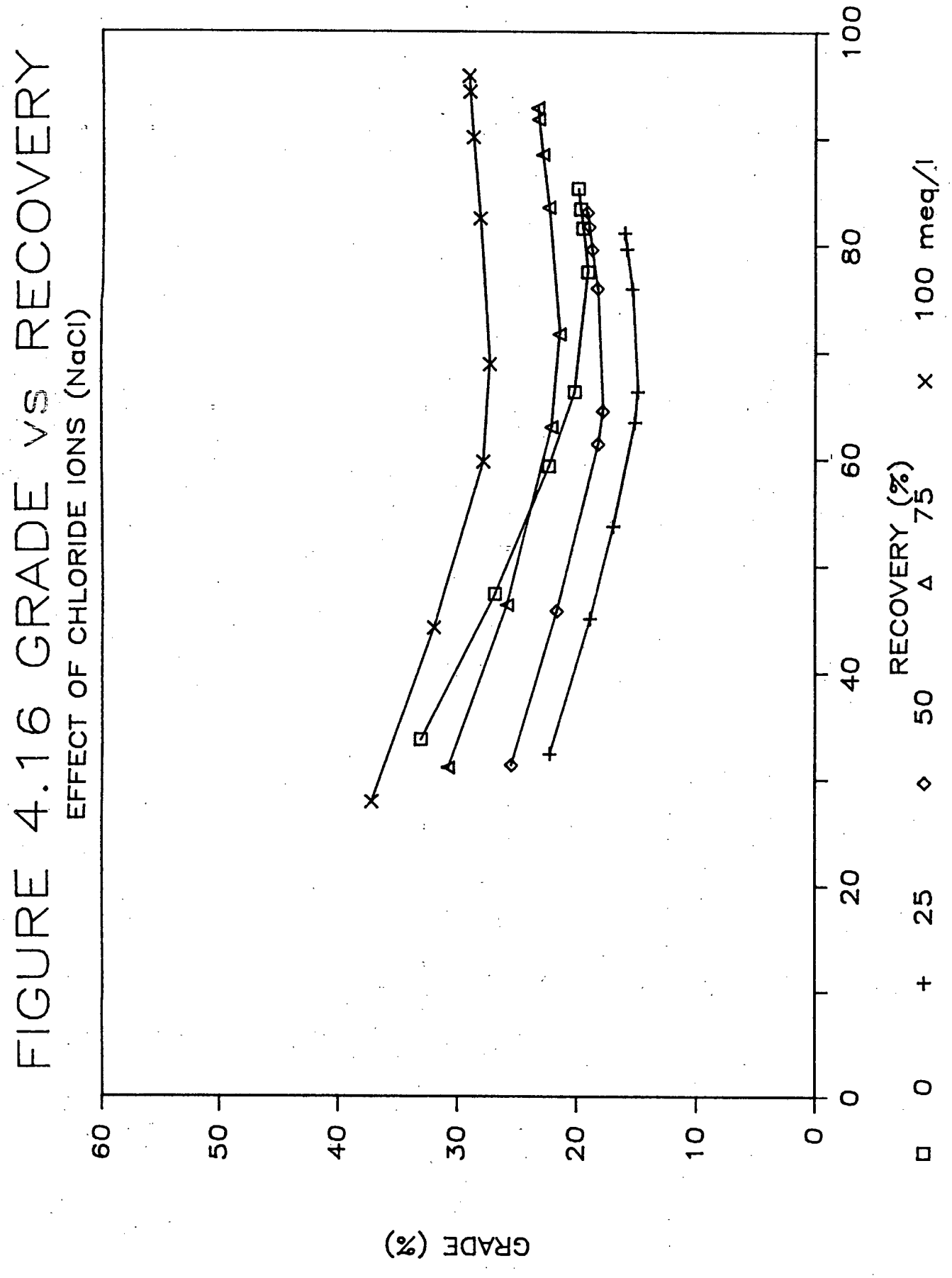
FIGURE 4.16 GRADE VS RECOVERY
EFFECT OF CHLORIDE IONS (NaCl)
GRADE (%)
RECOVERY (%)
0
10
20
30
40
50
60
0
20
40
60
80
100
□ 0
+ 25
◇ 50
△ 75
× 100 meq/l

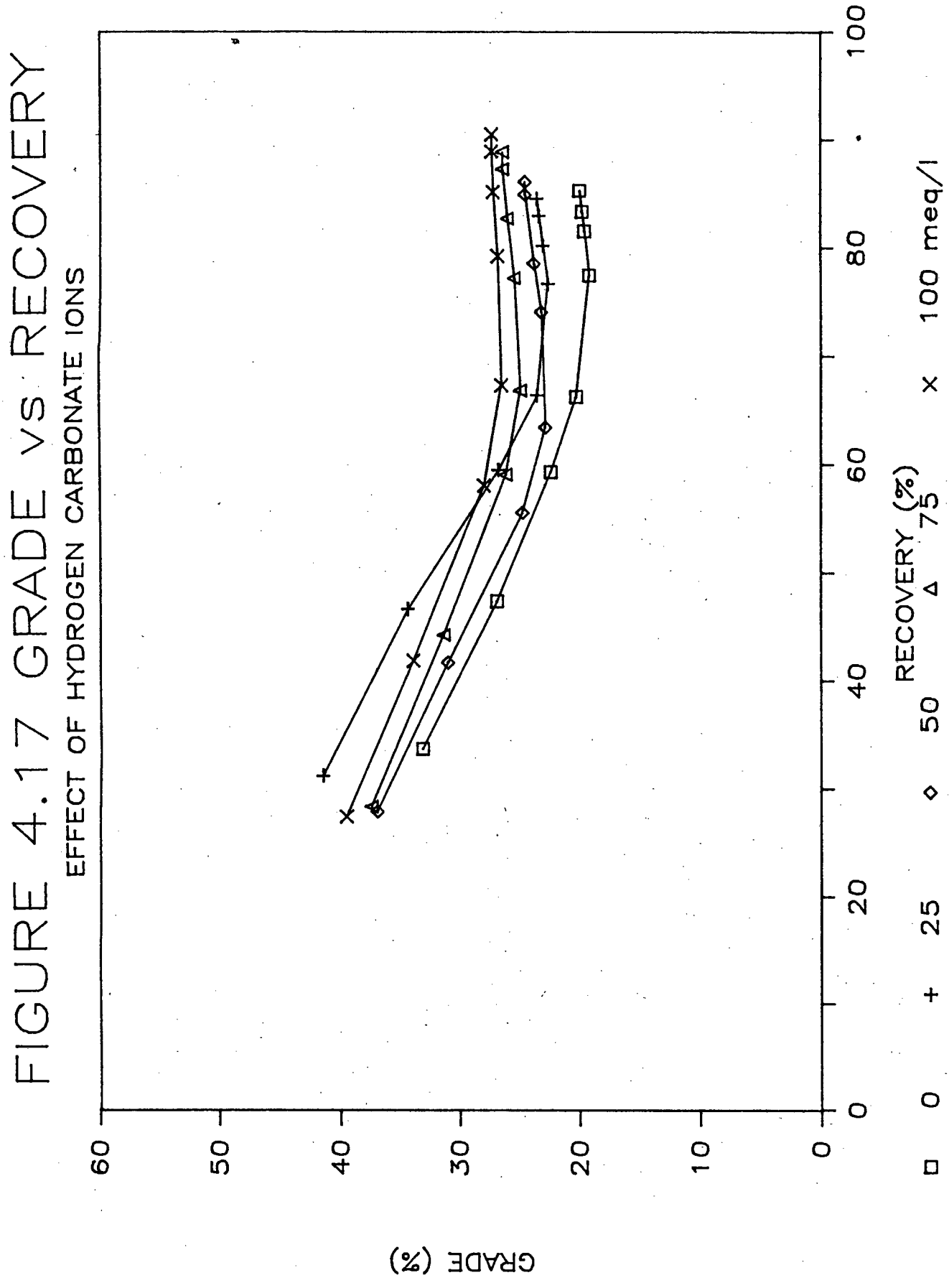
FIGURE 4.17 GRADE vs RECOVERY
EFFECT OF HYDROGEN CARBONATE IONS
GRADE (%)
60
50
40
30
20
10
0
0
20
40
60
80
100
RECOVERY (%)
□ 0 + 25 ◇ 50 △ 75 × 100 meq/l

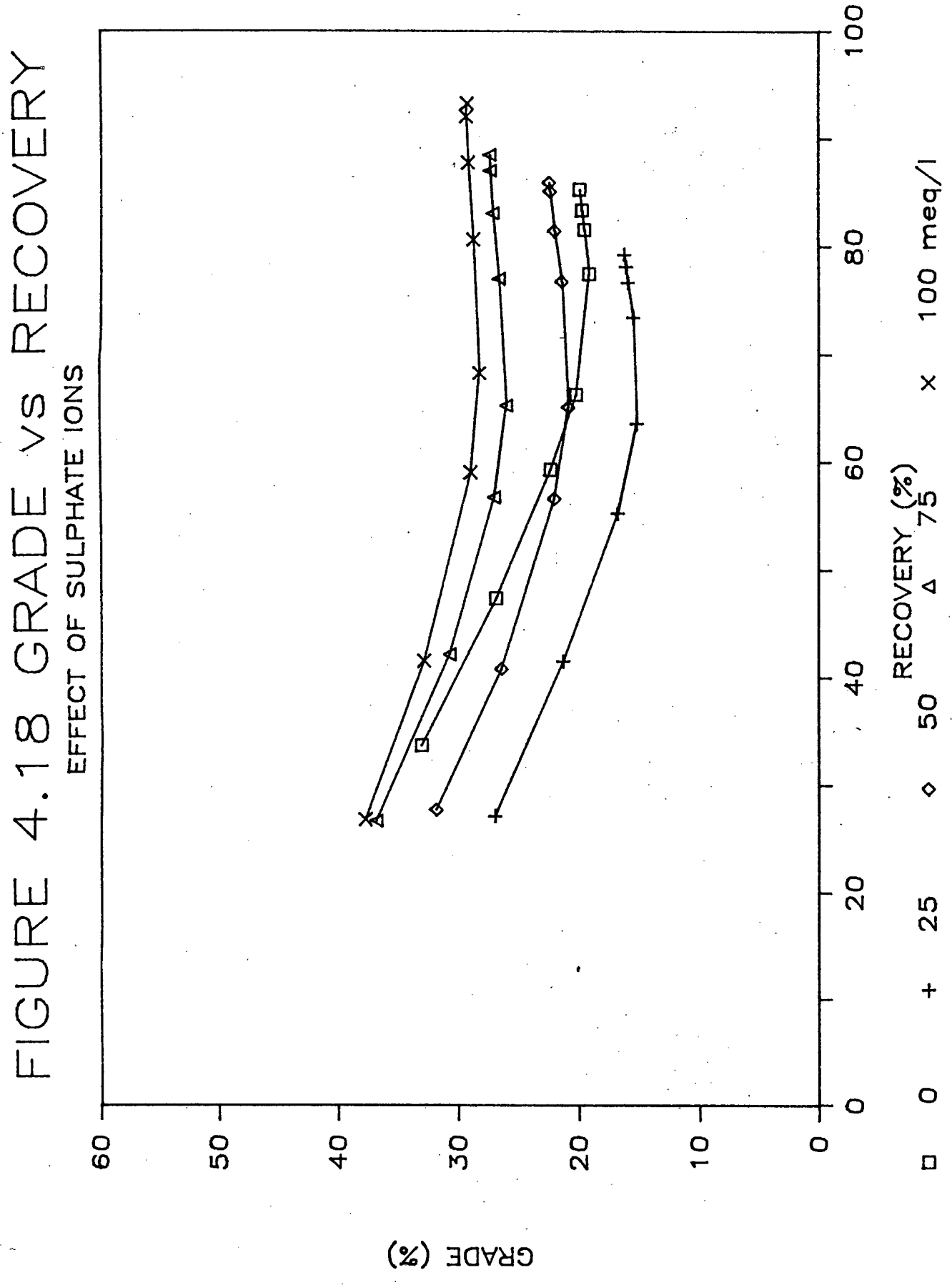
FIGURE 4.18 GRADE vs RECOVERY
EFFECT OF SULPHATE IONS
GRADE (%)
60
50
40
30
20
10
0
0
20
40
60
80
100
RECOVERY (%)
□ 0
+ 25
◇ 50
△ 75
× 100 meq/l

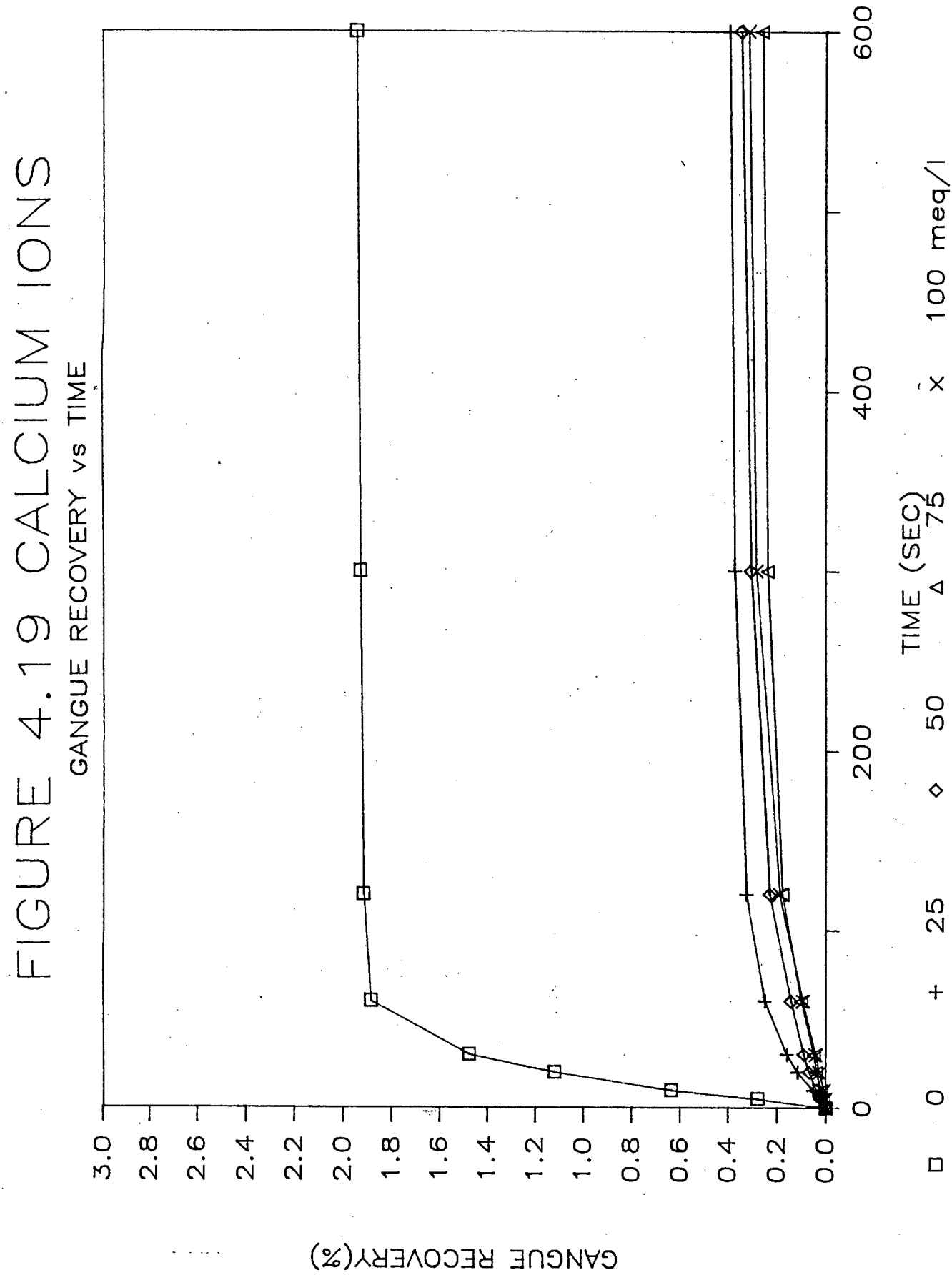
FIGURE 4.19 CALCIUM IONS
GANGUE RECOVERY vs TIME
GANGUE RECOVERY(%)
3.0
2.8
2.6
2.4
2.2
2.0
1.8
1.6
1.4
1.2
1.0
0.8
0.6
0.4
0.2
0.0
0
200
400
600
TIME (SEC)
□ 0
+ 25
◇ 50
△ 75
× 100 meq/l

FIGURE 4.20 MAGNESIUM IONS

GANGUE RECOVERY vs TIME

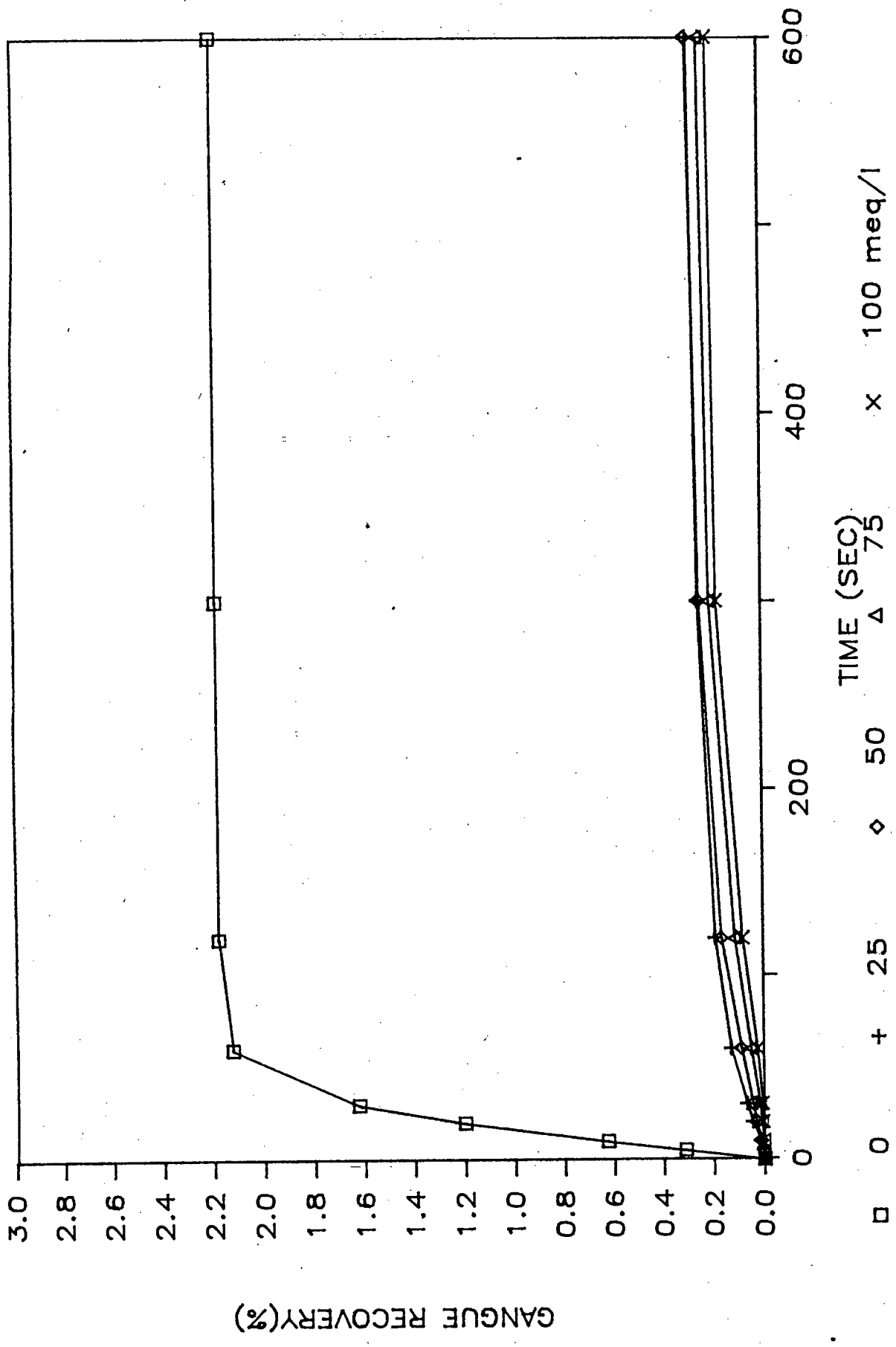

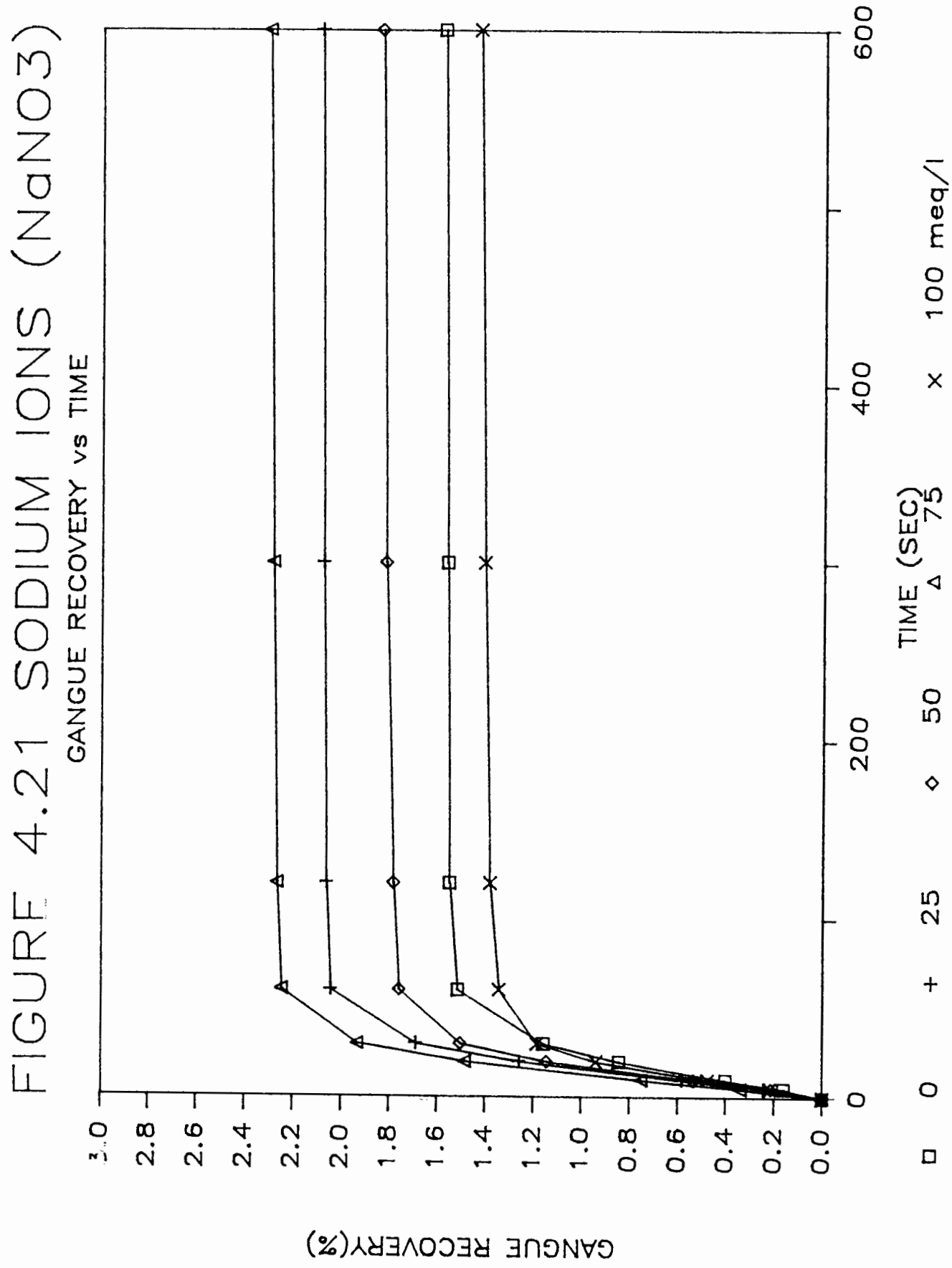
FIGURF 4.21 SODIUM IONS (NaNO3)
GANGUE RECOVERY vs TIME
GANGUE RECOVERY(%)
TIME (SEC)
□ 0 + 25 ◇ 50 △ 75 × 100 meq/l
0.0
0.2
0.4
0.6
0.8
1.0
1.2
1.4
1.6
1.8
2.0
2.2
2.4
2.6
2.8
3.0
0
200
400
600

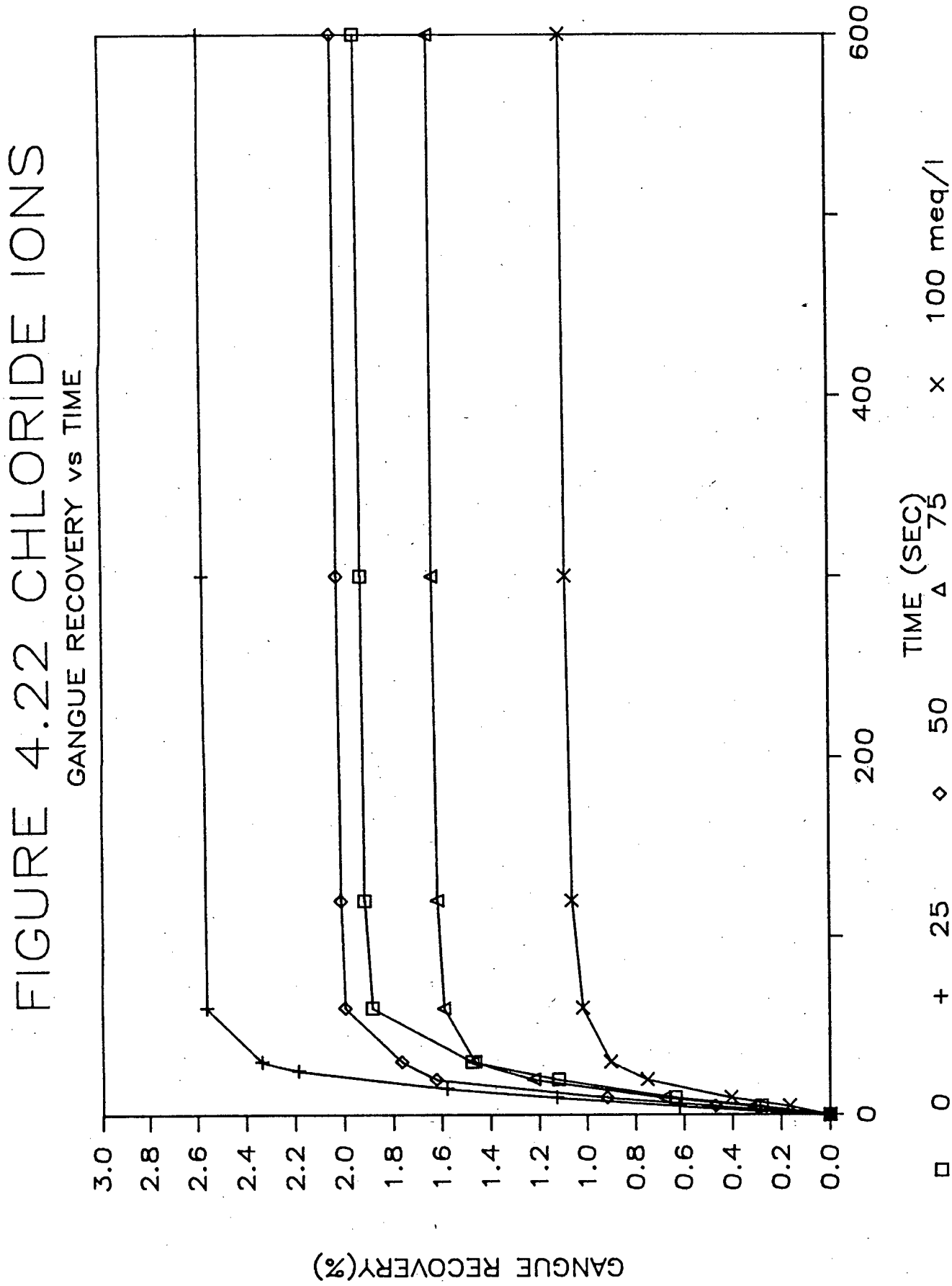
FIGURE 4.22 CHLORIDE IONS
GANGUE RECOVERY vs TIME
GANGUE RECOVERY(%)
3.0
2.8
2.6
2.4
2.2
2.0
1.8
1.6
1.4
1.2
1.0
0.8
0.6
0.4
0.2
0.0
0
200
400
600
TIME (SEC)
□ 0
+ 25
◇ 50
△ 75
× 100 meq/l

FIGURE 4.23 HYDROGEN CARBONATE IONS

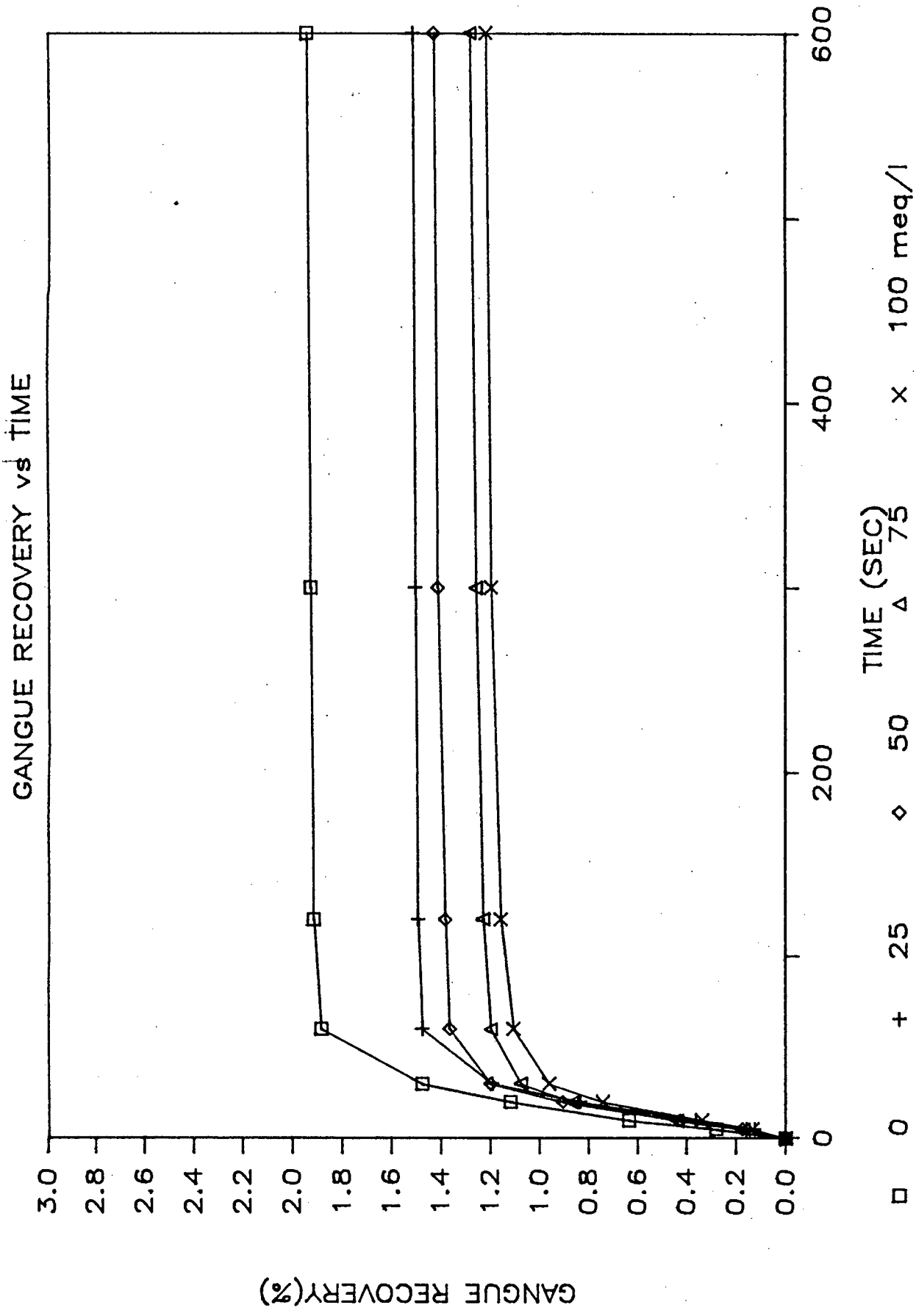

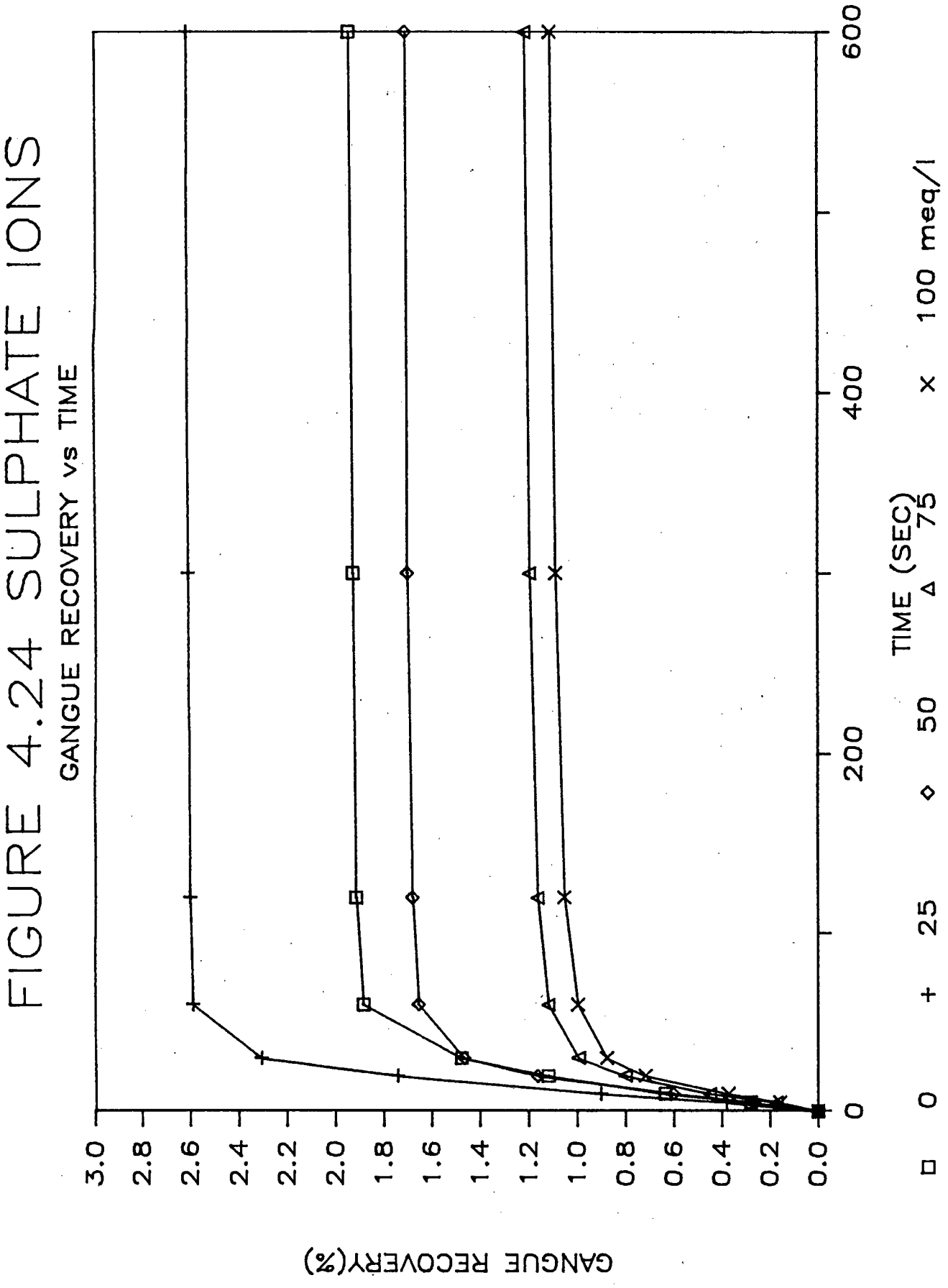
FIGURE 4.24 SULPHATE IONS
GANGUE RECOVERY vs TIME
GANGUE RECOVERY(%)
3.0
2.8
2.6
2.4
2.2
2.0
1.8
1.6
1.4
1.2
1.0
0.8
0.6
0.4
0.2
0.0
0
200
400
600
TIME (SEC)
□ 0
+ 25
◇ 50
△ 75
× 100 meq/l

FIGURE 4.25 CALCIUM IONS

GANGUE RECOVERY vs MASS of WATER

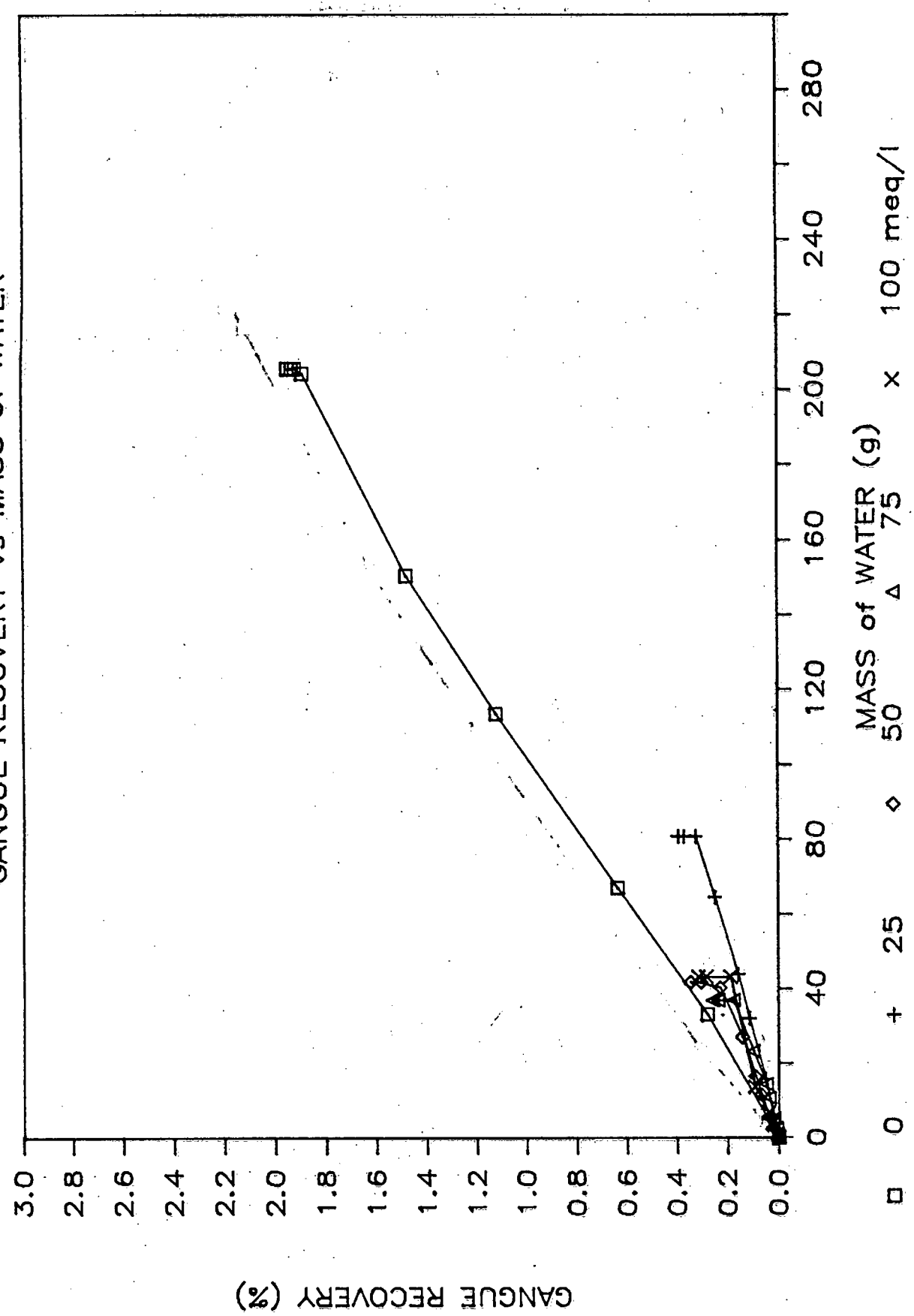

FIGURE 4.26 MAGNESIUM IONS

GANGUE RECOVERY vs MASS OF WATER

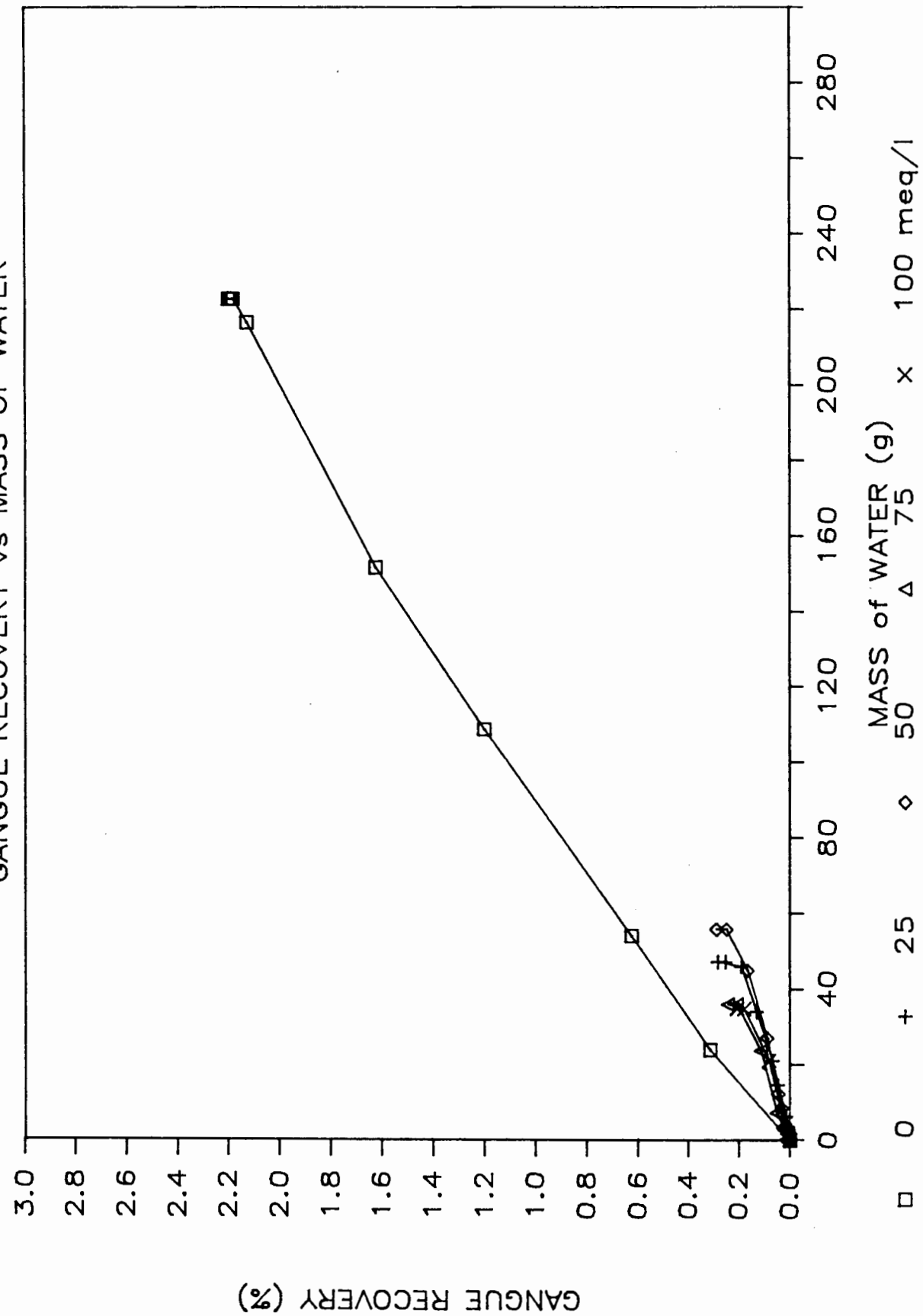

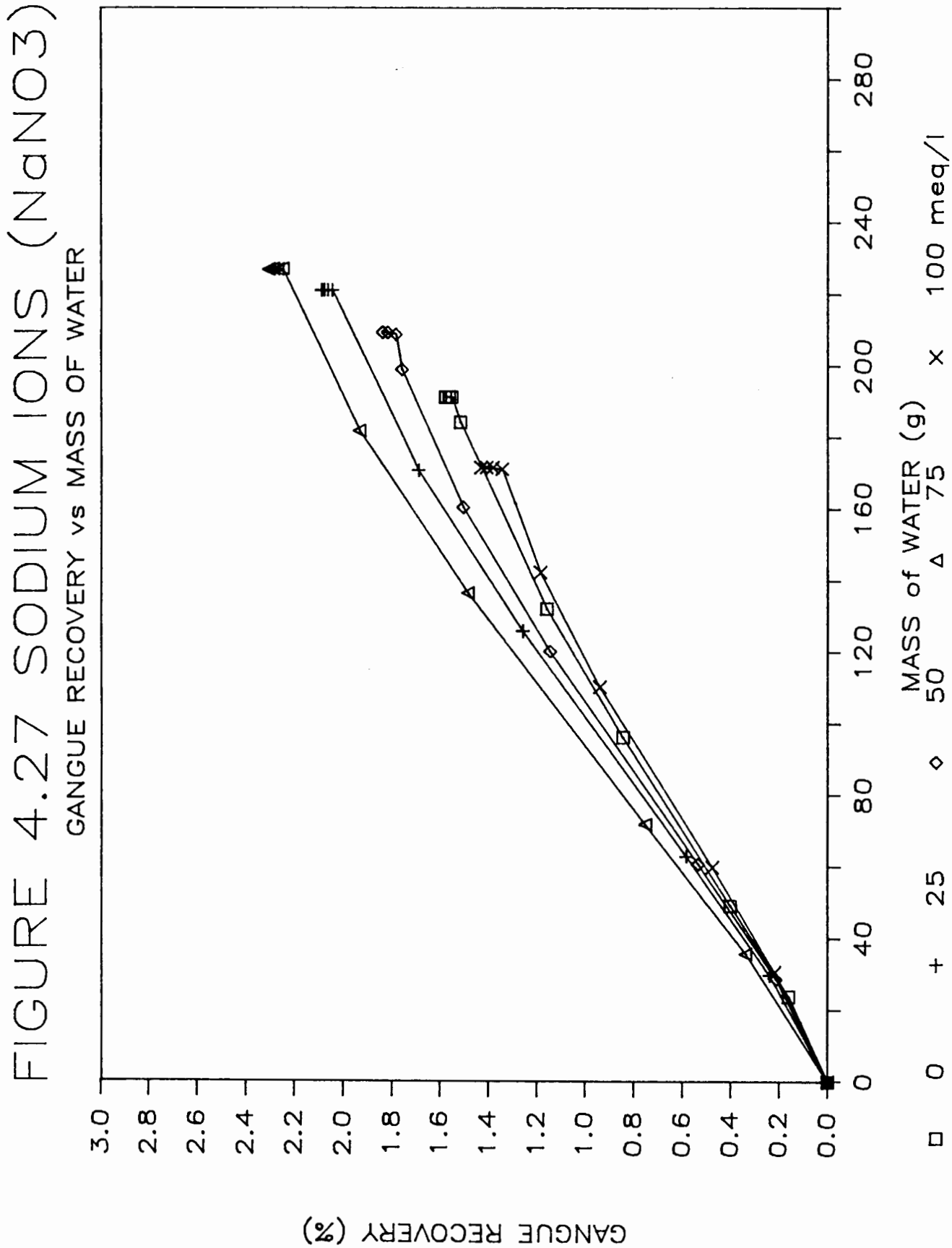
FIGURE 4.27 SODIUM IONS (NaNO3)
GANGUE RECOVERY vs MASS OF WATER
GANGUE RECOVERY (%)
3.0
2.8
2.6
2.4
2.2
2.0
1.8
1.6
1.4
1.2
1.0
0.8
0.6
0.4
0.2
0.0
0
40
80
120
160
200
240
280
MASS of WATER (g)
□ 0 + 25 ◇ 50 △ 75 × 100 meq/l

FIGURE 4.28 CHLORIDE IONS

GANGUE RECOVERY vs MASS of WATER

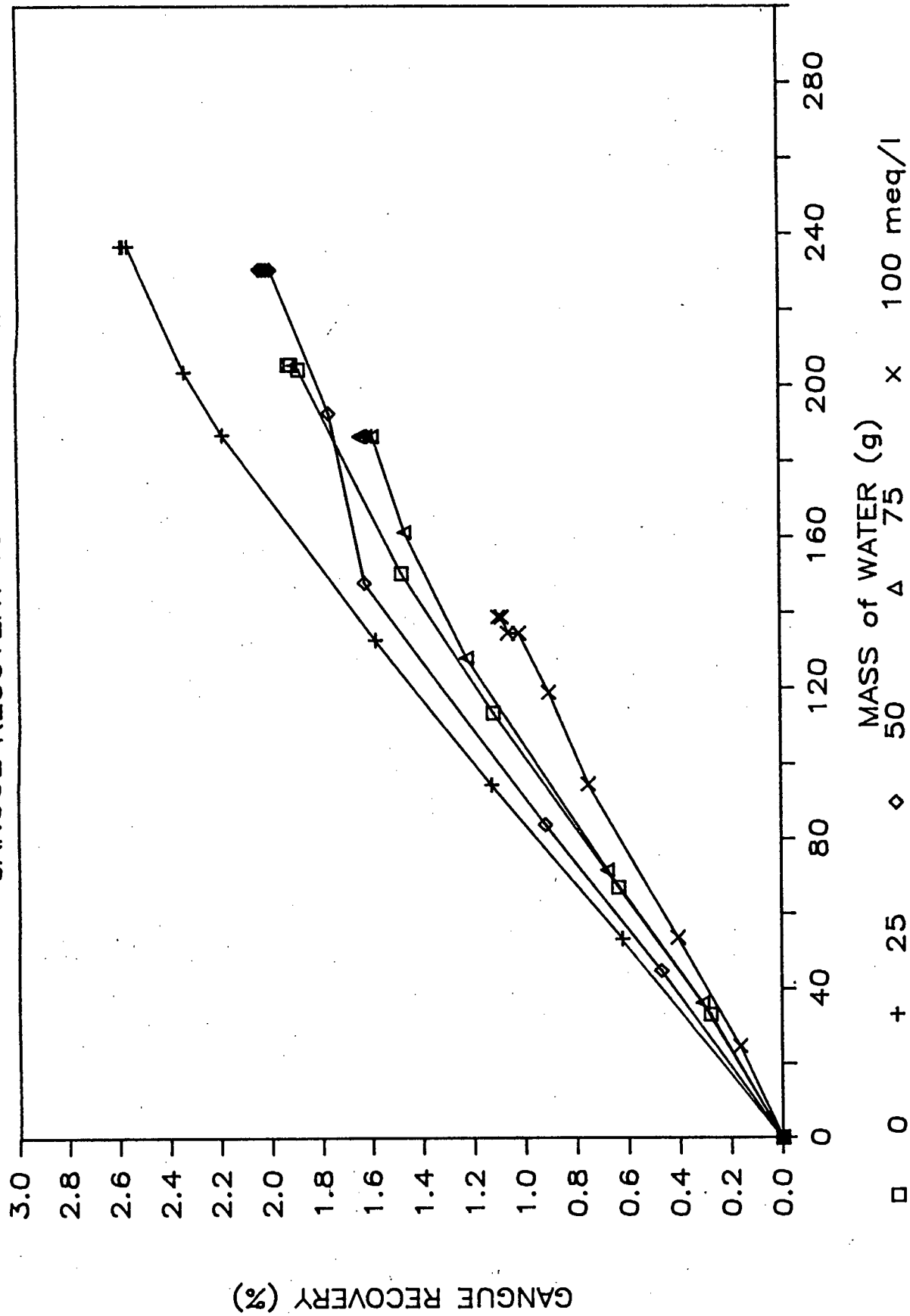

FIGURE 4.29 HYDROGEN CARBONATE IONS

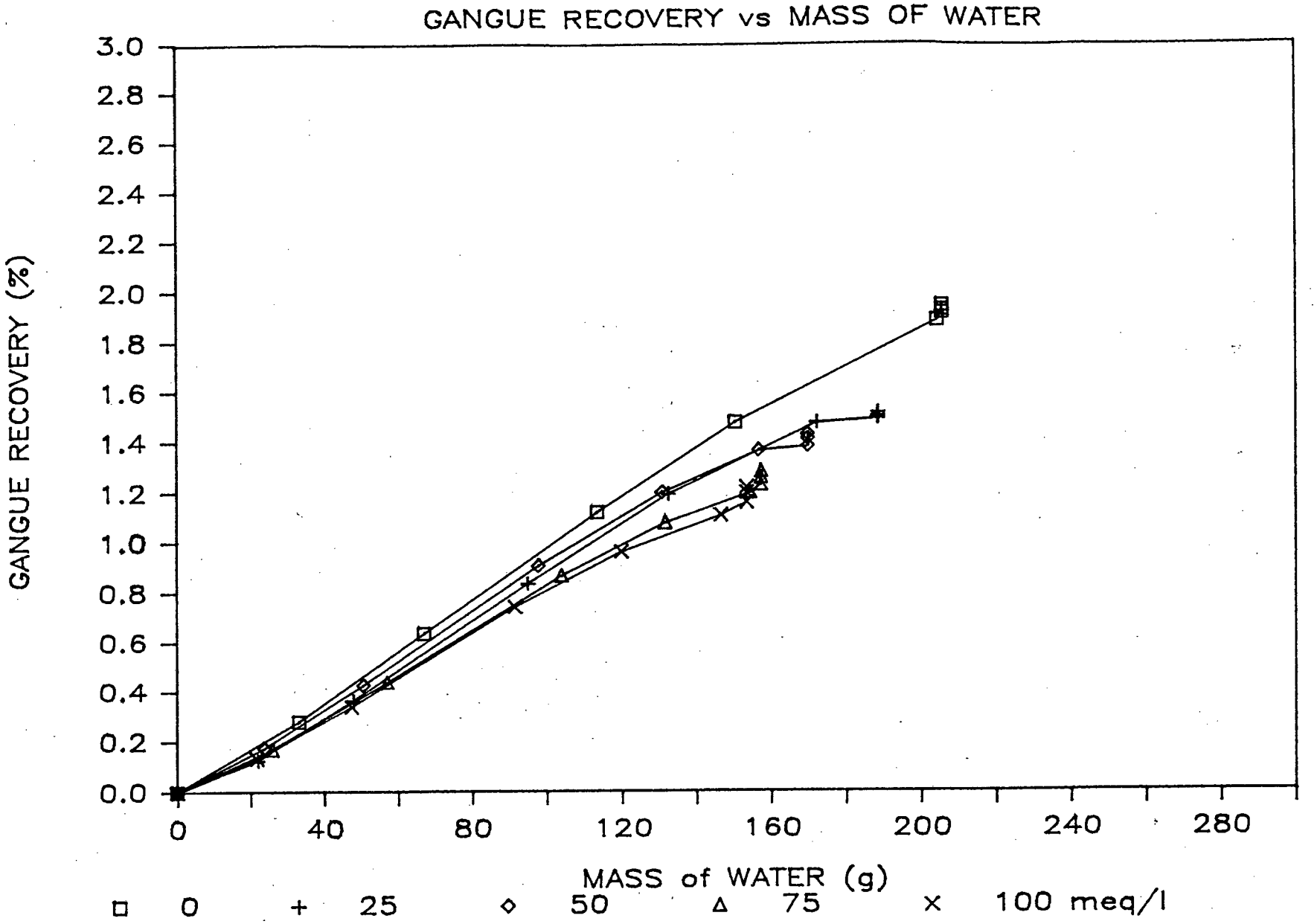

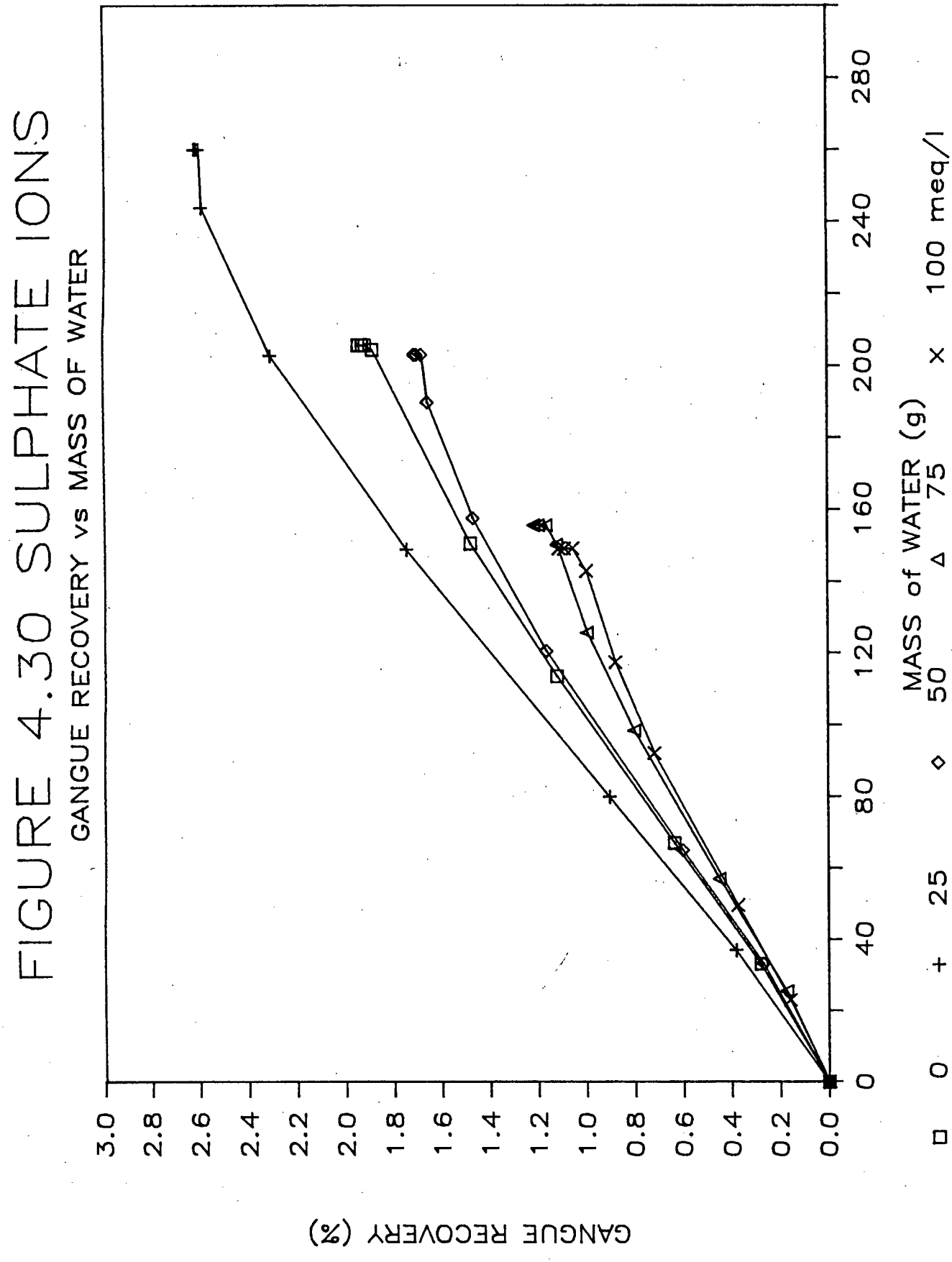
FIGURE 4.30 SULPHATE IONS
GANGUE RECOVERY vs MASS OF WATER
GANGUE RECOVERY (%)
3.0
2.8
2.6
2.4
2.2
2.0
1.8
1.6
1.4
1.2
1.0
0.8
0.6
0.4
0.2
0.0
0
40
80
120
160
200
240
280
MASS of WATER (g)
□ 0 + 25 ◇ 50 △ 75 × 100 meq/l

FIGURE 4.31 LEACHED ORE

RECOVERY (600sec) vs CONCENTRATION

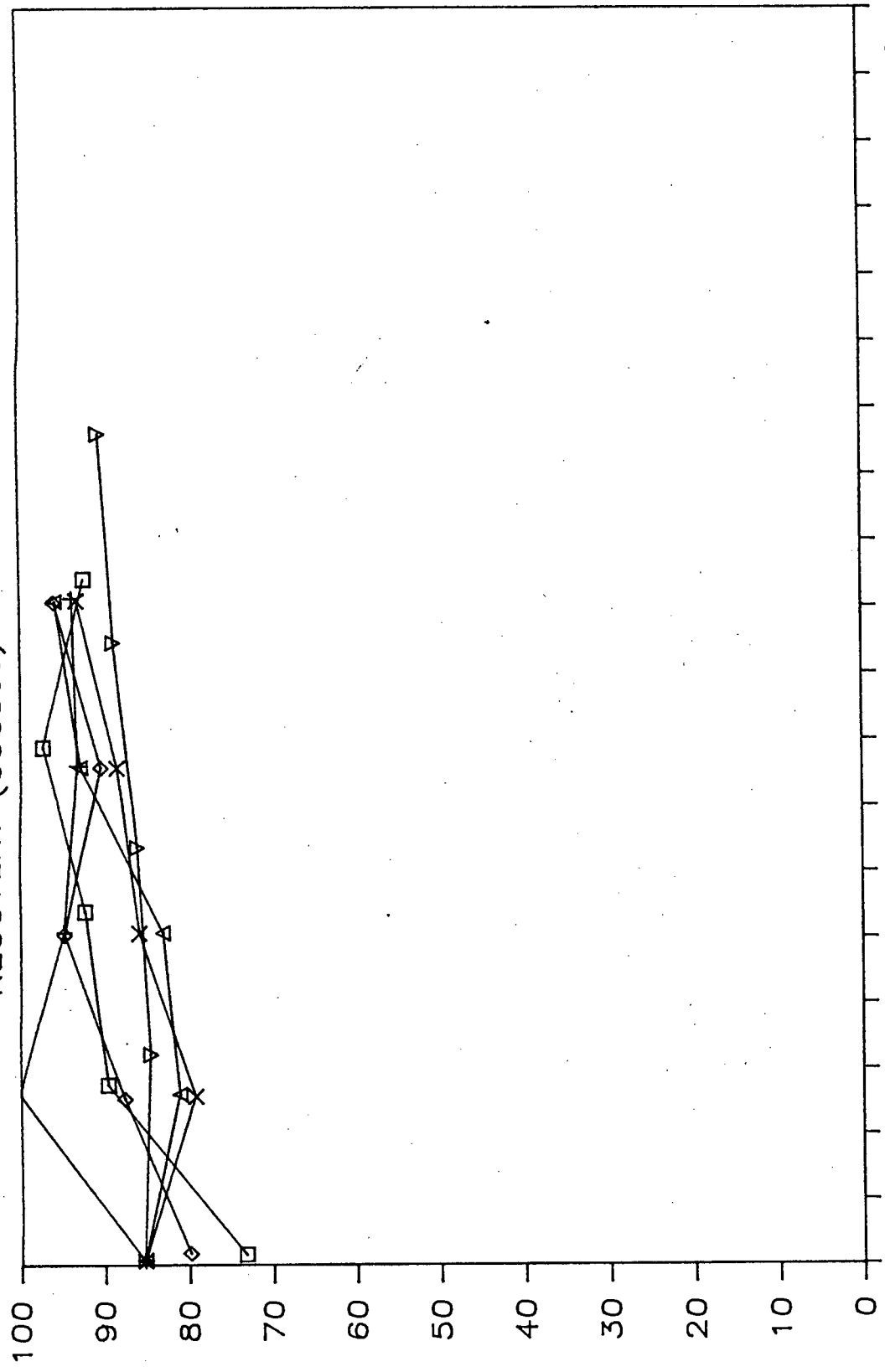

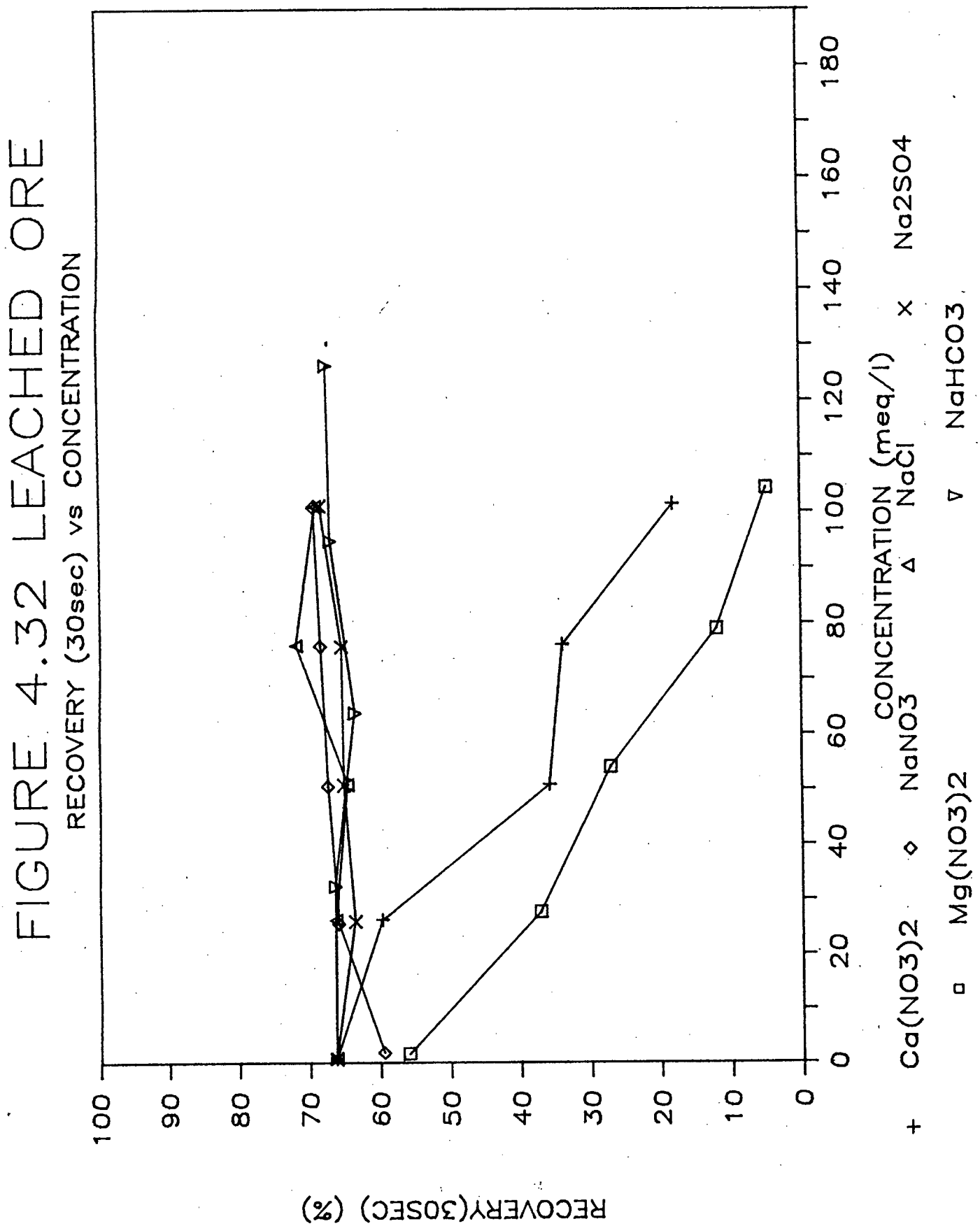
FIGURE 4.32 LEACHED ORE
RECOVERY (30sec) vs CONCENTRATION
RECOVERY(30SEC) (%)
100
90
80
70
60
50
40
30
20
10
0
0
20
40
60
80
100
120
140
160
180
CONCENTRATION (meq/l)
+ Ca(NO3)2
◇ NaNO3
△ NaCl
× Na2SO4
□ Mg(NO3)2
▽ NaHCO3

FIGURE 4.33 LEACHED ORE

GANGUE RECOVERY vs CONCENTRATION

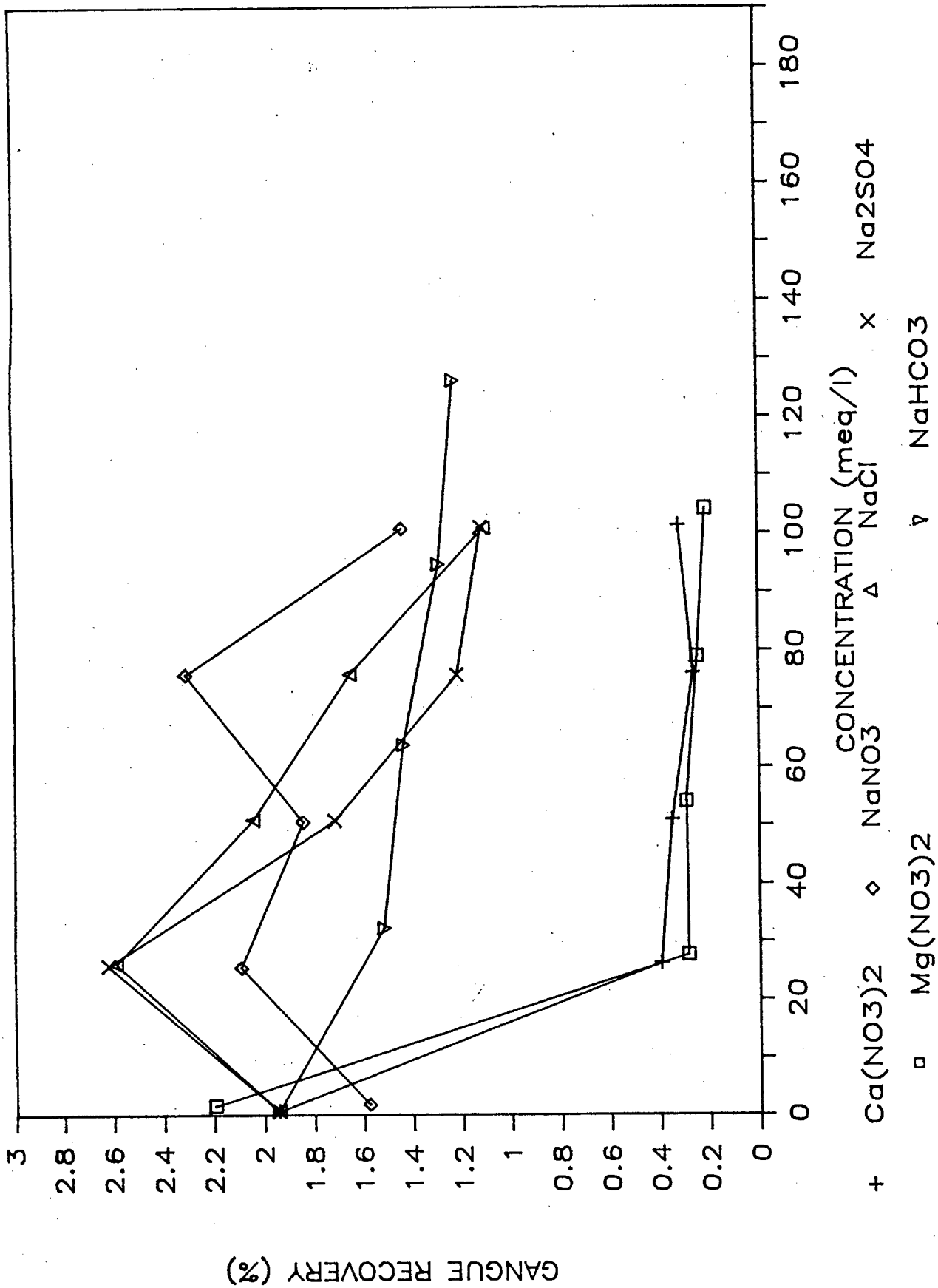

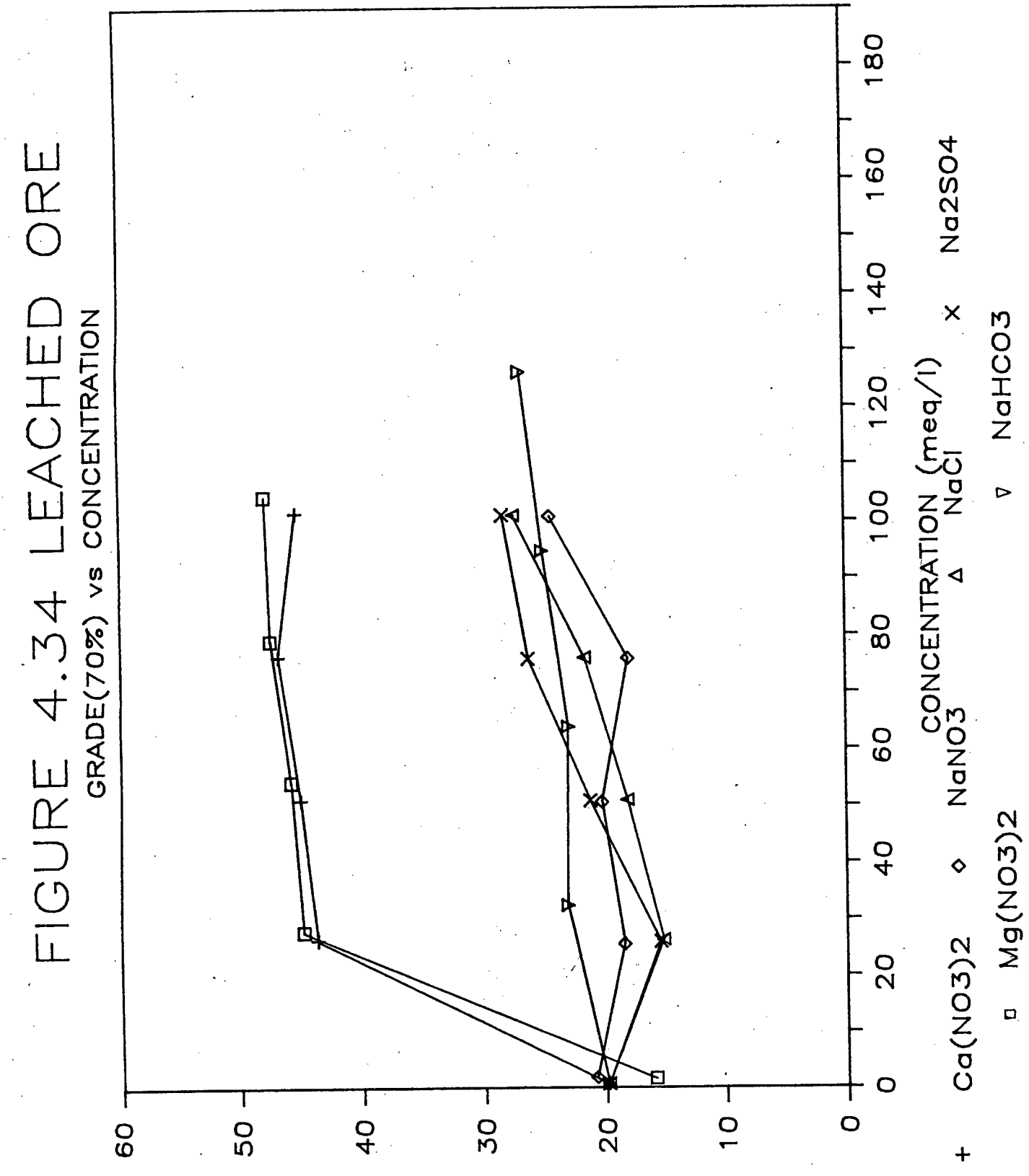
FIGURE 4.34 LEACHED ORE
GRADE(70%) vs CONCENTRATION
GRADE(70%) (%)
60
50
40
30
20
10
0
0
20
40
60
80
100
120
140
160
180
CONCENTRATION (meq/l)
+ Ca(NO3)2
◇ NaNO3
△ NaCl
× Na2SO4
▽ NaHCO3
□ Mg(NO3)2

From Figure 4.31 it was found that recovery at 10 minutes increased with an increase in concentration of ions added. This increase ranged from 5% to 20% depending on the salt used. No definite trends distinguishing differences between ions can be seen.

From Figure 4.32 the addition of the divalent cations, calcium and magnesium, resulted in a decrease of approximately 50% in R_{30} whereas the addition of the salts containing the sodium cation had very little effect.

In Figure 4.33 the gangue recovery resulting from the addition of the divalent ions decreased significantly from addition rates of 1 to 25 meq/l and then showed very little difference with higher additions. The gangue recoveries resulting from the addition of NaCl, $NaNO_3$ and Na_2SO_4 increased slightly and then decreased. The gangue recovery following the addition of $NaHCO_3$ decreased with increasing concentration. These differences were however only 0,2 to 0,3%.

From Figure 4.34 it can be seen that the grade at 70% recovery increased by approximately 25% for the divalent ions, but only by 5 to 10% for the other inorganic salts.

The froth produced during these runs varied with addition rate. At low additions the froth formation time was 10 to 13 seconds. Dry froth as described previously occurred after two minutes in the front of the cell. Increased additions of $NaNO_3$, NaCl, Na_2SO_4 and $NaHCO_3$ resulted in no change in the froth formation time but did result in a decrease in dry froth. Very little dry froth occurred with more than 50 meq/l ion added.

The addition of magnesium nitrate and calcium nitrate resulted in an immediate increase (from 0 to 25 meq/l) in the froth formation time which was 13 seconds at 0 meq/l, 20 seconds at 25, 50 and 75 meq/l and 30 seconds at 100 meq/l. No dry froth occurred, but at 100 meq/l the first layer of

froth had to be scraped off before the froth would increase sufficiently to flow over the lip.

Photographs of this froth are shown in Figures 4.35 to 4.37. The photographs show the froth at 0 seconds, 30 seconds, 2 minutes and 10 minutes. In Figure 4.35 where there was no ion addition except NaOH, the pH regulator, the dry froth can be seen at 2 minutes and 10 minutes. In Figure 4.36 it can be seen that no dry froth forms with the addition of 100 meq/l $NaNO_3$. In Figure 4.37 it can be seen that the bubbles are generally smaller and more evenly sized with the addition of 100 meq/l calcium nitrate than those formed with the equivalent addition of $NaNO_3$ in Figure 4.36.

Table 4.10 shows the concentration of species of each ion present at each addition rate at pH 9. The calculations are shown in Appendix E. These concentrations are the concentrations that would occur were no pyrite or quartz present. The predominant ions can be identified and possible mechanisms of the interactions of these ions and the system can be predicted.

Figure 4.35 Froth Formed with the Addition of 1.8 meq/l Na^+ at 0, 30, 120 and 600 seconds

Figure 4.36 Froth Formed with the Addition of 100 meq/l $NaNO_3$ at 0, 30, 120 and 600 seconds

Figure 4.37 Froth Formed with the Addition of 100 meq/l Calcium Nitrate at 0, 30, 120 and 600 seconds

Table 4.10 Concentration Levels of Species

ION	TOTAL CONCENTRATION		SPECIES			
Calcium Nitrate	Calcium meq/l	Calcium mmol/l	$CaOH^+$ mmol/l		Ca^{++} mmol/l	
	0,73	0,37	0,2E-3		0,37	
	26,2	13,1	4E-3		13,1	
	50,9	25,5	8E-3		25,4	
	76,1	38,1	12E-3		38,0	
	101,3	50,7	16E-3		50,6	
Magnesium Nitrate	Magnesium meq/l	Magnesium mmol/l	$MgOH^+$ mmol/l		Mg^{++} mmol/l	
	1,7	0,8	3E-3		0,8	
	27,7	13,9	0,05		13,8	
	54,1	27,1	0,1		27,0	
	78,9	39,5	0,15		39,3	
	104,2	52,1	0,2		51,9	
Sodium Nitrate	All additions completely dissociate to form Na^+ and NO_3^-					
Sodium Chloride	All additions completely dissociate to form Na^+ and Cl^-					
Na_2SO_4 and $Ca(OH)_2$ mmol/l	Sulphate	Calcium	Ca^{++}	$CaOH^+$	SO_4^{2-}	$CaSO_4$ s
	0	0,37	0,36	2E-4	0	0
	12,5	0,45	2E-6	6E-10	12,1	0,45
	25	0,40	1E-6	3E-10	24,6	0,40
	37,5	0,35	7E-7	2E-10	37,2	0,35
	50	0,45	5E-7	2E-10	49,6	0,45
$NaHCO_3$ and $Ca(OH)_2$ mmol/l	Carbonate	Calcium	HCO_3^-	CO_3^{2-}	$CaCO_3$	H_2CO_3
	0	0,3	0	0	0	0
	25	3,7	20,1	1,1	3,7	0,05
	50	6,9	40,7	2,3	6,9	0,10
	75	9,9	61,5	3,5	9,9	0,14
	100	13,1	82,1	4,6	13,1	0,19
			Ca^{++}	$CaOH^+$		
			0,3	2E-4		
			8E-9	3E-12		
			4E-9	1E-12		
			3E-9	8E-13		
			2E-9	6E-13		

From Table 4.10 it can be seen that the predominant species respectively for calcium nitrate, magnesium nitrate, sodium nitrate, sodium chloride, sodium sulphate and sodium hydrogen carbonate are Ca^{++}, Mg^{++}, Na^{+} (and NO_3^-), Na^{+} and Cl^-, Na^{+} and SO_4^{2-} and Na^{+} and HCO_3^- respectively. $CaCO_3$ and $CaSO_4$ precipitates do occur.

Two additional runs were made: one with no ions or pH regulator added and one with 100 meq/l CaCl2. The results are summarised in Table 4.11.

Table 4.11 R_{600} and R_{30} for no ion addition and the addition of 100meq/l $CaCl_2$

pH	CONCENTRATION	R_{600}	R_{30}	R_{6600}	$G_{70\%}$
5,9	0 meq/l	80,79	70,07	1,618	22,18
9,0	100meq/l CaCl2	90,83	2,95	0,202	46,78

The results produced by $CaCl_2$ are very similar to those obtained using calcium nitrate. The results obtained using no pH regulator at all are similar to those obtained using the pH regulators only. However the rate as expressed by R_{30} is slightly higher.

4.1.9 Effect of ions on unleached ore

The effect of different addition rates of four inorganic salts on unleached ore was investigated. The salts were magnesium nitrate, calcium nitrate, sodium nitrate and sodium chloride.

The recovery-time and recovery-grade graphs for each salt are shown in Figures 4.38 to 4.45. The variation of R_{600}, R_{30}, R_{6600} and G_{70x} with concentration are shown in Figures 4.46 to 4.49 and in Table 4.12.

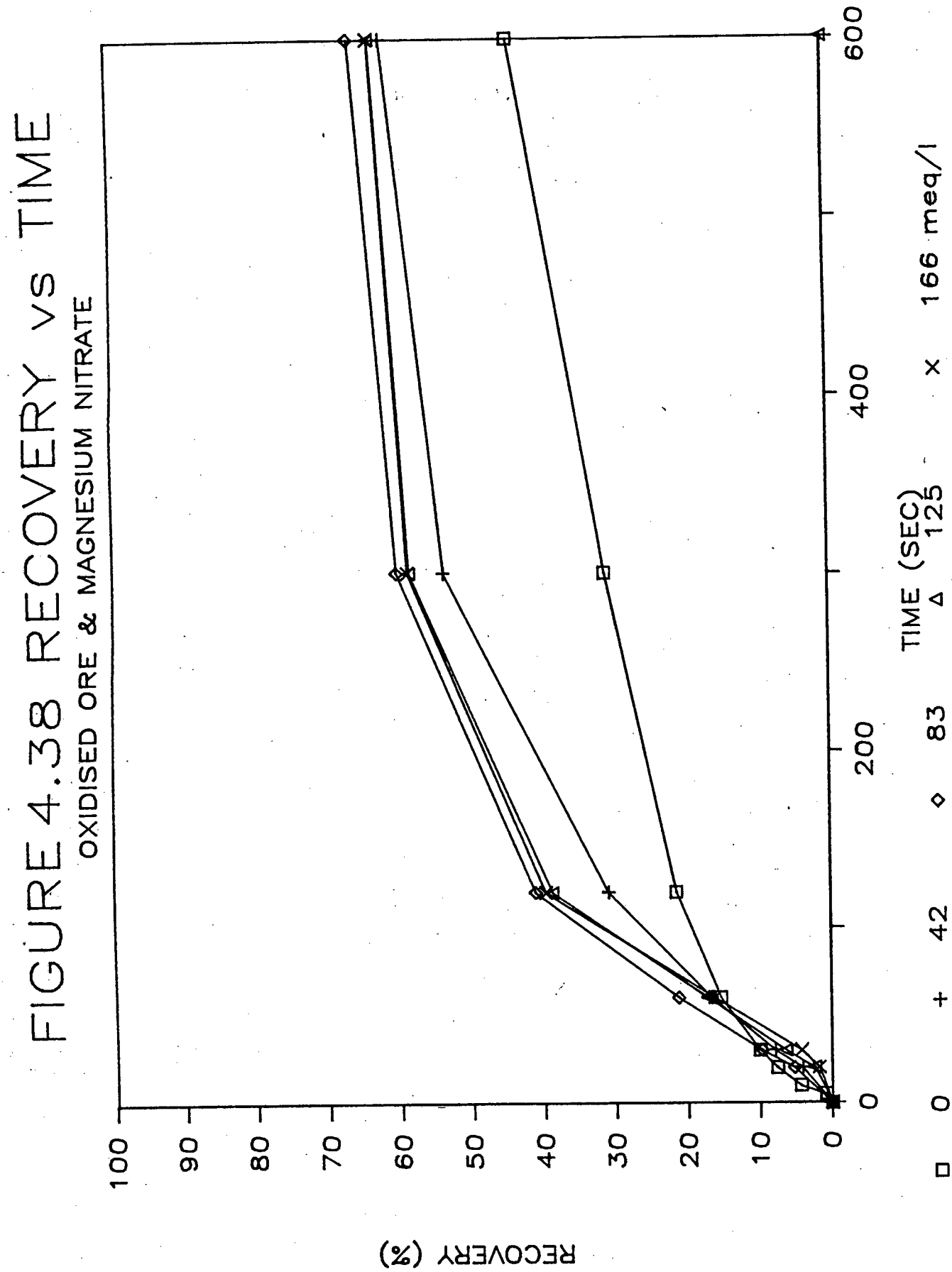
FIGURE 4.38 RECOVERY vs TIME
OXIDISED ORE & MAGNESIUM NITRATE
RECOVERY (%)
100
90
80
70
60
50
40
30
20
10
0
0
200
400
600
TIME (SEC)
□ 0
+ 42
◇ 83
△ 125
× 166 meq/l

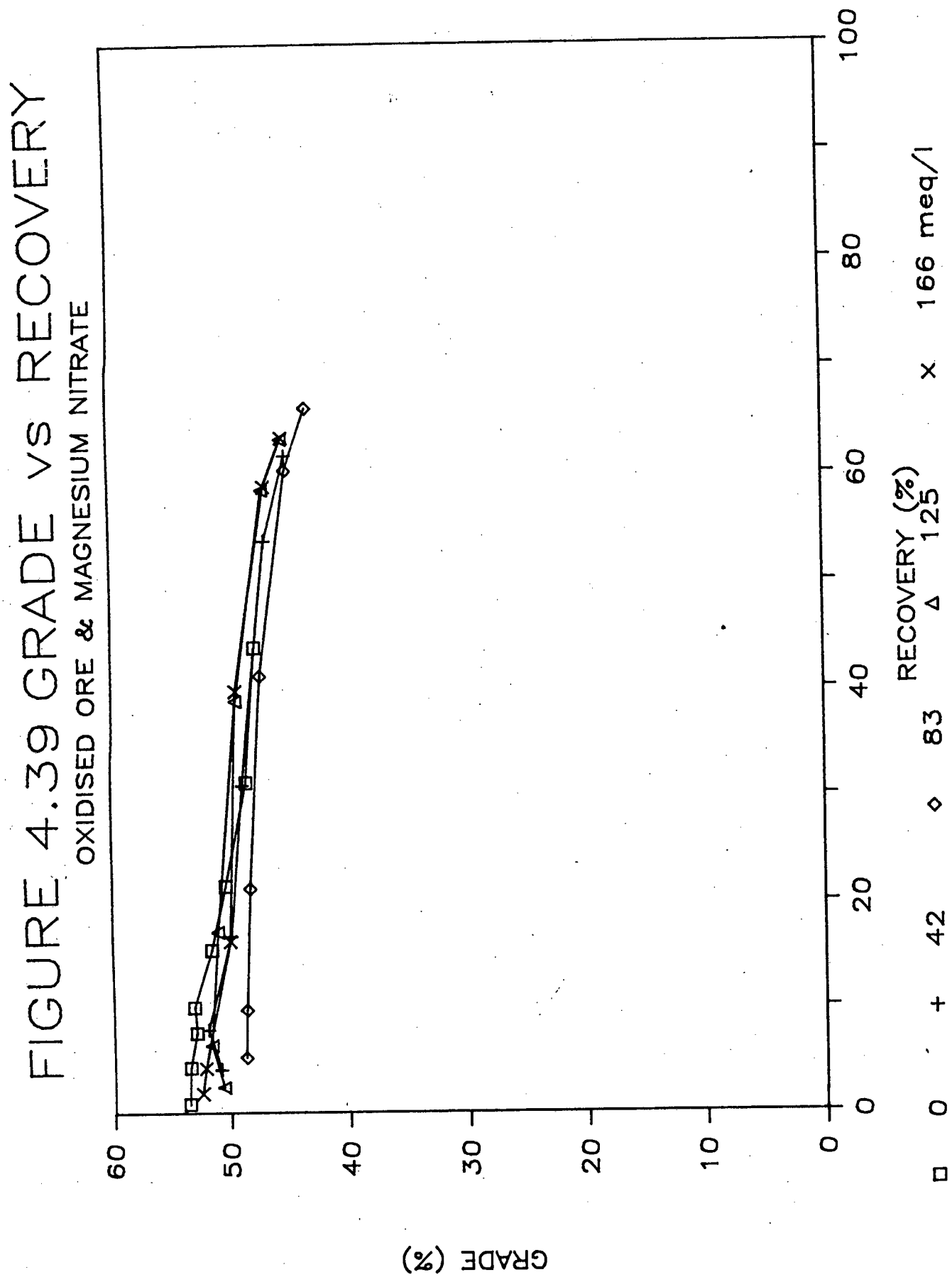
FIGURE 4.39 GRADE vs RECOVERY
OXIDISED ORE & MAGNESIUM NITRATE
GRADE (%)
60
50
40
30
20
10
0
RECOVERY (%)
0
20
40
60
80
100
□ 0
+ 42
◇ 83
△ 125
× 166 meq/l

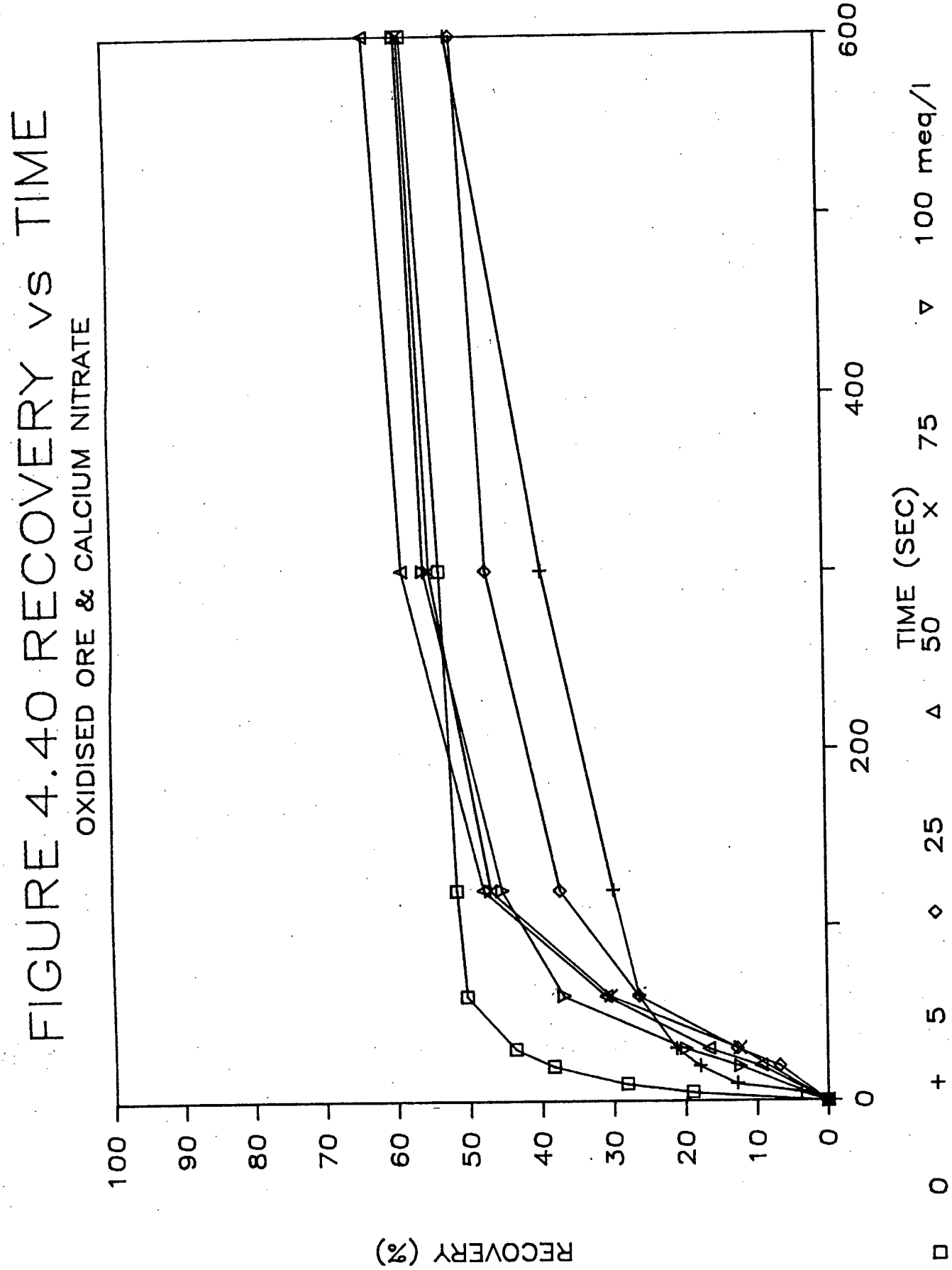
FIGURE 4.40 RECOVERY vs TIME
OXIDISED ORE & CALCIUM NITRATE
RECOVERY (%)
100
90
80
70
60
50
40
30
20
10
0
0
200
400
600
TIME (SEC)
0
5
25
50
75
100 meq/l

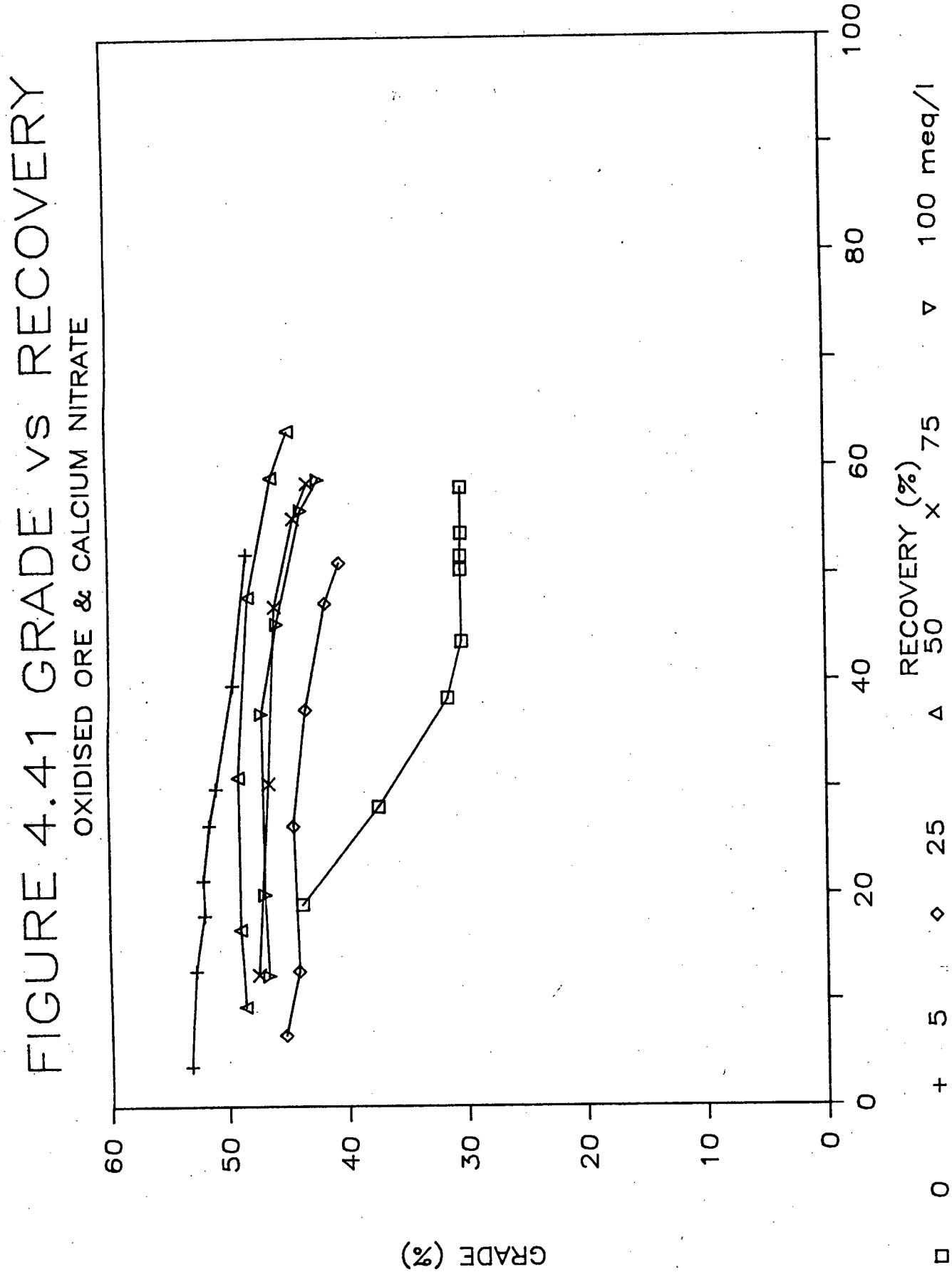
FIGURE 4.41 GRADE VS RECOVERY
OXIDISED ORE & CALCIUM NITRATE
GRADE (%)
RECOVERY (%)
0
10
20
30
40
50
60
0
20
40
60
80
100
0 meq/l
5
25
50
75
100 meq/l

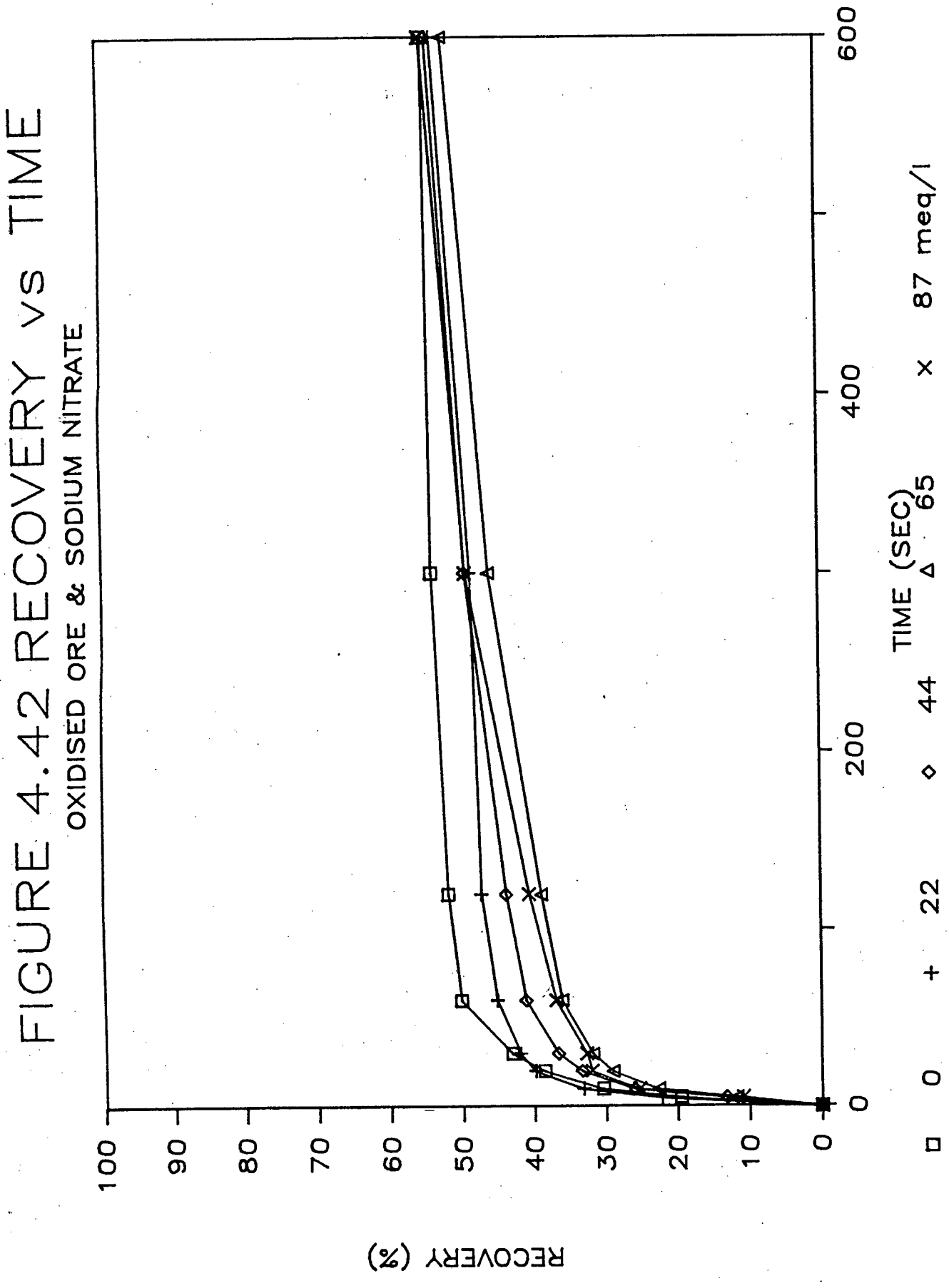
FIGURE 4.42 RECOVERY vs TIME
OXIDISED ORE & SODIUM NITRATE
RECOVERY (%)
100
90
80
70
60
50
40
30
20
10
0
0
200
400
600
TIME (SEC)
□ 0
+ 22
◇ 44
△ 65
× 87 meq/l

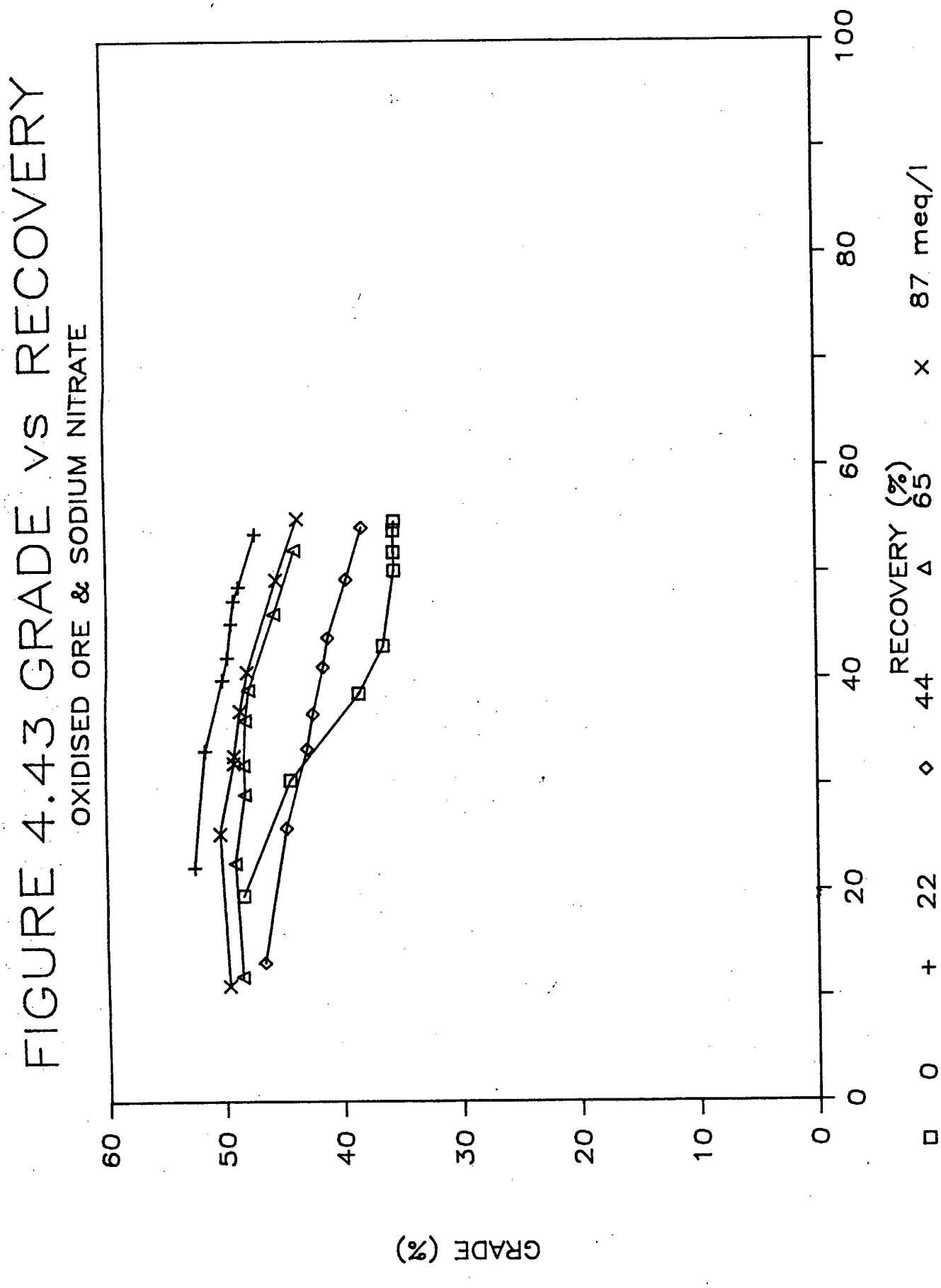
FIGURE 4.43 GRADE VS RECOVERY
OXIDISED ORE & SODIUM NITRATE
GRADE (%)
60
50
40
30
20
10
0
0
20
40
60
80
100
RECOVERY (%)
□ 0
+ 22
◇ 44
△ 65
× 87 meq/l

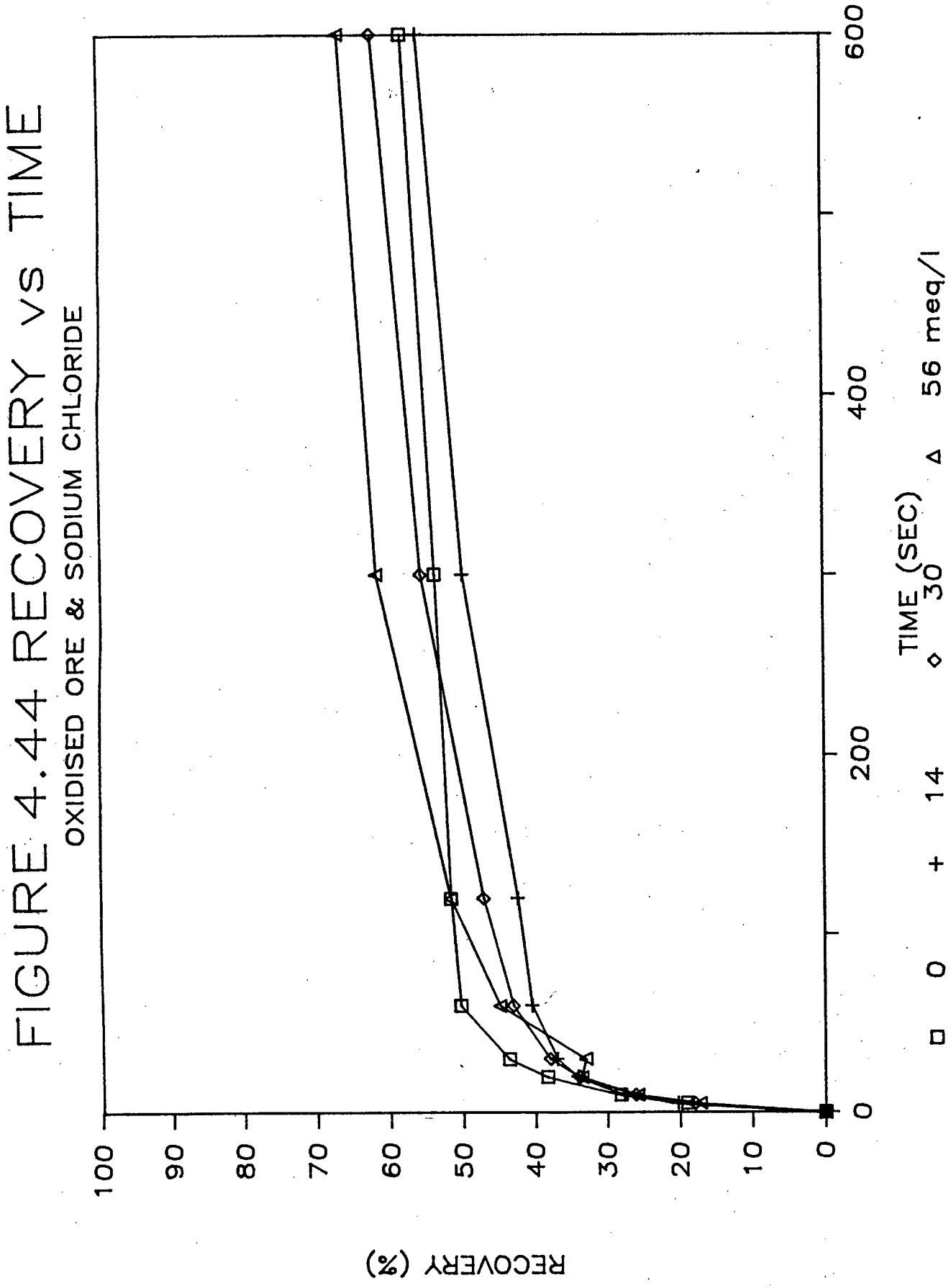
FIGURE 4.44 RECOVERY vs TIME
OXIDISED ORE & SODIUM CHLORIDE
RECOVERY (%)
100
90
80
70
60
50
40
30
20
10
0
0
200
400
600
TIME (SEC)
□ 0
+ 14
◇ 30
△ 56 meq/l

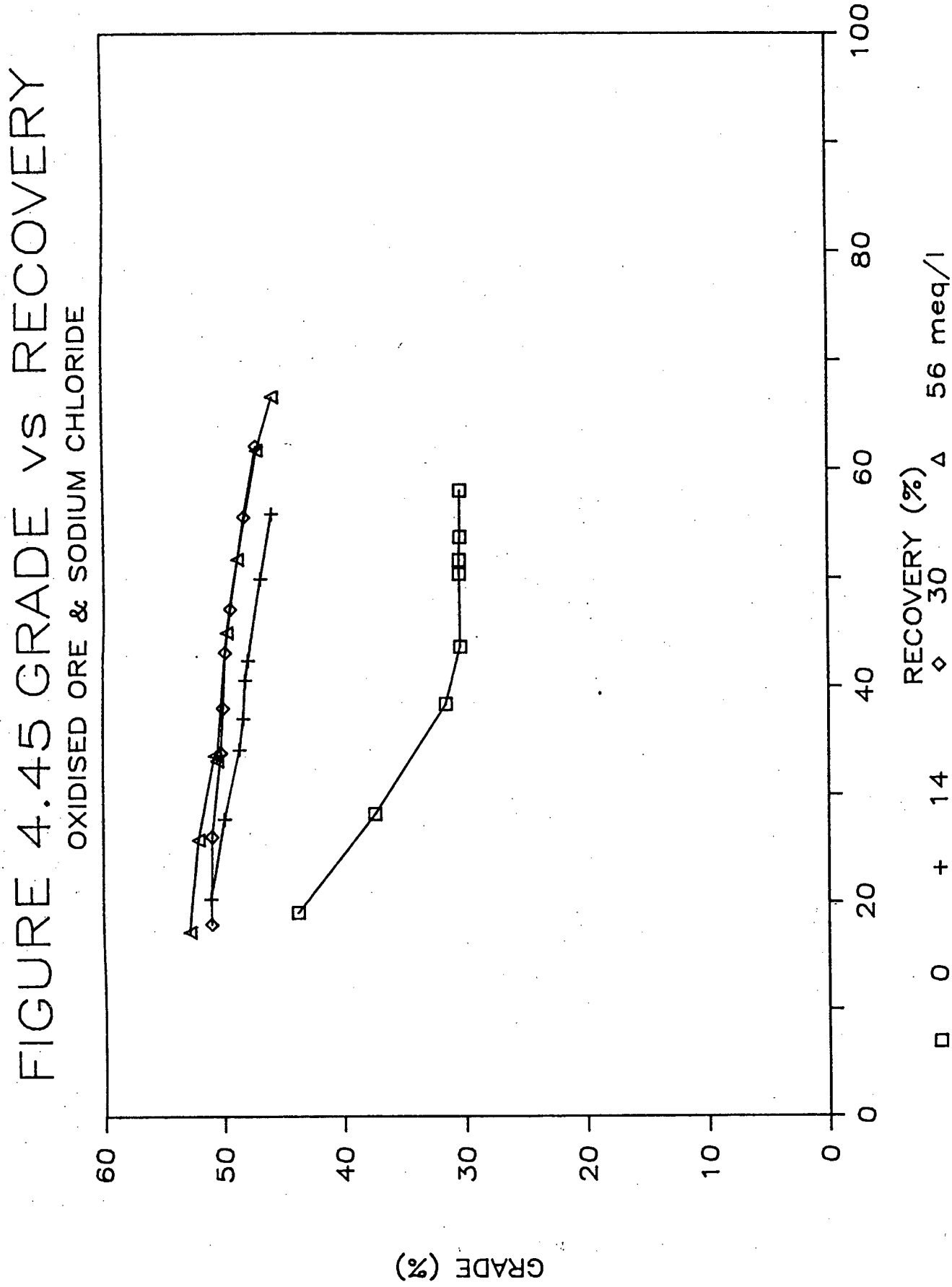
FIGURE 4.45 GRADE vs RECOVERY
OXIDISED ORE & SODIUM CHLORIDE
GRADE (%)
60
50
40
30
20
10
0
0
20
40
60
80
100
RECOVERY (%)
□ 0
+ 14
◇ 30
△ 56 meq/l

FIGURE 4.46 UNLEACHED ORE

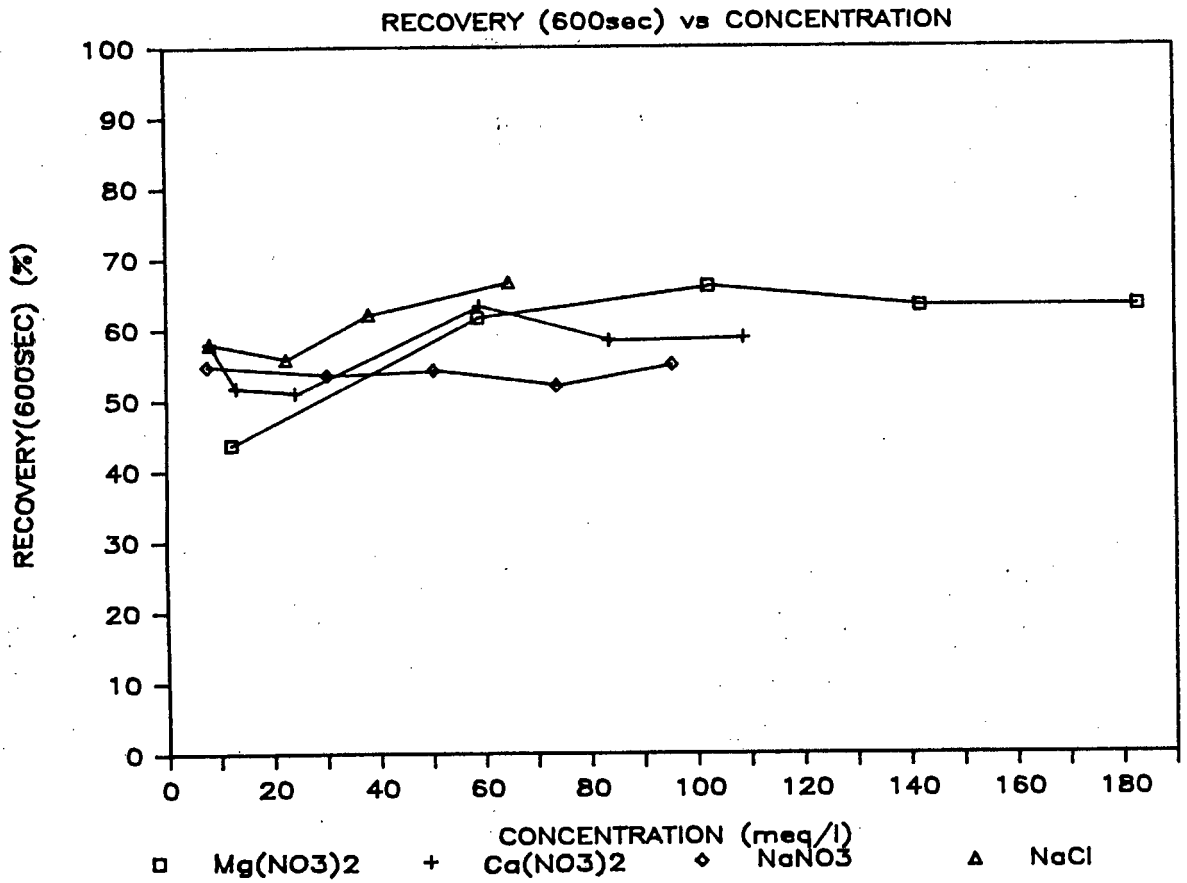

FIGURE 4.47 UNLEACHED ORE

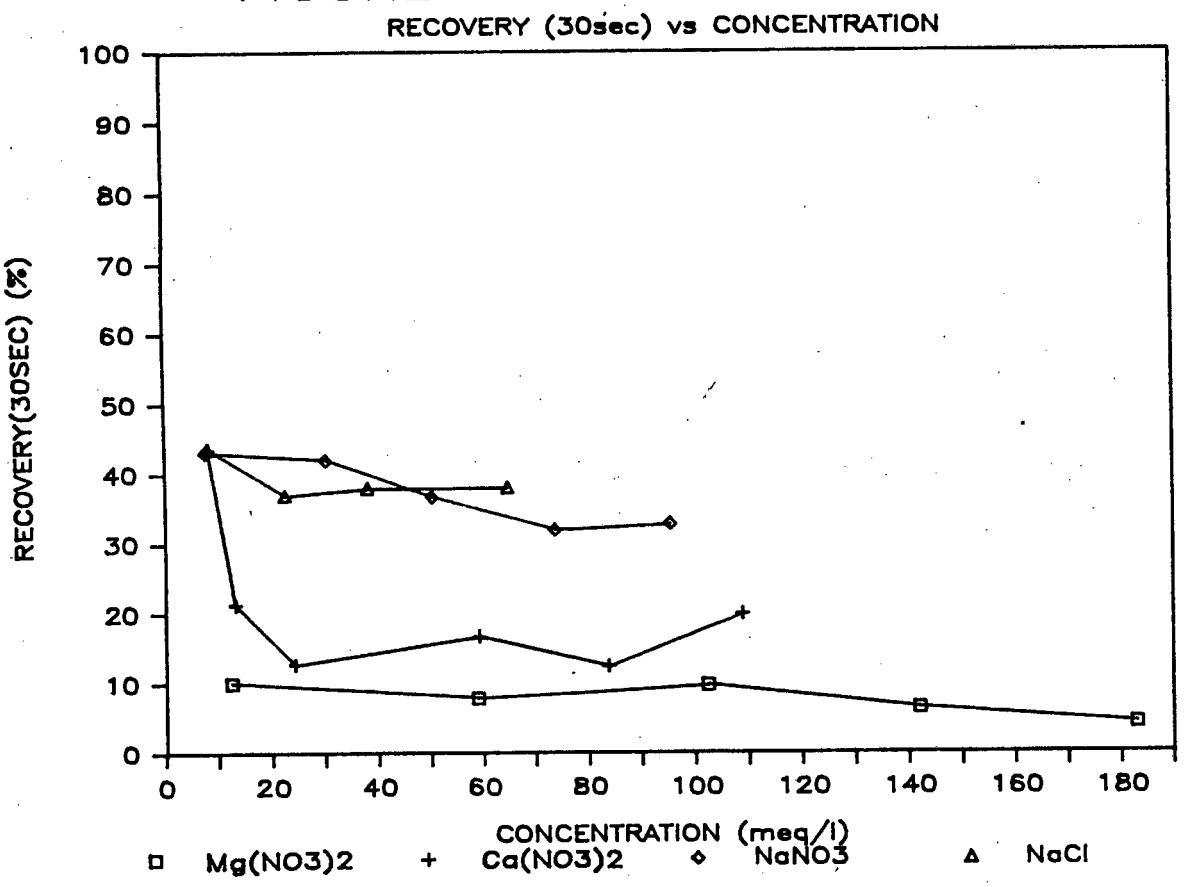

FIGURE 4.48 UNLEACHED ORE

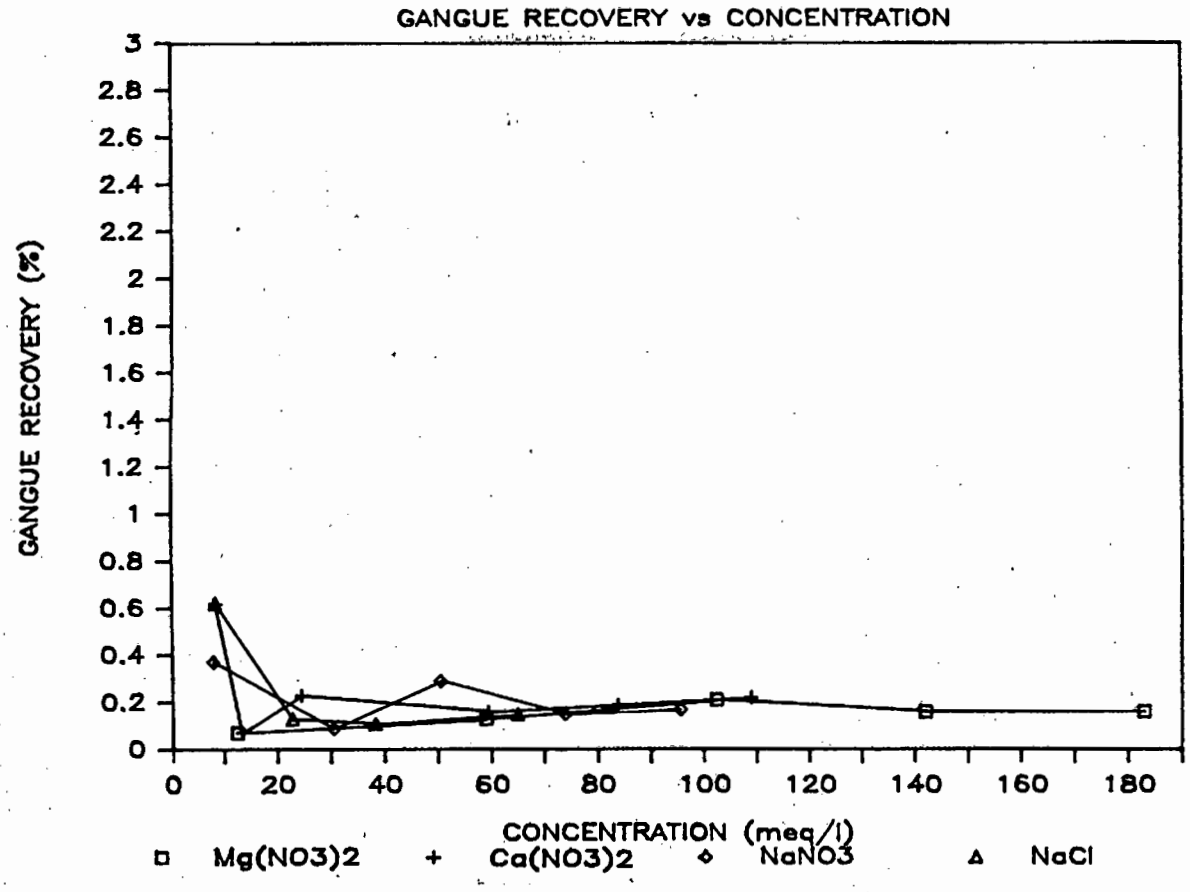

FIGURE 4.49 UNLEACHED ORE

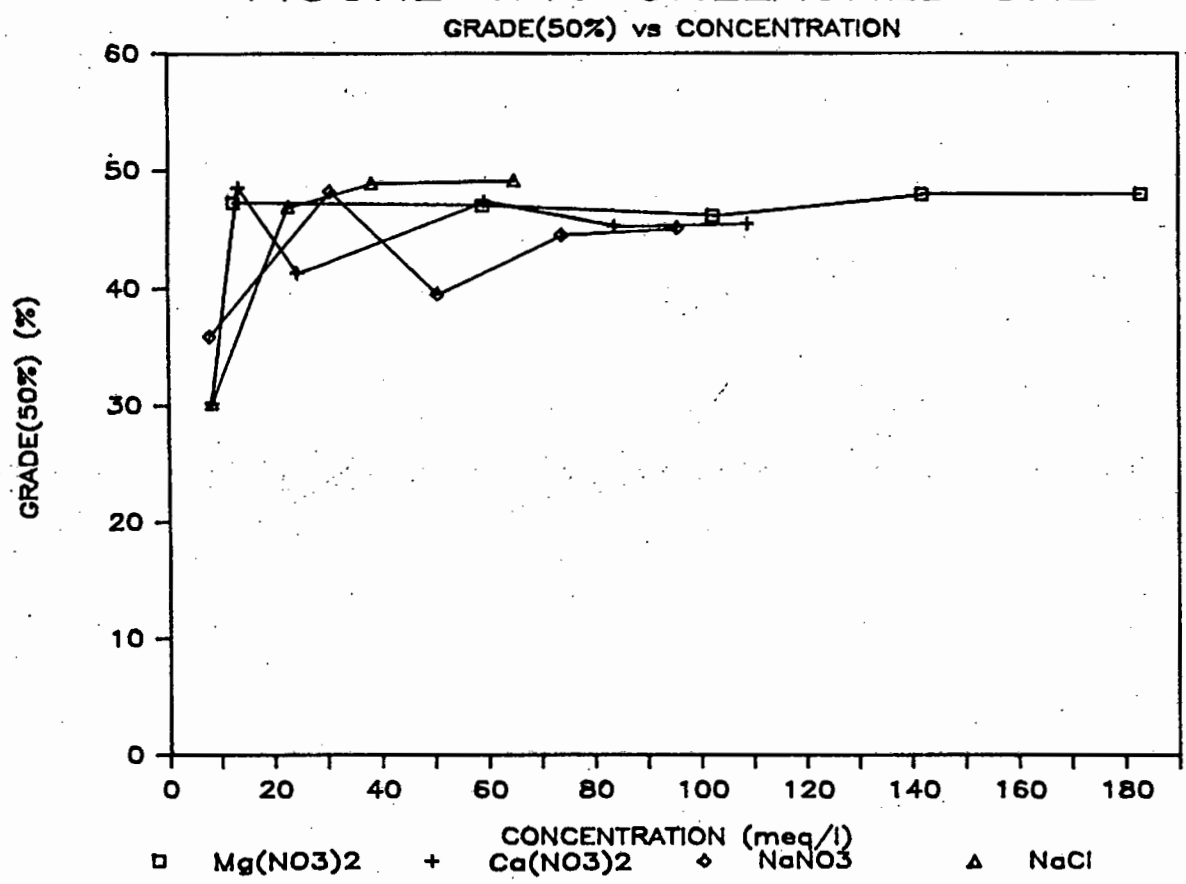

Table 4.12 Variation of Recovery and Grade with concentration of added ions using unleached ore

CONCENTRATION meq/l		R_{600}	R_{30}	R_{6600}	$G_{30\%}$
$Mg(OH)_2$	Magnesium Nitrate				
12,4		43,78	10,05	0,07	47,30*
17,3	41,7	61,63	7,89	0,13	47,03
19,1	83,3	66,02	9,73	0,21	46,16
17,0	125,0	63,18	6,40	0,16	48,01
16,3	166,7	63,26	4,23	0,16	48,00
$Ca(OH)_2$	Calcium Nitrate				
8,3		58,00	43,64	0,62	30,18
8,3	5	51,76	21,32	0,07	48,60
9,4	25	51,00	12,78	0,23	41,34
9,3	50	63,28	16,72	0,16	47,41
8,7	75	58,37	12,43	0,19	45,26
8,9	100	58,78	19,96	0,22	45,52
NaOH	$NaNO_3$				
7,9	0	54,76	43,09	0,37	35,89
8,7	21,7	53,56	41,97	0,09	48,22
6,9	43,5	54,21	36,69	0,29	39,52
8,5	65,2	52,03	31,90	0,15	44,53
8,5	87,0	55,00	32,73	0,17	45,14
$Ca(OH)_2$	NaCl				
8,3	0	58,00	43,64	0,62	30,18
8,6	14,1	55,85	37,01	0,13	46,96
8,7	29,5	62,07	38,00	0,11	48,96
8,6	56,3	66,63	38,06	0,15	49,18

* extrapolated point

From Figure 4.46 it can be seen that recovery increases slightly with concentration of ions. However there are no distinctive differences between the ions.

From Figure 4.47 it can be seen that the divalent cations, calcium and magnesium, have a much lower R_{30} and therefore rate of flotation. This is also shown by the froth formation time which is 15 seconds for all $NaNO_3$ and NaCl runs but increased with the addition of calcium and magnesium nitrate. The times were 20, 60, 60, 120 and 120 seconds for additions of 0, 500, 1000, 1500 and 2000ppm

respectively. An increased ion concentration after 25 eq/l had little effect on R_{30} for either of the ions.

From Figure 4.48 the gangue recovery decreased slightly with concentration. No differences between the ions can be seen.

In Figure 4.49 the grade at 50% recovery initially increased from 0 to 40 eq/l but thereafter remained fairly constant. No distinct differences between the ions can be seen.

Two runs were made to investigate the effect of the two ions, Na^+ and Ca^{++}, on the flotation of the ore at the natural pH of 3,7. The results are shown in Table 4.13.

Table 4.13 Flotation of oxidized ore at natural pH

CONCENTRATION	R_{600}	R_{30}	R_{6600}	$G_{50\%}$
50meq/l Ca^{++}	94,33	61,58	0,22	50,83
44 meq/l Na^+	93,35	64,49	0,23	51,17

There is very little difference between the effect of the two ions. When comparing these runs with those at pH 9 it can be seen that the recoveries are far higher but the grades and gangue recoveries are the same. The froth formation time was 15 seconds for both runs compared with the delay of 60 seconds when using calcium nitrate at pH9.

4.1.10 Effect of tap water on pyrite

The results of several runs using tap water are shown in Table 4.14. The analysis of the tap water has already been shown in Section 1.2.2 in Table 1.2.

Table 4.14 Effect of tap water on flotation

pH	CONCENTRATION	ORE	R_{600}	R_{30}	R_{6600}	$G_{50\%}$
10	10 meq/l Na^{+}	ox	57,43	46,03	4,06	10,56
10	20 meq/l Ca^{++}	ox	67,28	48,25	0,67	32,25
9	8 meq/l Na^{+}	ox	62,65	52,18	0,74	29,33
9	10 meq/l Ca^{++}	ox	66,82	49,02	0,32	40,55
9	1 meq/l Ca^{++}	leach	77,29	60,44	2,78	19,14

Very little dry froth occurred during these runs. From this table it can be seen that the addition of sodium results in lower grades and higher gangue recoveries than with calcium. Higher pH levels result in increased gangue recovery. Leaching the pyrite results in a higher recovery rate and gangue recovery and a lower grade.

When comparing values from Tables 4.9 and 4.12 it can be seen that the use of tap water results in increased recoveries and rates for oxidised ore but decreased recovery and rate for leached ore. With oxidised ore and sodium the use of tap water resulted in an increase in the grades at 50% recovery but with calcium it resulted in a decrease in grade. Tap water had little effect on the grade of leached ore. The gangue recovery increased using leached ore and calcium ions as well as oxidised ore and sodium ions but decreased using oxidised ore and calcium ions.

4.2 FROTH TESTS

4.2.1 Two phase system

The effect of calcium, magnesium and sodium ions on the froth height and breakdown rate of the two phase system (air and water) was investigated. De-ionised water and Cape Town tap water was used. The pH was 10.

The change of froth height with concentration of ions is shown in Figures 4.50 and 4.51. Detailed tables are given in Appendix H.

In Figure 4.50 and 4.51 it can be seen that the froth height increased with increasing concentration of sodium and magnesium but remained constant with increasing concentration of calcium ions. A comparison of the ions showed a decrease in froth height in the order of magnesium, sodium and calcium ions.

The greatest difference between tap water and de-ionised water was found in the calcium system where froth heights using tap water were double the heights using de-ionised water.

From the tables in Appendix H it can be seen that the species present in highest concentration in the calcium system is the Ca^{++} ion and in the magnesium system the $Mg(OH)_2$ precipitate.

The breakdown rates are shown in Figures 4.52 and 4.53.

The breakdown rate decreased with increasing concentration of ions using de-ionised water but remained fairly constant with tap water.

Using de-ionised water, the breakdown rate decreased in the order sodium, magnesium and calcium. Using the tap water there is very little difference between the ions.

FIGURE 4.50 DE-IONISED WATER

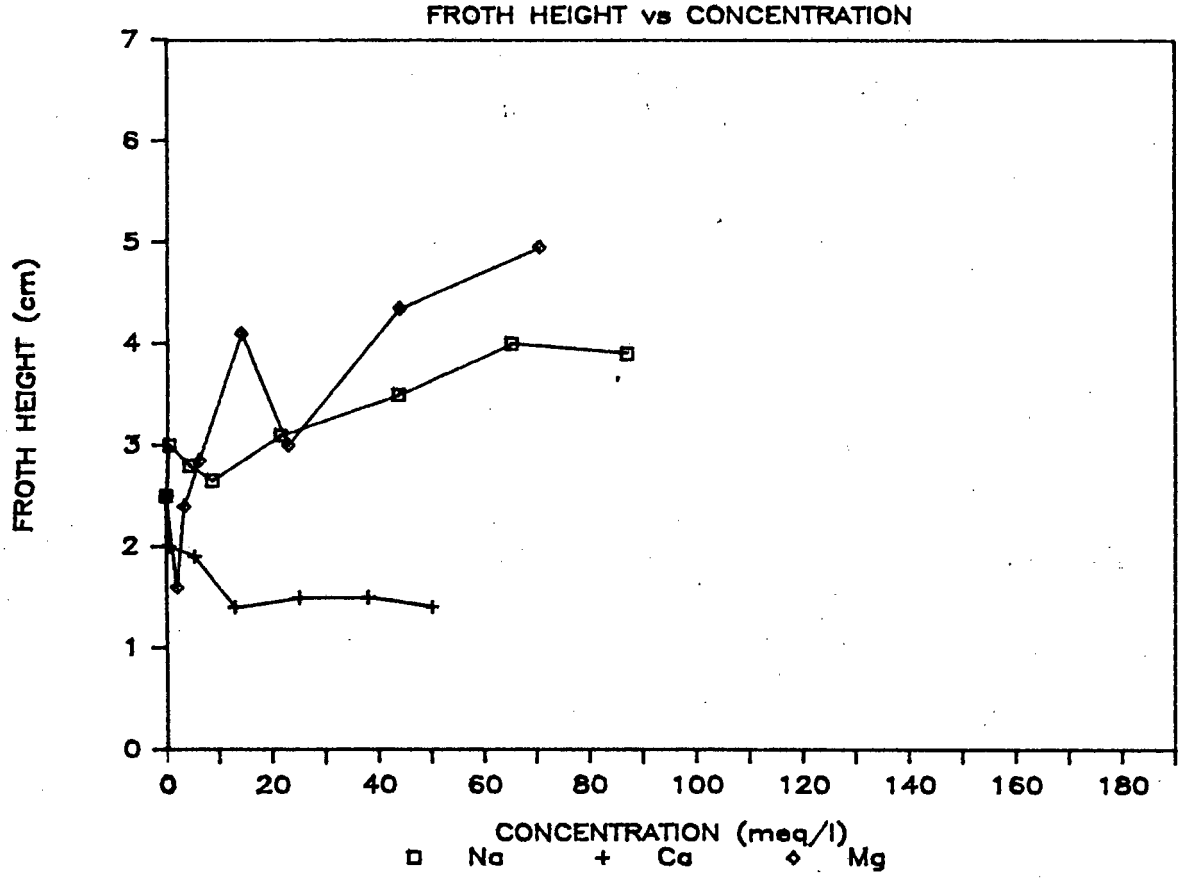

FIGURE 4.51 TAP WATER

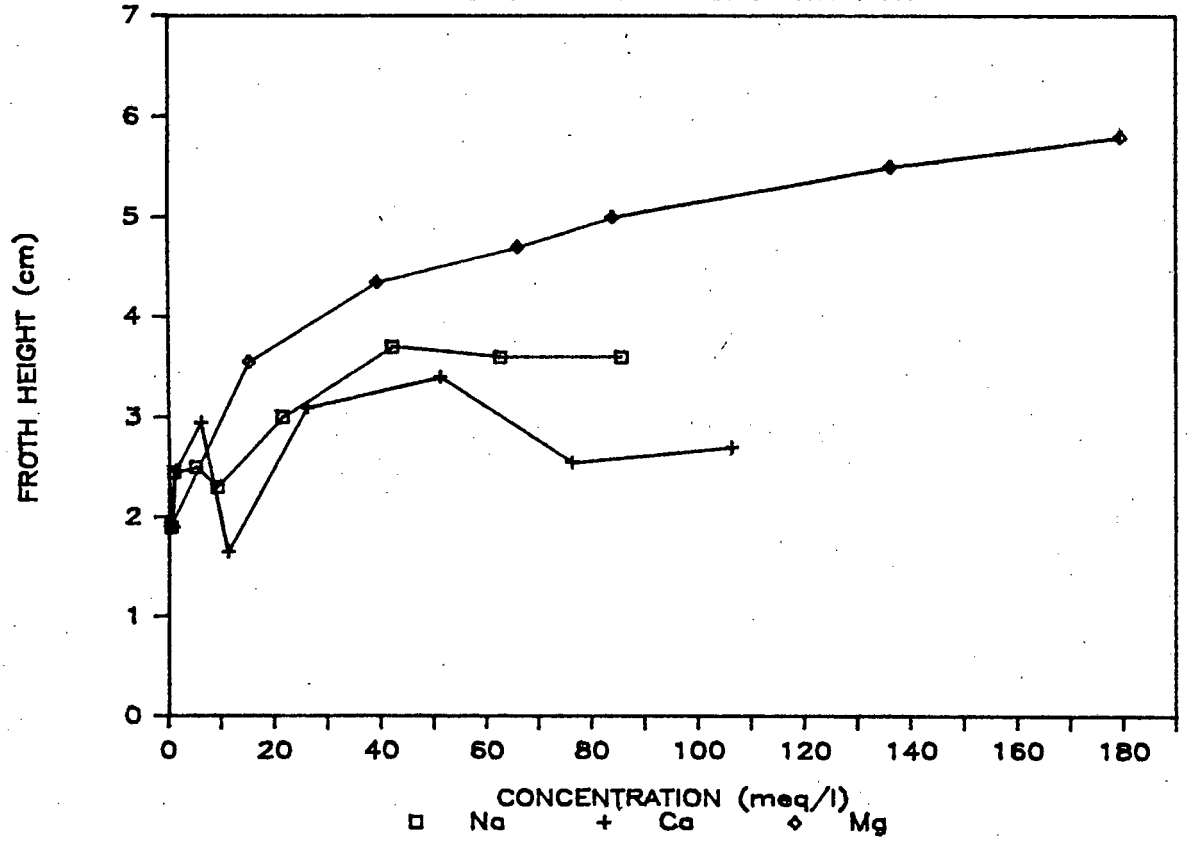

FIGURE 4.52 DE-IONISED WATER

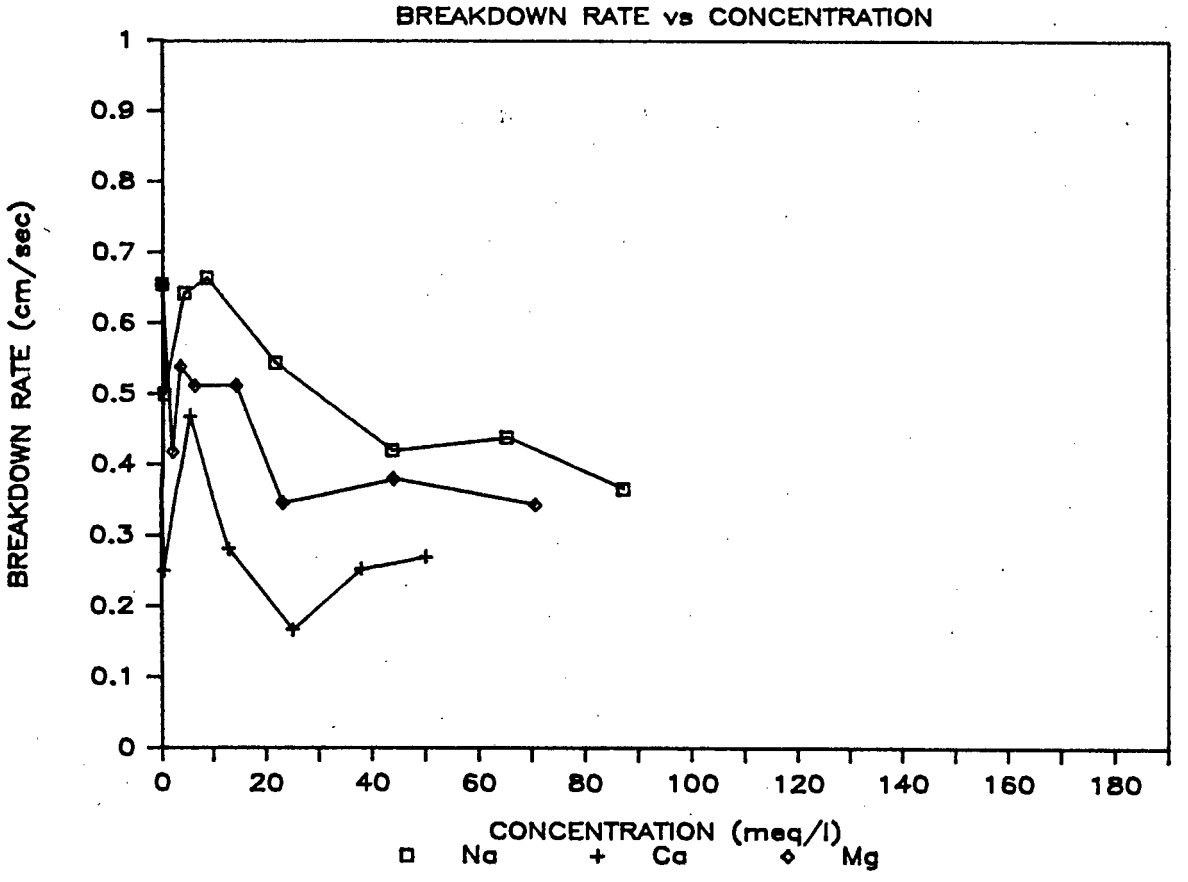

FIGURE 4.53 TAP WATER

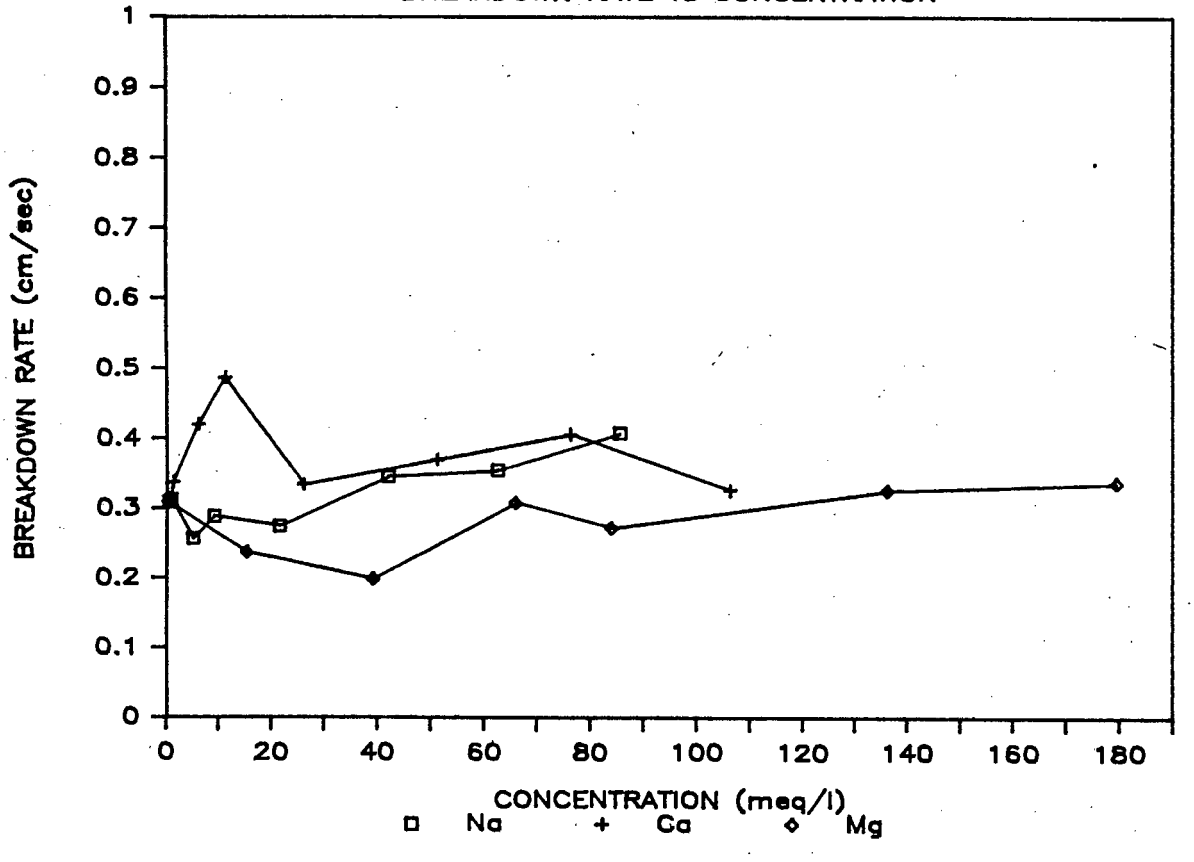

4.2.2 Three phase system

4.2.2.1 Quartz

The effect of calcium, magnesium and sodium ions on the froth height of the three phase system comprising quartz, air and water at pH 10 was investigated. De-ionised water and Cape Town tap water was used.

The change of froth height with concentration is shown in Figure 4.54 and 4.55.

Froth heights obtained were very low. Little difference can be seen with an increase in salt addition between the different ions or between tap and de-ionised water.

4.2.2.2 Quartz and Pyrite

The effect of sodium nitrate, calcium nitrate and sodium chloride on the three phase system comprising quartz, pyrite, air and water at pH 9 was investigated. De-ionised water was used.

The change of froth height and breakdown rate with concentration is shown in Figures 4.56 and 4.57. Detailed tables are given in Appendix H.

The froth height increased with increasing concentration of all ions. Calcium nitrate and sodium nitrate have similar heights with calcium producing the highest froths. Sodium chloride produced significantly lower froths at low addition rates.

Breakdown rates increased slightly with increased concentration of sodium nitrate and sodium chloride but remained fairly constant with increasing concentration of calcium nitrate. The breakdown rate using calcium nitrate was slightly higher initially than the other two salts.

Two runs using oxidised pyrite and calcium nitrate are also shown in Figure 4.56. The froth height obtained is approximately half of that obtained using leached pyrite.

FIGURE 4.54 DE-IONISED WATER AND QUARTZ

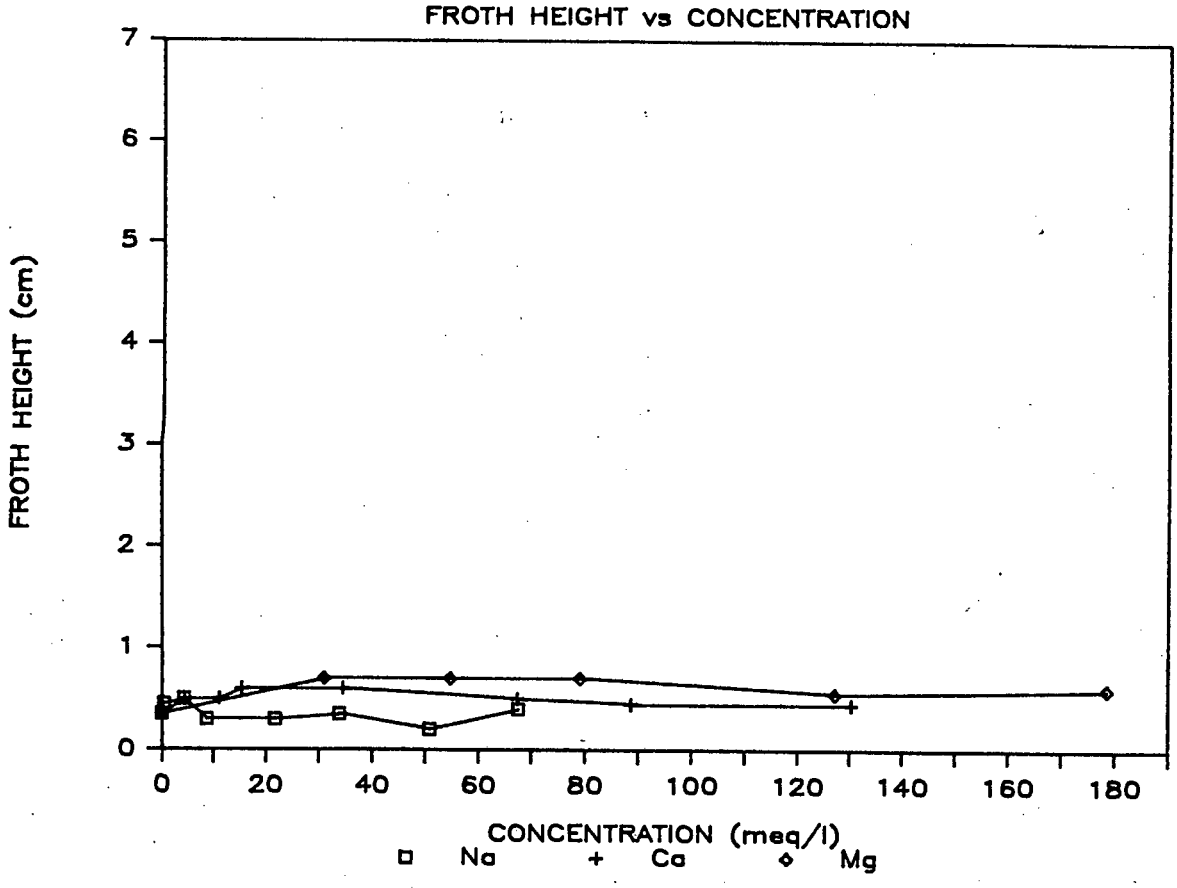

FIGURE 4.55 TAP WATER AND QUARTZ

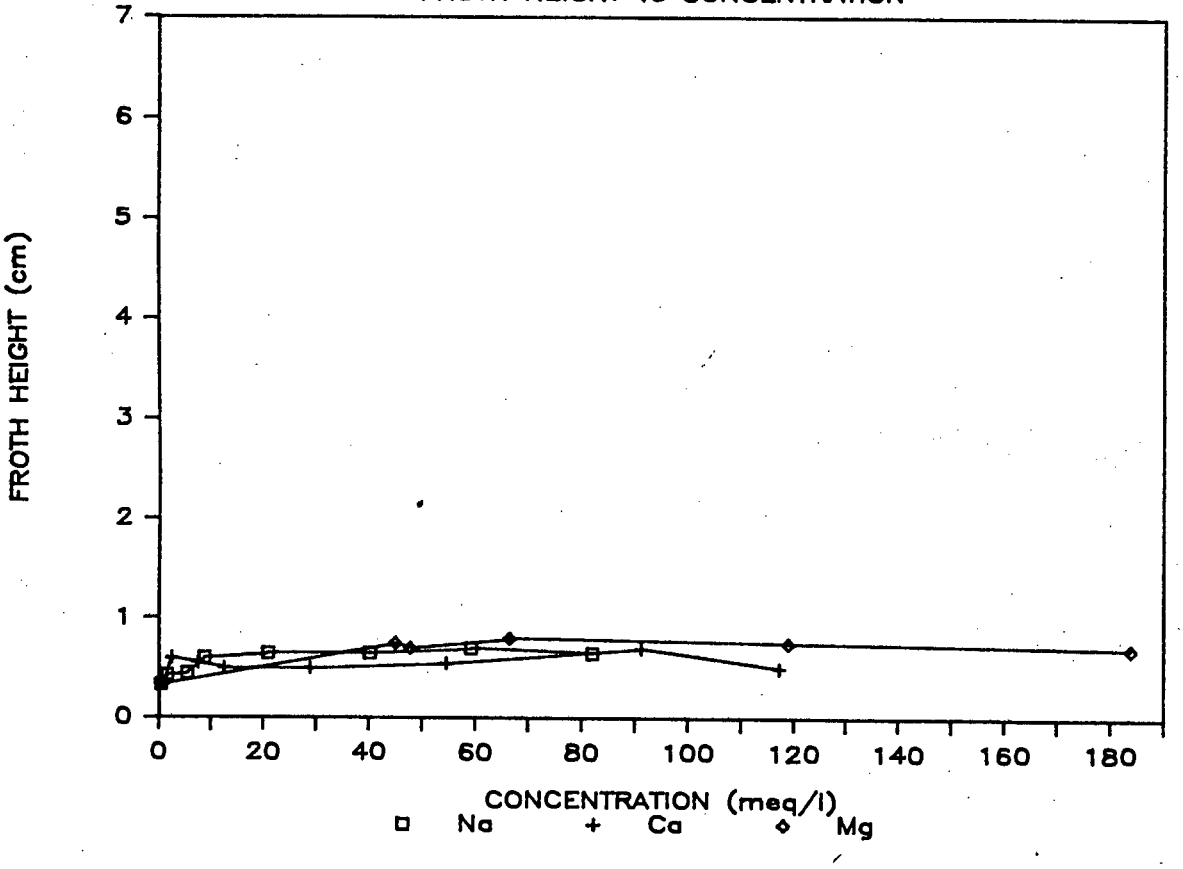

FIGURE 4.56 QUARTZ AND PYRITE

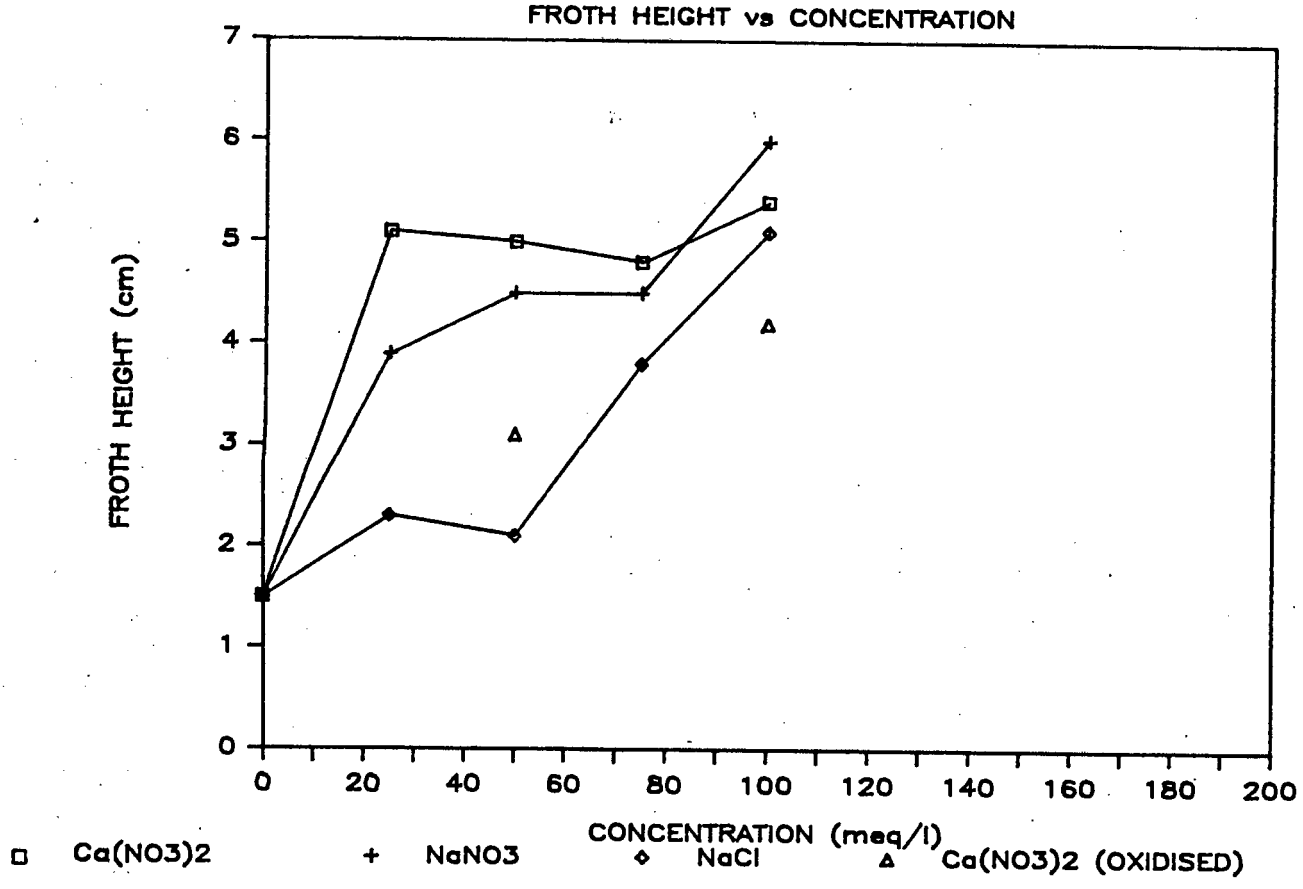

FIGURE 4.57 QUARTZ AND PYRITE

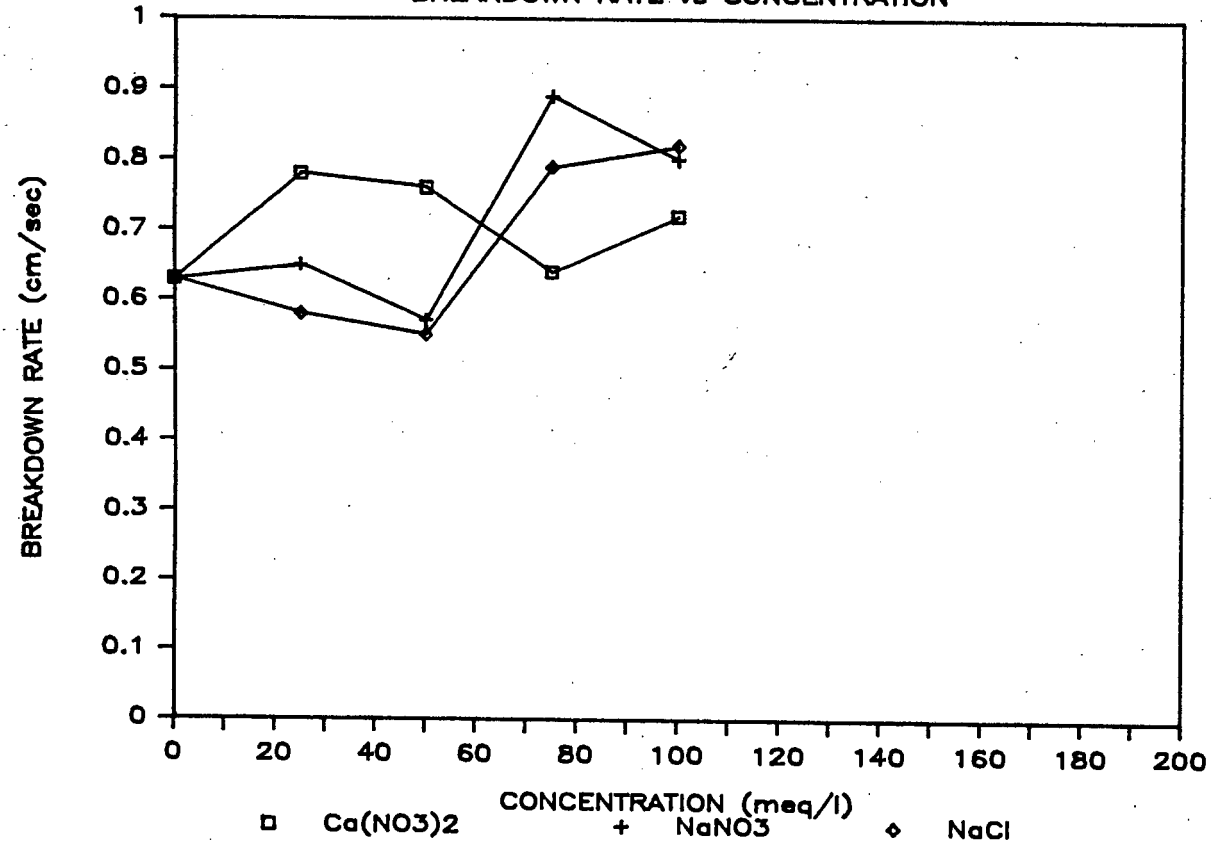

4.3 ADSORPTION TESTS

4.3.1 Effect of ions on sodium ethyl xanthate

The effect of five ions on the adsorbance of sodium ethyl xanthate was investigated using a U.V. spectrophotometer.

The five ions used were calcium nitrate, magnesium nitrate, sodium nitrate, sodium chloride and sodium sulphate.

The results are shown in Figure 4.58.

The ions have no effect on the adsorbance of SEX at the peak at 300 nm. The peak at 220 nm using sodium, calcium and magnesium nitrate is due to the nitrate peak.

Figure 4.58 Effect of Ions on Sodium Ethyl Xanthate

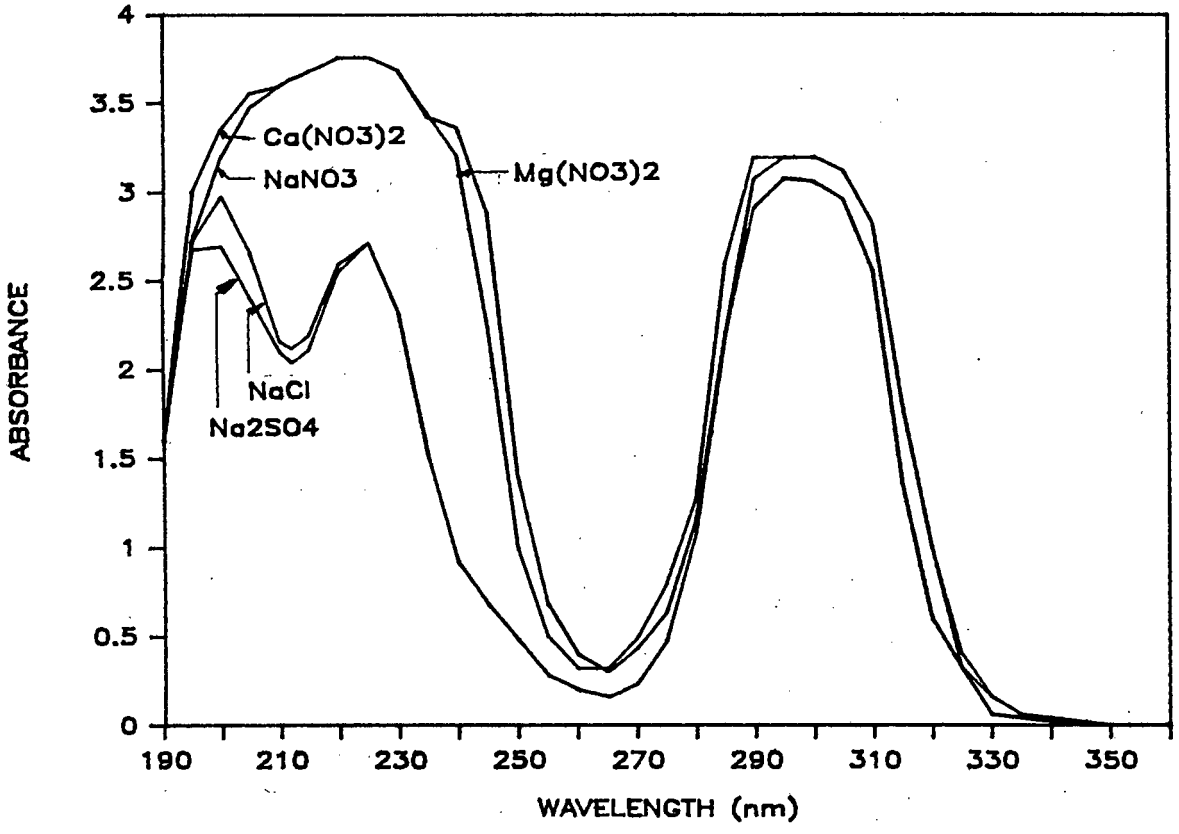

4.3.2 The effect of ions on the adsorbance of SEX by pyrite

4.3.2.1 Reproducibility

The reproducibility of the method is shown in Figure 4.59. The average standard deviation for A/A_0 is ±0,02.

Figure 4.59 also shows the difference between leached and unleached ore. There is far less xanthate adsorption onto unleached ore. The reproducibility using unleached ore is poor.

4.3.2.2 The effect of ions

The effect of sodium nitrate, sodium chloride, calcium chloride and calcium nitrate on the adsorption of SEX was investigated at two addition rates, viz 50 and 100 meq/l.

The adsorption-time curves are shown in Figures 4.61 to 4.64 and the adsorption-concentration curve in Figure 4.60 and listed in Table 4.15.

Table 4.15 Effect of ions on adsorption of SEX on pyrite

ION	CONCENTRATION meq/l	A/AO 240 sec
$NaNO_3$	0	0,226
	50	0,368
	100	0,484
$Ca(NO_3)_2 \cdot 4H_2O$	0	0,226
	50	0,307
	100	0,418
NaCl	0	0,226
	50	0,226
	100	0,222
$CaCl_2$	0	0,226
	50	0,188
	100	0,177

The adsorption decreases slightly with calcium chloride, remains constant with sodium chloride and increases with calcium nitrate and sodium nitrate.

FIGURE 4.59 ADSORPTION vs TIME

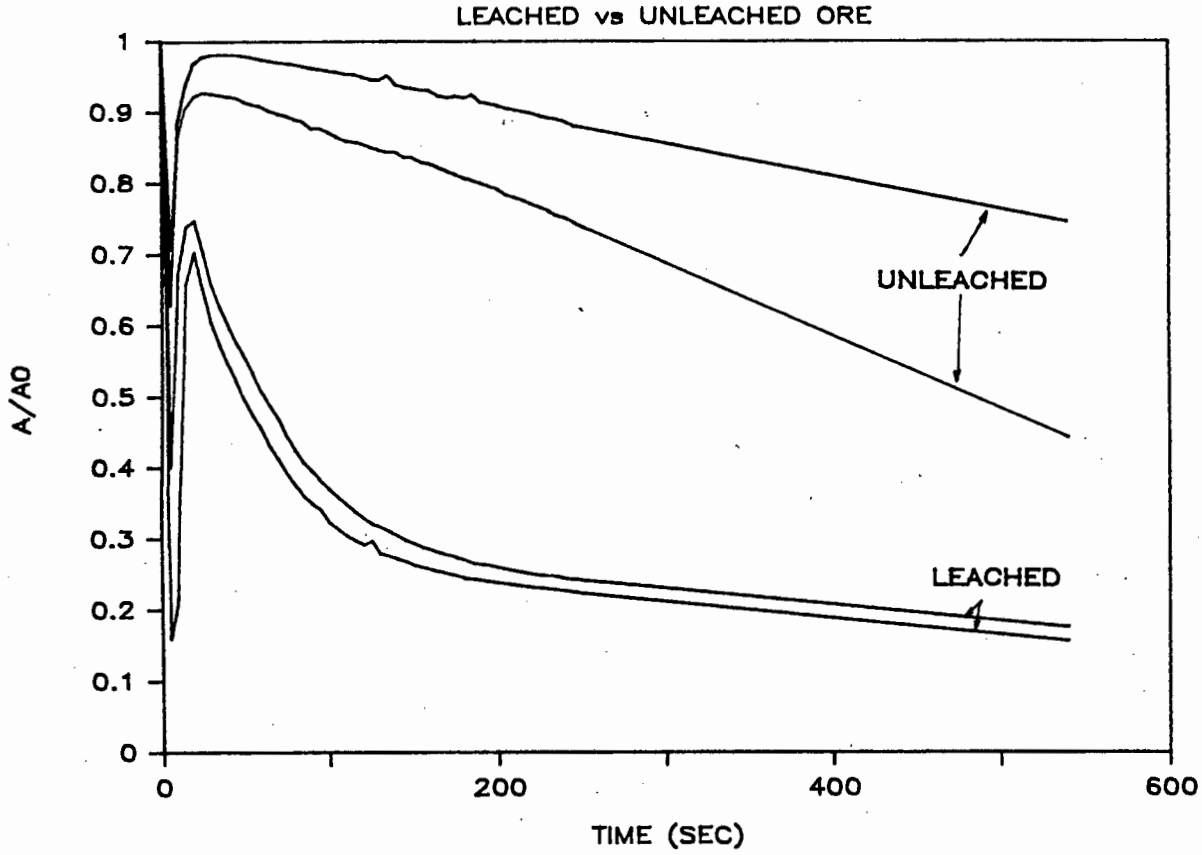

FIGURE 4.60 ADSORPTION vs CONCENTRATION

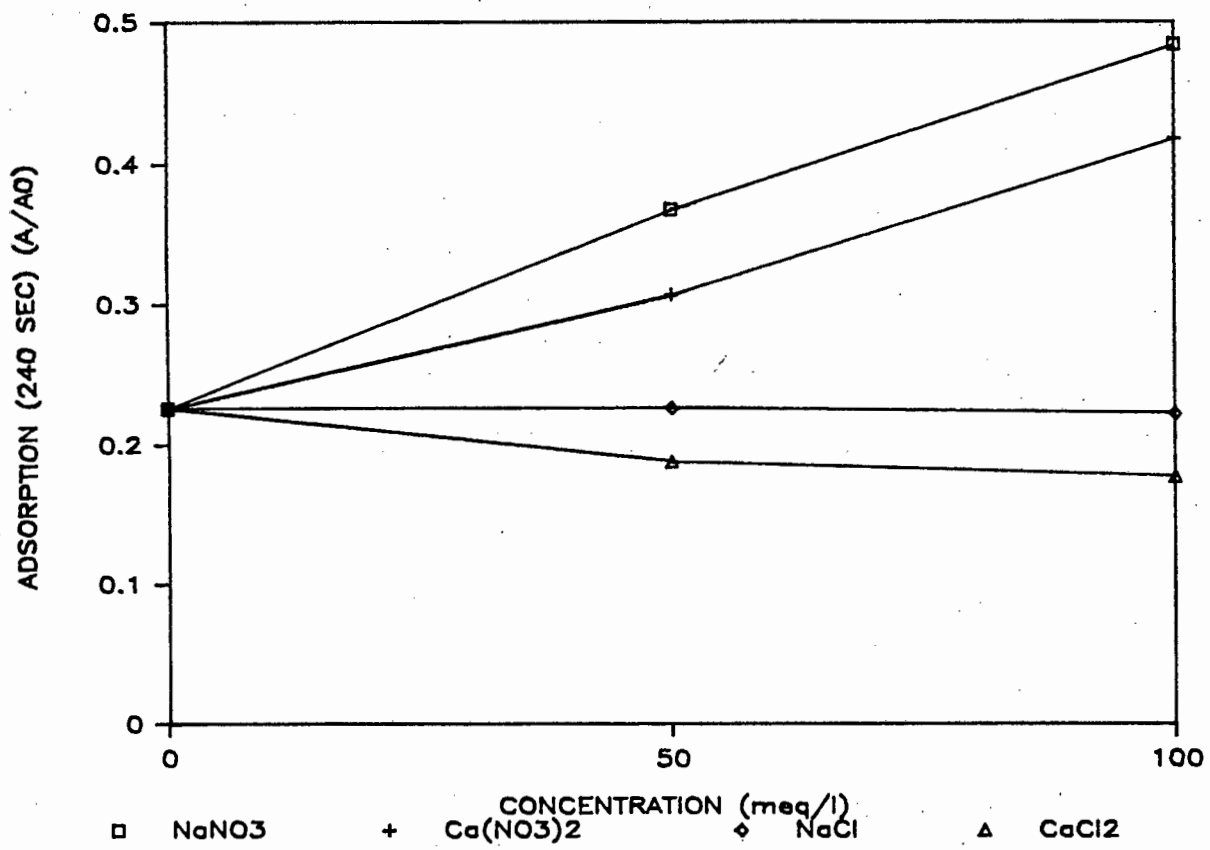

FIGURE 4.61 ADSORPTION vs TIME

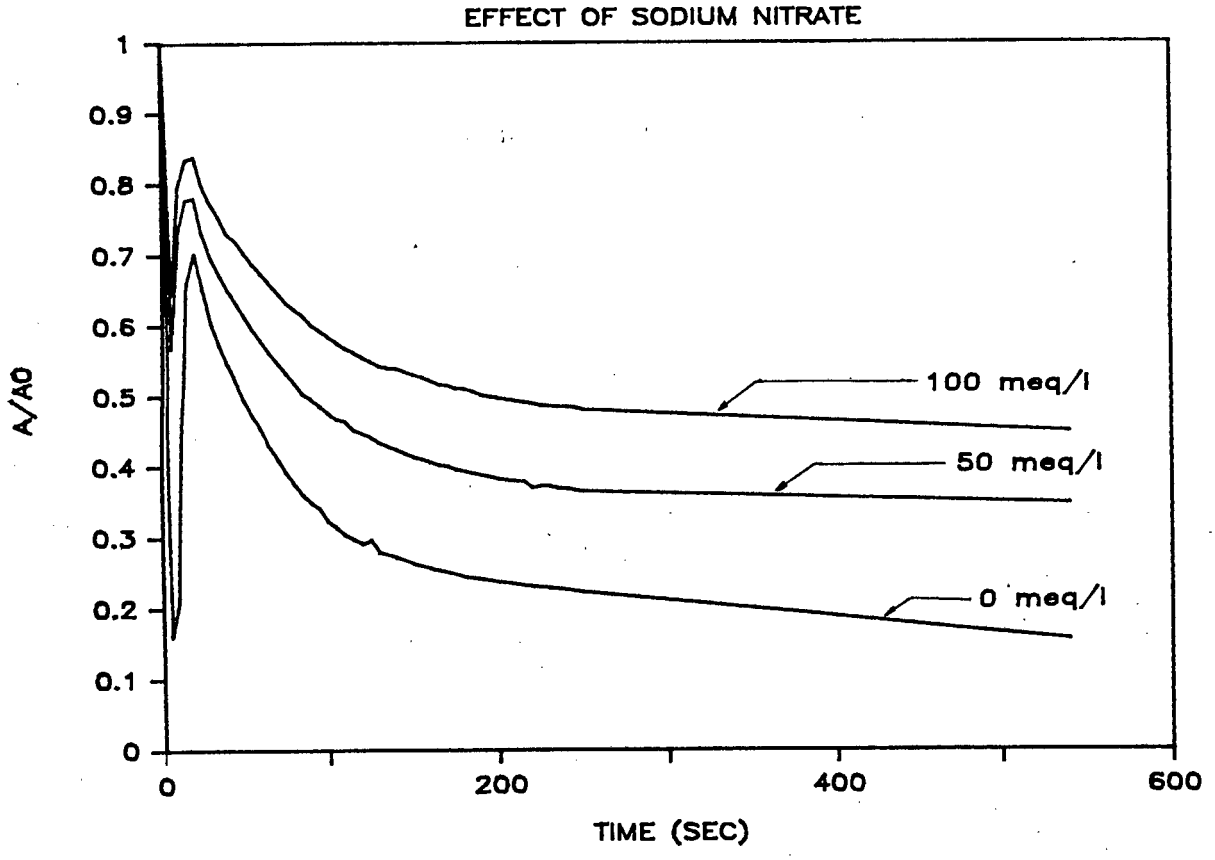

FIGURE 4.62 ADSORPTION vs TIME

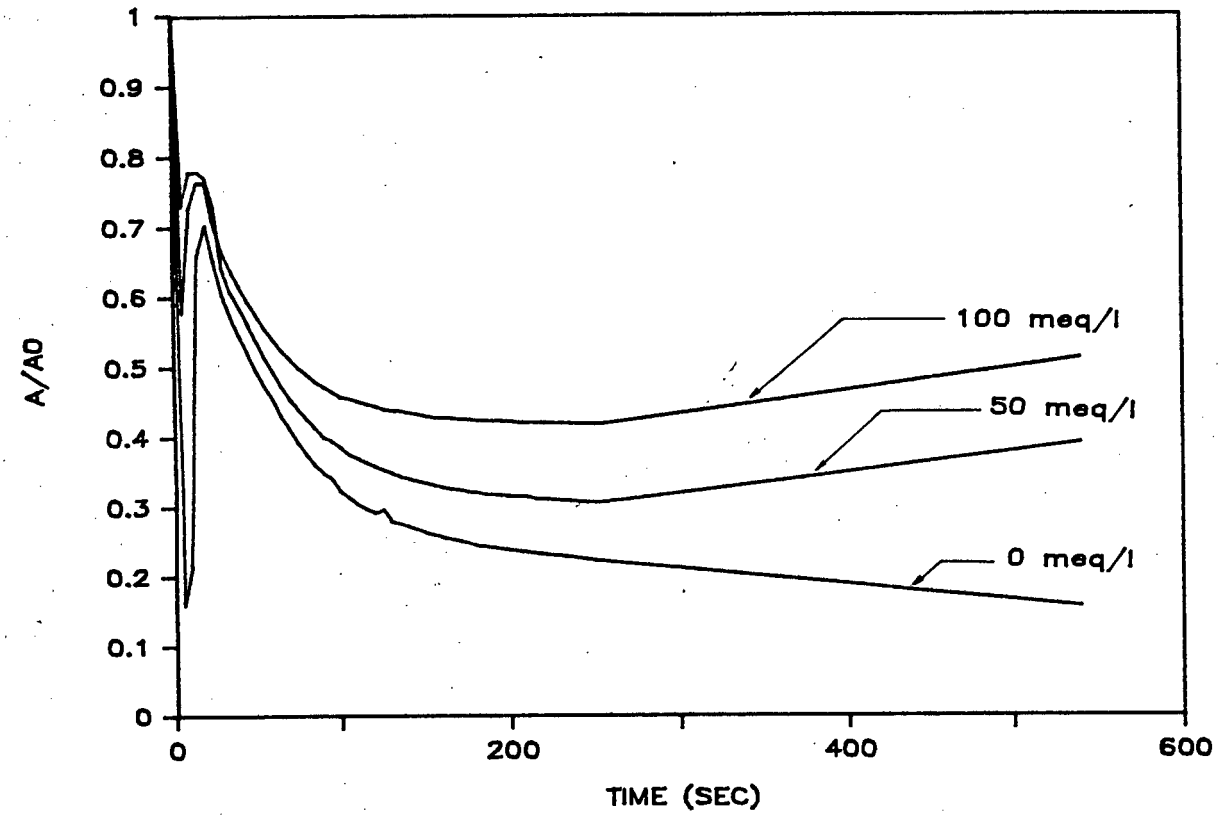

FIGURE 4.63 ADSORPTION vs TIME

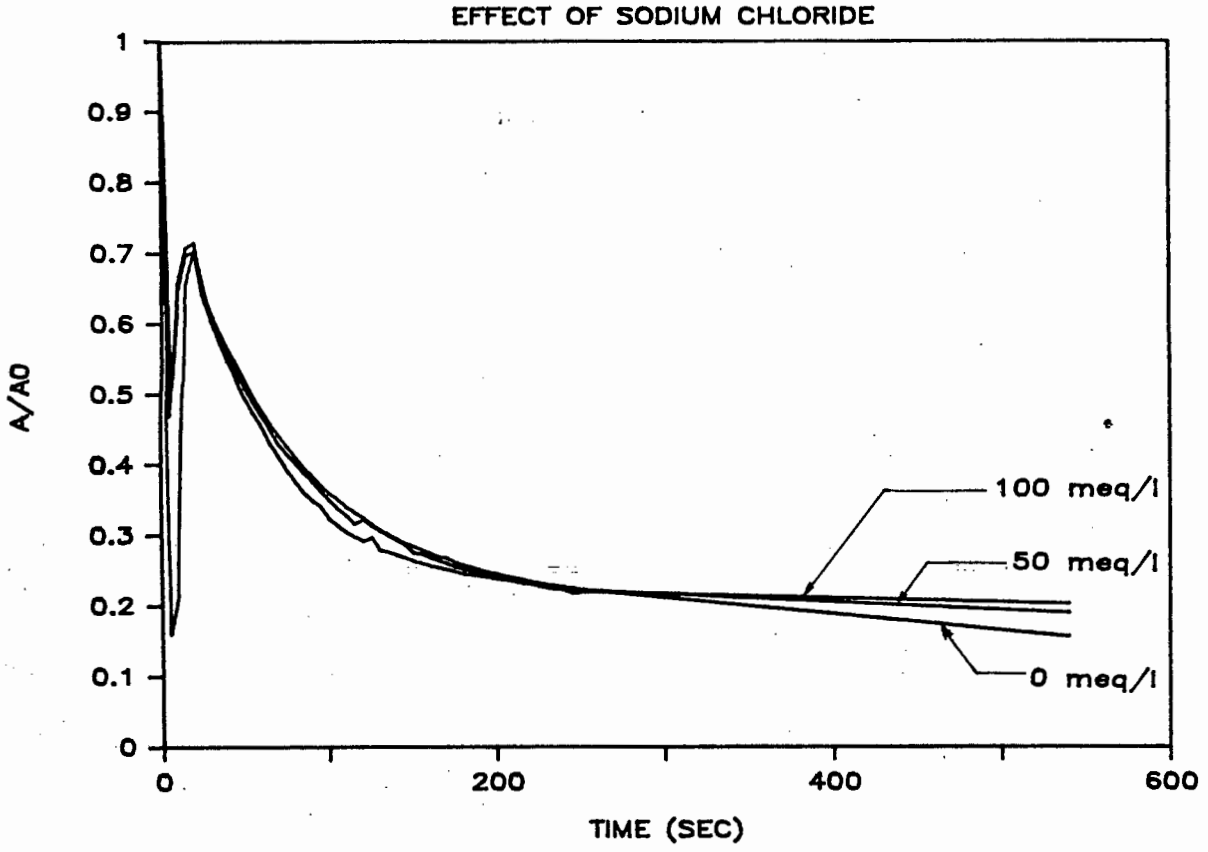

FIGURE 4.64 ADSORPTION vs TIME

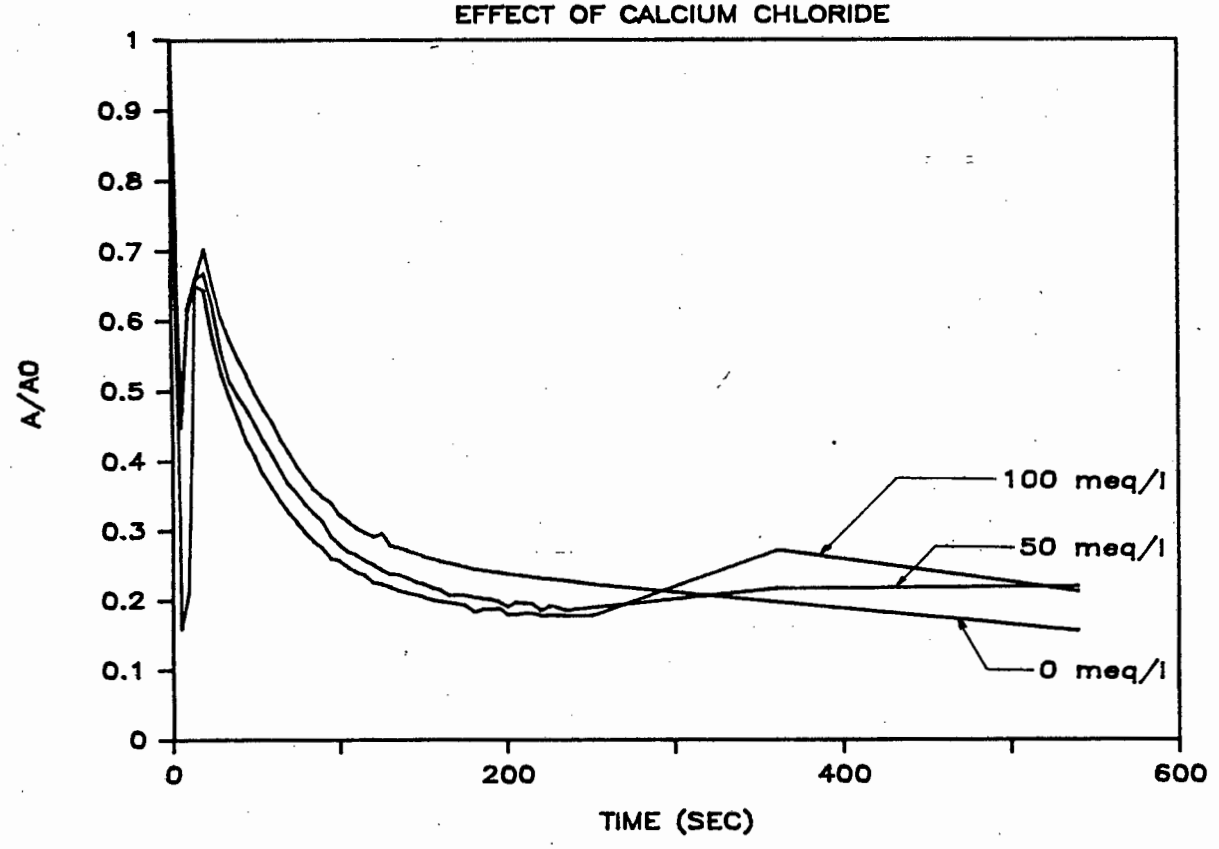

5. DISCUSSION

From the flotation experiments it was found that the most reproducible system was that using leached pyrite and the collector, sodium ethyl xanthate (SEX). Further it was established that the the modified Leeds cell produced acceptable reproducibility. A paddle was used to remove the froth. Different pH values, collector concentrations and the presence of trace organics did not have a significant effect on the reproducibility. A pH of 9 was selected as at this pH the predominant species formed upon the addition of the nitrate salts are the Ca^{++} and Mg^{++} ions. At higher pH values calcium hydroxide ions and magnesium hydroxide precipitates are formed.

The improvement in reproducibility with the use of leached ore in the flotation tests was also reflected in the reproducibility of the adsorption tests (Figure 4.59).

Oxidised pyrite is covered with a layer of iron hydroxide. The surface however is not uniformly oxidized (Wark and Sutherland 1955) and this probably accounts for the poor reproducibility obtained.

The improved reproducibility obtained when using SEX as opposed to SIBX was possibly due to the decrease in the extent of the occurence of "dry froth" when using SEX. It has been found that hydrophobic particles with high contact angles (usually above 90° but possibly lower depending on the particle shape) cause destabilization of the froth. Since SIBX is a stronger collector than SEX with the contact angles for SIBX and SEX being 78° and 60° respectively (Glembotski V.A. 1970), the above observation may be due to the hydrophobicity resulting from the two collectors. It has also been found that galena and KEX (contact angle equal to 60°) tended to destabilize froth less than galena and KHX (contact angle of 80°) (Dippenaar 1978). The effect of longer chained xanthates on the froth stability is said to be due to the effect of the larger contact angle which

results in the replacement of water by the air at the solid-water-air interface. The elutriation of the water in the bubble film is increased resulting in a dryer froth and possible rupture of the bubble wall (Wark and Sutherland 1955).

The best froth removal method was found to result from using the paddle which avoids the effect of variables such as contamination from the porous plate or changes in water flow rate through the plate.

Three major effects were found in these flotation tests carried out on leached ore:

(i) There was a general increase in recovery as the concentration of the inorganic salts increased. This was accompanied by a decrease in "dry froth" after additions of 50 meq/l for the sodium salts and 25 meq/l for calcium and magnesium nitrate.

(ii) The rate, as expressed by R_{30}, remained unchanged with increased addition of sodium salts but decreased upon addition of magnesium or calcium nitrate. The froth formation time remained 13 seconds for all concentrations of sodium salts but increased from 13 to 30 seconds for additions from 0 to 100 meq/l of both magnesium and calcium nitrate.

(iii) When magnesium or calcium nitrate was added, the grades increased sharply from 0 to 25 meq/l but remained constant with a further increase in concentration. This is accompanied by a sharp decrease in gangue and water recovery. There was a slight increase in grade and water recovery and a decrease in gangue recovery as the concentration of sodium salts increased.

The results of the adsorption tests showed that the calcium, sodium, chloride and nitrate ions had no effect on the characteristic absorption wavelength of SEX, thus indicating that these ions did not complex with the collector molecules and change their chemical nature. The addition of calcium

nitrate or sodium nitrate resulted in a decrease in SEX adsorption but the addition of sodium or calcium chloride had no effect on the adsorption. Thus the nitrate ion seems to cause the decrease in adsorption, though the reason for this is not known. Unleached ore adsorbed very little SEX.

The results of the froth tests showed that the froth height increased with an increase in concentration of any of the ions. In the three phase system, viz. pyrite, quartz and de-ionised water, the froth height decreased in the order calcium nitrate, sodium nitrate and sodium chloride whereas in the two phase system it decreased in the order magnesium, sodium and calcium nitrate. The breakdown rates for the ions in the three phase system were similar but in the two phase system decreased in the order sodium, magnesium and calcium. The use of unleached ore resulted in a decrease in froth height.

Experimental results have shown a slight decrease in quartz recovery with sodium ions and a significant decrease in quartz recovery with the divalent ions. The main effects of an increased addition of cations on quartz has been found to be a decrease in electrokinetic potential (Klaasen and Mokrousov 1963), thus causing the compression of the double layer, a decrease in electrostatic repulsion and coagulation of particles. It has been found that the mechanism of quartz recovery is mainly due to the entrainment of fine particles (Dimou 1985, Trahar W.J. 1981). Therefore if the quartz were to coagulate, the larger particles formed might not be entrained, thus resulting in a cleaner froth, higher grades and less gangue recovery. Less quartz is recovered when using calcium and magnesium than sodium ions and this may be due to the fact that the coagulation phenomenon is more pronounced when using divalent salts (Yarar and Kitchener 1970, Read and Hollick 1976). In addition, the froth stability tests using quartz showed no increase in the natural floatability of quartz with the addition of the Ca^{++} or the Mg^{++} ions. The recovery of quartz by anionic flotation has been found to occur at pH values greater than

10 where the predominant species, $CaOH^+$ ions and $Mg(OH)_2$ precipitate are said to activate the quartz (Iwasaki et al 1980).

Anions do not affect quartz recovery as quartz has a negative charge and would thus repel these ions.

The effect of the cations on the adsorption of the collectors on the pyrite has been shown to be negligible. The addition of sodium nitrate however, causes the zeta potential of pyrite to become less negative (Fuerstenau D.W. and Mishra R.K. 1980) and this could, as in the case of quartz, result in the coagulation of pyrite. Very fine particles (-10μm), unlike larger particles, tend not to adhere to the bubbles in the pulp during collisions. Therefore a possible result of cation addition to the pulp, especially divalent cations, could be to cause pyrite coagulation with a resultant increase in bubble mineralization in the pulp.

The effect of the anions on the pyrite varied. Chloride ions had no effect on the adsorption of xanthate whereas nitrate ions resulted in decreased xanthate adsorption. This would usually imply that nitrate ions would cause lower recoveries. The flotation tests however, did not indicate this, and thus it is unlikely that the changes in extent of reagent adsorption due to the presence of ions have any significant effect on subsequent recoveries.

In the froth phase the main components are ions, water and solid particles. The effects of particles on the froth phase is dependent on their size, hydrophobicity and quantity. Fine hydrophobic particles tend to break the froth by accelerating the coalescence of bubbles whereas larger hydrophobic particles slow down bubble coalescence (Lovell 1976). Therefore the decrease in "dry froth" with ion concentration could be due to coagulation of pyrite particles and a resultant increase in froth stability. The effect of the "dry froth" is to decrease the mass pull which

results in a decrease in recovery. Therefore the observed increase in recovery with ion concentration may be due to the increased froth stability caused by coagulation of pyrite particles.

The effect of particle loading is to decrease the rate of ascent of the bubbles (Wark and Sutherland 1955). As the rate of flotation is proportional to the rate of ascent of bubbles, the more loaded the bubble the slower will be the rate of flotation. From the flotation runs it can be seen that the water recovery is lower for the divalent ions than the sodium ions with the water content in the concentrate being respectively 70 to 75% of the mass of the concentrate as opposed to 80 to 85%. Therefore divalent ions appear to produce more heavily mineralized bubbles which have a slow rate of ascent and thus a slow rate of flotation (Figure 4.32).

In the froth tests the increase in froth height with increased ion concentration is due to an increase in the froth stability. This was also shown by the froth stabilizing effect of tap water on flotation (resulting in higher water recovery) and the stable froth obtained with unleached Ergo ore which increased the ionic strength of the pulp. The flotation results also showed a decrease in "dry froth" with an increase in the concentration of ions. It has been found that ions in the two phase system without frother increase the viscosity and the film drainage time which results in a decrease in coalescence which then increases the froth stability (Parekh et al 1983). Other researchers have found that electrolytes decrease film stability in the presence of various frothers (Wark and Sutherland 1955). However these tests were not done with the frother, DF400, and results might differ with different types of frother and different concentrations of ions.

In studying the flotation of oxidized ore the following observations were made:

(i) The recovery increased with ion concentration but the recovery levels were 20% lower than those found with unleached ore.

(ii) The rates expressed by R_{30} for calcium and magnesium nitrate decreased sharply initially with an increase in ion addition from 0 to 25 meq/l after which the rates remained constant. The rates were unaffected by increased concentration of sodium salts.

(iii) The grades for all the salts were high with the associated low gangue recovery.

Clearly the oxidation of the pyrite resulted in low recoveries. The adsorption tests also showed that far less xanthate was adsorbed onto the pyrite. This effect would contribute to a decreased recovery. The three phase froth tests without collector also showed a reduced froth height for the oxidised ore indicating that the natural floatability of the pyrite was reduced.

The other effects are very similar to those observed for the leached ore system and the same mechanisms are proposed. However the lack of good reproducibility in the oxidised system makes interpretation of these results difficult.

In the two phase froth stability tests using tap water it was found that the froth heights increased and breakdown rates decreased compared to the case for de-ionized water. It was also shown that the ions in tap water increased the froth stability in flotation tests. The effects of using tap water were probably due to the effect of ions present. The froth stability increased, resulting in a higher mass pull due to a decrease in "dry froth" and a higher gangue recovery.

6. CONCLUSIONS

This work has investigated the effect of various ions on pyrite flotation at a pH of 9. A minimum concentration of any ions is necessary in order to stabilize the froth and thus produce a reasonable recovery of pyrite.

An increase in the concentration of the monovalent cation, sodium, resulted in an increase in pyrite recovery and a slight decrease in gangue recovery. Further it resulted in a decrease in "dry froth" formation thus showing that froth stability improved with ion addition. The adsorption of xanthate ions however, was not affected by the cation addition.

An increase in the concentration of the divalent cations, calcium and magnesium, resulted in an increase in pyrite recovery, and a sharp decrease in gangue recovery and the rate of flotation. Froth stability improved with the addition of the cations. Xanthate adsorption was not affected by the divalent cations.

The addition of the nitrate anion resulted in a reduction in the adsorption of xanthate on the pyrite. This however did not have a significant effect on the flotation of pyrite. The other anions did not differ significantly in their effect on the pyrite flotation, froth stability or the adsorption of xanthate.

Particle size has a considerable effect on froth stability and therefore the effect of univalent and divalent cations in conjunction with the effect of particle size should be considered. Other species such as the calcium hydroxide ion or magnesium hydroxide precipitate which occur at higher pH values might also be significant in the pyrite or quartz flotation and should be investigated.

REFERENCES

Allison, S.A., Goold, L.A, Nicol, M.J. and Granville, A, A determination of the products of reaction between various sulfide minerals and aqueous xanthate solution, and a correlation of the products with electrode rest potentials, Metallurgical Transactions, Vol 3, October 1972

Butler, J.M., Ionic Equilibrium - a Mathematical Approach, Addison Wesley Publishing Co 1964.

CRC Handbook of Chemistry and Physics, Ed R.C. Weast, 61st edition, CRC Press 1980

Dimou, A, MSc Thesis, U.C.T., 1986

Dippenaar, A. and Harris, P.J., The effect of particles on the stability of flotation froths, MINTEK Report No 1988, 1978

Dudenkov, S.V. and Livshits, A.K., Effect of collectors on the dispersion of air bubbles, Tvet. Metally, vol 32,. No 7, 1959

Finch, J.A. and Smith, G.W., Contact angle and wetting, Minerals Sci Engng, Vol 11, No 1, Jan 1979

Fuerstenau, D.W., Mineral-water interfaces and the electrical double layer, Principles of Flotation, Ed R.P. King, SAIMM, Johannesburg, 1982

Fuerstenau, D.W. and Fuerstenau, M.C., The flotation of oxide and silicate minerals, Principles of Flotation, Ed R.P. King, SAIMM, Johannesburg, 1982

Fuerstenau, D.W. and Mishra, R.K., On the mechanism of flotation with xanthate collectors, Complex Sulphide Ores, Pap. Conf. 1980, 271-8(Eng), Ed Jones, M.J., Inst. Min. Metall, London

Fuerstenau, M.C., Sulphide mineral flotation, Principles of Flotation, Ed R.P.King, SAIMM 1982

Fuerstenau, M.C., Elgillani D.A. and Miller J.D., Adsorption mechanisms in non-metallic activation systems, AIME Transactions, Vol 247, 1970

Glembotskii, V.A., The hydrophobization effect of anionic collectors during flotation, Flotation Agents and Effects, Editor V.I. Solnyshkin, AKADEMIA NAUK SSR 1970.

Glembotskii, V.A., Klassen, V.I. and Plaksin, I.N., Flotation, Primary Sources, New York 1972

Goldhaber, M.B., Experimental study of metastable sulfur oxyanion formation during pyrite oxidation at pH 6-9 and 30°, American Journal of Science, Vol 283, March 1983

Gaudin, A.M., Flotation, 1st Edition, McGraw-Hill Book Company, New York and London, 1932

Gaudin, A.M. and Charles, W.D., Trans. AIME, 196, p195, 1953

Harris, P.J., Frothing phenomena and frothers, Principles of Flotation, Ed R.P. King, SAIMM 1982

Heerema, R.H. and Iwasaki, I, Chemical precipitation of alkaline earth cations and its effect on flocculation and flotation of quartz, Mining Engineering, October 1980

Hoberg, H, Loesche, T. and Schneider, F.-U, Investigations on the floatability of sulphides after dry grinding, Aufbereitungs-Technik, Nr 4, 1985

Hoover, M.R., Water chemistry effects in the flotation of sulphide minerals - a review and discussion for molybdenite, Conference: Complex Sulphide Ores, Inst Min Metall, London 1980

Iwasaki, I, Smith, K.A., Lipp, R.J and Sato, H, Effect of calcium and magnesium ions on selective desliming and cationic flotation of quartz from iron ores, Fine Particles Processing, Ed P. Somasundaran, AIME, 1980

James, R.O. and Healy, T.W., Adsorption of hydrolyzable metal ions at the oxide-water interface, J. Colloid & Interface Science, Vol 40, No 1, July 1972

Klaasen, V. and Mokrousov, V., An Introduction to the Theory of Flotation, London, Butterworths 1963

Klimpel, R.R., The engineering analysis of dispersion effects in selected mineral processing operations, Fine Particles Processing, Ed P. Somasundaran, AIME, 1980

Laskowski, J and Iskra, J, Role of capillary effects in bubble-particle collision in flotation, Trans Instn Min Metall, Vol 79, 1970

Lloyd, P.J.D., The flotation of gold, uranium and pyrite from Witwatersrand ores, Journal of South African Institute of Mining and Metallurgy, February 1981

Loewenthal, R.E. and Marais, G. vR, Carbonate Chemistry of Aquatic Systems: Theory and Application, Ann Arbor Science, Michigan 1976

Lovell, V.M., Froth characteristics in phosphate flotation, A.M. Gaudin Memorial Volume, Vol 2, Ed M.C. Fuerstenau, 1976

Majima, H., Electrochemistry of pyrite and its significance in sulphide flotation, AIME Centennial Annual Meeting, New York, 1971

OFS Metallurgical Scheme, Anglo American Corporation of South Africa Ltd, September 1981

Palmer, B.R., Gutierrez, B. and Fuerstenau, M.C., Mechanism involved in the flotation of oxides and silicates with anionic collectors: Part 1 and 2, American Institute of Mining, Metallurgical and Petroleum Engineers, V 258, 1975

Parekh, V.V, Raper, J.A. and Jameson, G.J., The effect of electrolyte concentration on froth stability, CHEMECA 83, 11th Australian Chemical Engineering Conference, Brisbane, 1983

Perry, R.H. and Chilton, C.H., Chemical Engineers Handbook, 5th edition, International Student Edition, McGraw Hill, 1973

Pryor, E, Mineral Processing, 3rd Ed, Elsevier Co Pty Publishing 1965

Read, A.D and Hollick, C.T., Selective flocculation technique for recovery of fine particles, Miner Sci. Eng., Vol 8, No 3, July 1969

Read, A.D. and Kitchener, J.A., Wetting films on silica, J. Colloid Interface Sci., Vol 30, No 3, July 1969

Ross, V.E., Dunne, R.C. and Burger, R., The flotation of pyrite from Buffelsfontein mine material, MINTEK Report, 1984

Shaw, P., Characterisation of frothers, SAIMM Colloquium, 1983

Trahar, W.J., A rational interpretation of the role of particle size in flotation, International Journal of Mineral Processing, Vol 8, 1981

Viviers, J.M.P., The effect of water quality on mineral flotation, MINTEK Report, 1979

Wark, I.W. and Sutherland, K.L., Principles of Flotation, Australasian Institute of Mining and Metallurgy 1955

Warren, L.J., Determination of the contributions of true flotation and entrainment in batch flotation tests, Int. J. of Mineral Processing, 14, 1985

Westwood, R.J., Stander, G.S. and Carlisle, H.P., The recovery of pyrite at Government Gold Mining Areas Limited, Journal of South Africa Institute of Mining and Metallurgy, Jan. 1970

Yarar, B. and Kitchener, J.A., Selective flocculation of minerals, Inst. Min. Metall. Trans., Sec C, Vol 76, 1970

APPENDIX A : SULPHUR ANALYSIS

1. METHOD

The sulphur content of the pyrite samples was determined by burning the pyrite in oxygen at a high temperature in a Leco induction furnace. Combustion products obtained were SO_2 and SO_3. The SO_2 produced was then analysed using the iodate titration method.

The reactions during the titration are:

$$KIO_3 + KI + 6HCl \rightarrow 3I_2 + 6KCl + 3H_2O$$

$$SO_2 + I_2 + 2H_2O \rightarrow H_2SO_4 + 2HI$$

The iodine and starch indicator form a complex which gives the solution a blue colour. The addition of SO_2 reduces the iodine to iodide thus removing this complex and therefore the blue colour. The addition of KIO_3 as a titrant is used to maintain a light blue colour in the solution throughout the reaction.

The experimental procedure was:

1. A sample with a mass of approximately 0,05g was placed in a disposable ceramic crucible. A vanadium pentoxide disc was placed inside the crucible which was covered with a porous ceramic disc.
2. The sample was placed in a Leco induction furnace. The Variac setting was 230V with a grid current of 100mA and a plate current of approximately 250mA.
3. The oxygen flow (purified through a bed of magnesium perchlorate) was set at 0,5 l/min.
4. The combustion products were titrated with a 1,1125 g/l KIO_3 solution for 5 minutes after which it was assumed that the reaction was complete.

2. ANALYSIS

From the known volume of KIO_3 the mass of SO_2 can be calculated. However an unknown volume of SO_3 was also produced during combustion of the pyrite. Therefore to calculate the total percentage sulphur in pyrite, the percentage of sulphur in SO_2 released has to be multiplied by a calibration factor. This calibration factor was determined from MINTEK standards and the mean of 3 analyses done for each sample. The factors are shown in Table A1.

Table A1 : Calibration Factors obtained for MINTEK Standards

MINTEK STANDARD	MEAN	CALIBRATION FACTOR
1,15	1,084	1,061
7,3	7,125	1,025
13,9	13,010	1,068
33,3	30,666	1,085
50,15	46,337	1,082

From these results it was decided to use different calibration factors for different percentage sulphur ranges. These factors were calculated by taking the average of two calibration factors found in the range selected. The factors are shown in Table A2.

Table A2 : Calibration Factors used in Sulphur Analysis

PERCENTAGE SULPHUR	CALIBRATION FACTOR
Less than 1%	1,061
1-5%	1,049
5-10%	1,051
10-20%	1,059
20-40%	1,078
Greater than 40%	1,084

The percentage of sulphur in the sample can then be calculated from the volume of KIO_3, the mass of the sample

and the calibration factor. The calculations are shown below.

$KIO_3 + KI + 6HCl \rightarrow 3I_2 + 6KCl + 3H_2O$

$SO_2 + I_2 + 2H_2O \rightarrow H_2SO_4 + 2HI$

$$\text{Titre of } KIO_3 = Vml * \frac{1,1125g}{1000ml} * \frac{1mol}{214g}$$

1 mol KIO_3 reacts with 3 mol SO_2

mol SO_2 released = V * 3 * 1,1125E-3 / 214
mol S released = V * 1,1125E-3 / 71,33
mass S released = V * 1,1125E-3 / 2,229
% S released = mass S released / mass of sample * 100
= V / (mass * 20,037)

This result is then multiplied by the calibration factor to obtain the final value.

APPENDIX B : CALCULATION OF GRADE AND RECOVERY

1. GRADE

$$\text{Grade (cumulative \%S)} = \frac{C_1 c_1 + C_2 c_2 + \ldots + C_n c_n}{C_1 + C_2 + \ldots + C_n} * 100$$

where C_i = mass of fraction i
c_i = sulphur analysis of fraction i

2. RECOVERY

$$\text{Recovery } R = \frac{C_1 c_1 + C_2 c_2 + \ldots + C_n c_n}{Ff} * 100$$

where F = mass of feed
f = % S in feed

3. GANGUE RECOVERY

$$\% \text{ pyrite} = \% S * \frac{\text{mass of 1 mol } FeS_2}{\text{mass of 2 mol S}}$$
$$= \% S * 1,875$$

therefore
$f_g = 100 - 1,875 * f$
$c_{gi} = 100 - 1,875 * c_i$

$$\text{Recovery of gangue } R_g = \frac{C_1 c_{g1} + C_2 c_{g2} + \ldots + C_n c_{gn}}{Ff_g} * 100$$

where f_g = % gangue in feed
c_{gi} = % gangue in concentrate i

APPENDIX C : KLIMPEL MODEL

Grade and recovery data are calculated using the values of sulphur assays and concentrate masses as shown in Appendix B.

A model has been developed by Klimpel analysing the recovery-time profile. This model shown below is based on the assumption that the size of the feed is approximately uniform.

The model is:

$$r = R \{ 1 - (1/kt)(1 - \exp(-kt))\}$$

where r - cumulative recovery at time t
k - first order rate constant of total mass removal
R - ultimate equilibrium recovery at time t - ∞

(Klimpel 1980)

The values of R and k are obtained by Nelder-Mead optimisation minimising the error between calculated and observed values of r. The Nelder-Mead program is shown in Appendix D.

APPENDIX D : NELDER-MEAD OPTIMISATION PROGRAM

```
10 REM ************************************************************
20 REM *                                                          *
30 REM * This program uses a Nelder - Mead optimisation method to *
40 REM * approximate the constants in the Klimpel model. The      *
50 REM * constants are : " R " = ultimate recovery      and       *
60 REM *                 " k " = rate constant                    *
70 REM *                                                          *
80 REM ************************************************************
90 CLS : PRINT "    KLIMPEL  MODEL   ":PRINT "     ==============  "
100 DIM T(20),R(20),RR(20),E1(20)
110 REM
120 REM
130 REM * INPUT DATA *
140 REM
150  PRINT "READ YIELD TIME DATA":PRINT:PRINT
160 INPUT "NO OF DATA POINTS ",N
170 FOR I = 1 TO N
180 INPUT "TIME";T(I):INPUT "RECOVERY";R(I)
190 NEXT I
200 CLS : LOCATE 2,1 : PRINT "TIME (s)" : LOCATE 2,20 : PRINT "RECOVERY (%)"
210 P=4
220 FOR I = 1 TO N
230 LOCATE P,1 : PRINT T(I)
235 LOCATE P,20 : PRINT USING "##.##";R(I)
236 LOCATE P,45 : PRINT "OK Y/N"
240 A$=INKEY$:IF A$="" THEN 240
250 IF A$="Y" OR A$="y" THEN 290
260 INPUT "INPUT NUMBER OF DATA POINT",I
270 INPUT "TIME= ",T(I):INPUT "RECOVERY",R(I)
280 LOCATE P,1 :PRINT T(I) :LOCATE P,20 : PRINT R(I)
290 P=P+1
300 NEXT I
310 REM * NELDER -MEAD OPTIMISATION *
320 N2 = 2 :AL = 1 :BT = .5 :GM = 2
330 A = 1
340 DIM F(N2 + 5),X(N2+5,N)
350 X(1,1) = R(N)
360 X(1,2) = .075
370 FL = N2
380 P = A/FL/SQR(2)*(FL-1+SQR(FL+1))
390 Q1 = A/FL/SQR(2)*(SQR(FL+1)-1)
400 LOCATE 10,45 : PRINT "I AM CALCULATING - BE PATIENT"
410 FOR I =  2 TO N2+1
420 FOR J = 1 TO N2
430 IF J = I-1 GOTO 450
440 X(I,J) = X(I,J)+Q1 : GOTO 460
450 X(I,J) = X(I,J)+P
460 NEXT J : NEXT I
470 FOR I = 1 TO N2 + 1
480 GOSUB 1380
490 NEXT I
500 IB = 1 :IW = 1
510 FOR I = 1 TO N2 + 1
520 IF F(I) < F(IB) THEN IB = I
530 IF F(I) > F(IW) THEN IW = I
    NEXT I
```

```
550 FOR J = 1 TO N2
560 X(N2+2,J) = 0
570 FOR I = 1 TO N2 +1
580 X(N2+2,J) = X(N2+2,J) + X(I,J)
590 NEXT I
600 X(N2+2,J) = (X(N2+2,J) - X(IW,J)) / FL
610 NEXT J : I = N2+2
620 GOSUB 1380
630 EP = 0
640 FOR I = 1 TO N2 + 1
650 EP = EP + (F(I)-F(N2+2))*(F(I)-F(N2+2))
660 NEXT I
670 EP = SQR((EP-(F(IW)-F(N2+2))*(F(IW)-F(N2+2)))/FL)
680 IF EP < .00001 GOTO 1090
690 FOR J = 1 TO N2
700 X(N2+3,J) = X(N2+2,J) +AL * (X(N2+2,J) - X(IW,J))
710 NEXT J : I = N2 +3
720 GOSUB 1380
730 IF F(N2+3) > F(IW) GOTO 760
740 IF F(N2+3) > F(IB) GOTO 790
750 GOTO 930
760 FOR J = 1 TO N2
770 X(N2+4,J) = X(N2+2,J)-BT*(X(N2+2,J)-X(IW,J))
780 NEXT J :I = N2 + 4 : GOTO 820
790 FOR J = 1 TO N2
800 X(N2+4,J) = X(N2+2,J)- BT*(X(N2+2,J) - X(N2+3,J))
810 NEXT J : I = N2 +4
820 GOSUB 1380
830 IF F(N2+4) > F(IW) GOTO 880
840 FOR J = 1 TO N2
850 X(IW,J) = X(N2+4,J)
860 NEXT J
870 F(IW) = F(N2+4) : GOTO 500
880 FOR I = 1 TO N2+1
890 FOR J = 1 TO N2
900 X(I,J) =( X(I,J) + X(IB,J))/2
910 NEXT J : NEXT I
920 GOTO 470
930 FOR J = 1 TO N2
940 X(N2+5,J) = X(N2+2,J) + GM * (X(N2+3,J)-X(N2+2,J))
950 NEXT J :I = N2+5
960 GOSUB 1380
970 IF F(N2+5) < F(IB) GOTO 1030
980 FOR J = 1 TO N2
990 X(IW,J) = X(N2+3,J)
1000 NEXT J
1010 F(IW) = F(N2+3)
1020 GOTO 500
1030 FOR J = 1 TO N
1040 X(IW,J) = X(N2+5,J)
1050 NEXT J
1060 F(IW) = F(N2+5)
1070 GOTO 500
1080 REM * OUTPUT DATA *
1090 CLS : LOCATE 10,1:PRINT STRING$(80," ")
1100 LOCATE 2,1 : PRINT "TIME (s)" : LOCATE 2,20 : PRINT "RECOVERY (%)"
1110 FOR I = 1 TO N:P=3+I
1120 LOCATE P,1 :PRINT T(I) :PRINT B$ : LOCATE P,20 :PRINT R(I)
1130 NEXT I
1140 LOCATE 14,10 :PRINT " MIN = ";F(IB)
1150 LOCATE 16,10 :PRINT "   R = ";X(IB,1)
1160 LOCATE  18,10 :PRINT "   K = ";X(IB,2)
1170 LOCATE 2,40 :PRINT "PRED. RECOVERY "
```

```
1180 FOR J = 1 TO N
1190 LOCATE 3+J,45 :PRINT RR(J)
1200 NEXT J
1210 LOCATE 22,1
1220 INPUT "TO LINE PRINTER Y/N ",A$
1230 IF A$="N" OR A$="n" THEN 1360
1240 LPRINT TAB(1) "TIME (s)" ;
1250 LPRINT TAB(20) "RECOVERY (%)";
1260 LPRINT TAB(40) "PRED. RECOVERY"
1270 FOR I = 1 TO N:P=3+I
1280 LPRINT TAB(1) T(I) ;
1290 LPRINT TAB(20) ;
1295 LPRINT USING "##.##" ;R(I);
1300 LPRINT TAB(45);
1305 LPRINT USING "##.##" ;RR(I)
1310 NEXT I
1320 LPRINT " " : LPRINT " "
1330 LPRINT TAB(18) " MIN = ";F(IB)
1340 LPRINT TAB(18) "   R = ";X(IB,1)
1350 LPRINT TAB(18) "   K = ";X(IB,2)
1360 END
1370 REM * CALCULATE PREDICTED RECOVERIES *
1380 PH = X(I,1) : K = X(I,2) : ER =0
1390 IF K < 0 GOTO 1410
1400 GOTO 1420
1410 F(I) = 1E+08 : GOTO 1480
1420 FOR J = 1 TO N
1430 RR(J) = PH * (1- (1/(K*T(J)))*(1-EXP(-K*T(J))))
1440 E1(J) = (RR(J) - R(J))^2
1450 ER = ER + E1(J)
1460 NEXT J
1470 F(I) = ER
1480 RETURN
```

APPENDIX E : CALCULATION OF CONCENTRATIONS OF IONS

1. CALCIUM

K_1 = 32,359
K_{s0} = 5,4954E-4
K_{s1} = 1,7783E-3 (Butler)

For unsaturated solutions

a. $[CaOH^+] < K_{s1} / [OH^-]$
$< 10^{-3,75} / [OH^-]$

If the concentration of $CaOH^+$ is higher than this calculated value $Ca(OH)_2$ precipitates out.

b. Mass Balance
$[Ca^{++}] + [CaOH^+] = C_T$
where C_T is the total calcium concentration

Equilibria Equation
$K_1 = [CaOH^+] / ([Ca^{++}][OH^-])$

$[CaOH^+] = K_1 [Ca^{++}][OH^-]$
$= K_1 (C_T - [CaOH^+]) [OH^-]$

therefore

$$[CaOH^+] = \frac{K_1 K_W C_T}{[H^+] + K_1 K_W}$$

$[Ca^{++}] = C_T - [CaOH^+]$

From the above equations at pH = 9
$[CaOH^+] = 3,235E-4 * C_T$
$[Ca^{++}] = 0,9997 * C_T$

2. MAGNESIUM

$\log K_{s0} = -10,74$

$\log K_{s1} = -8,16$

$\log K_1 = 2,58$ (Butler)

a. Unsaturated solution

Mass Balance

$[Mg^{++}] + [MgOH^+] = C_T$

where C_T is the total magnesium concentration

Equilibria equation

$K_1 = [MgOH^+] / [Mg^{++}][OH^-]$

therefore $[MgOH^+] > \dfrac{K_1 K_w C_T}{[H^+] + K_1 K_w}$

for saturation $[MgOH^+] > K_{s1} / [OH^-]$

at a pH = 9 $[MgOH^+] > 6,918E-4$ mol/l

Therefore at pH = 9

$[MgOH^+] = 3,787E-3 * C_T$

$[Mg^{++}] = 0,9962 * C_T$

b. Saturated solution

Mass balance

$[Mg^{++}] + [MgOH^+] + [Mg(OH)_2(s)] = C_T$

Equilibria equation

$[Mg^{++}] = K_{s0} / [OH^-]^2 = K_{s0} [H^+]^2 / K_w^2$

$[MgOH^+] = K_{s1} / [OH^-] = K_{s1} [H^+] / K_w$

therefore $K_{s0}[H^+]^2/K_w^2 + K_{s0}[H^+]/K_w + [Mg(OH)_2(s)] = C_T$

$[Mg(OH)_2(s)] = C_T - K_{s0}[H^+]^2/K_w^2 - K_{s0}[H^+]/K_w$

$= C_T - 1,8197*10^{17} [H^+]^2 - 6,9183*10^5 [H^+]$

$$[MgOH^+] = K_{s1}[H^+]/K_w$$
$$\simeq 6,9183*10^5\ [H^+]$$

$$[Mg^{++}] = C_T - [Mg(OH)_2(s)] - [MgOH^+]$$

3. SODIUM SULPHATE AND CALCIUM HYDROXIDE

For the calcium system

$K_1 = 32,359$

$$[Ca^{++}][SO_4^{2-}] = K_{SP} = 2,45E-5$$

Mass balances

$$C_{Ca} = [Ca^{++}] + P + [CaOH^+]$$
$$C_{SO4} = [SO_4^{2-}] + P$$

where C_{Ca} is the total calcium concentration
C_{SO4} is the total sulphate concentration
P is the calcium sulphate precipitate

therefore

$$C_{Ca} - C_{SO4} = [Ca^{++}] - [SO_4^{2-}] - [Ca^{++}]K_1K_w/[H^+]$$
$$= [Ca^{++}](1 + K_1K_w/[H^+]) - 2,45E-5/[Ca^{++}]$$

therefore $[Ca^{++}]$ can be obtained by solving

$$[Ca^{++}]^2(1+K_1K_w/[H^+]) - [Ca^{++}](C_{Ca} - C_{SO4}) - 2,45E-5 = 0$$

$$[SO_4^{2-}] = 2,45E-5 / [Ca^{++}]$$
$$[CaSO_4(s)] = C_{SO4} - [SO_4^{2-}]$$
$$[CaOH^+] = C_{Ca} - [Ca^{++}] - [CaSO_4(s)]$$

4. SODIUM HYDROGEN CARBONATE AND CALCIUM HYDROXIDE

For the carbonate system

$K_1 = 10^{-6,37}$

$K_2 = 10^{-10,25}$

$$[Ca^{++}][CO_3^{2-}] = 0,87E-8 = K_{SP}$$

$$C_T = [CO_3^{2-}] + [HCO_3^-] + [H_2CO_3^*] + P$$

$$C_{Ca} = [Ca^{++}] + [CaOH^+] + P$$

where C_T is the total carbonate concentration

C_{Ca} is the total calcium concentration

P is the calcium carbonate precipitate

$$C_T - C_{Ca} = [CO_3^{2-}] + [HCO_3^-] + [H_2CO_3^*] - [Ca^{++}](1+K_1K_W/[H^+])$$

Using equations from section 1.3.3 and the solubility product equation

$$[HCO_3^-]^2 (K_2/[H^+] + 1 + [H^+]/K_1) (K_2/[H^+]) - [HCO_3^-] (K_2/[H^+]) (C_T-C_{Ca}) - K_{SP} (1+ K_1K_W/[H^+]) = 0$$

Values of other ions can be determined using the $[HCO_3^-]$ value found from this equation.

APPENDIX F : RECOVERY DATA FOR FLOTATION TESTS

Table F1 : Recovery Data for Leached Ore and Sodium Nitrate

TIME	RECOVERY				
	0 meq/l	25 meq/l	50 meq/l	75 meq/l	100 meq/l
5	28,00	27,88	27,05	28,72	29,25
10	39,61	41,40	41,21	42,50	43,46
20	52,74	57,53	58,34	59,17	60,10
30	59,53	65,91	67,31	68,25	69,20
60	70,88	78,50	79,54	80,92	81,96
120	75,73	82,66	85,41	85,68	88,81
300	78,21	86,16	92,15	89,35	93,12
600	79,91	87,61	94,79	90,33	95,92

Table F2 : Recovery Data for Leached Ore and Calcium Nitrate

TIME	RECOVERY				
	0 meq/l	25 meq/l	50 meq/l	75 meq/l	100 meq/l
5	33,73	15,46	8,80	9,36	1,61
10	47,39	31,36	15,37	15,97	4,65
20	59,32	48,60	26,05	26,43	11,71
30	66,27	59,66	35,80	33,90	18,05
60	77,45	77,54	57,21	55,88	38,91
120	81,54	89,41	78,03	81,08	76,63
300	83,35	96,92	90,40	90,79	90,93
600	85,28	100,16	94,76	93,13	93,74

Table F3 : Recovery Data for Leached Ore and Magnesium Nitrate

TIME	RECOVERY				
	0 meq/l	25 meq/l	50 meq/l	75 meq/l	100 meq/l
5	19,34	6,52	3,43		
10	33,82	13,99	10,65	2,12	
20	48,37	26,22	19,20	7,02	2,67
30	55,94	37,13	27,09	11,90	4,80
60	67,00	58,37	49,72	29,78	18,61
120	71,42	74,21	73,98	66,68	58,35
300	72,34	85,28	87,92	91,63	88,46
600	73,24	89,53	92,30	97,24	92,32

Table F4 : Recovery Data for Leached Ore and Sodium Chloride

TIME	RECOVERY				
	0 meq/l	25 meq/l	50 meq/l	75 meq/l	100 meq/l
5	33,73	32,35	31,30	31,07	27,84
10	47,39	45,03	45,77	46,33	44,18
20	59,32	53,65	61,40	62,99	59,70
30	66,27	63,40	64,48	71,68	68,86
60	77,45	66,25	75,93	83,51	82,43
120	81,54	75,83	79,54	88,41	90,05
300	83,35	79,56	81,69	91,77	94,30
600	85,28	81,08	83,02	92,83	95,80

Table F5 : Recovery Data for Leached Ore and Sodium Sulphate

TIME	RECOVERY				
	0 meq/l	25 meq/l	50 meq/l	75 meq/l	100 meq/l
5	33,73	27,14	27,73	26,74	26,82
10	47,39	41,85	40,86	42,24	41,57
20	59,32	55,22	56,60	56,77	59,05
30	66,27	63,53	65,06	65,27	68,24
60	77,45	73,37	76,74	77,01	80,62
120	81,54	76,62	81,44	83,08	87,74
300	83,35	78,09	85,07	86,99	92,03
600	85,28	79,22	85,87	88,45	93,22

Table F6 : Recovery Data for Leached Ore and Sodium Hydrogen Carbonate

TIME	RECOVERY				
	0 meq/l	25 meq/l	50 meq/l	75 meq/l	100 meq/l
5	33,73	31,25	27,92	28,37	27,43
10	47,39	46,66	41,75	44,26	41,90
20	59,32	59,48	55,53	59,08	58,03
30	66,27	66,37	63,42	66,79	67,30
60	77,45	76,67	74,08	77,25	79,23
120	81,54	80,20	78,54	82,72	85,13
300	83,35	82,94	84,90	87,23	88,89
600	85,28	84,51	86,09	88,81	90,45

APPENDIX G : GRADE DATA FOR FLOTATION TESTS

Table G1 : Grade Data for Leached Ore and Sodium Nitrate

TIME	GRADE				
	0 meq/l	25 meq/l	50 meq/l	75 meq/l	100 meq/l
5	37,43	32,64	33,77	29,20	34,96
10	30,52	26,18	27,29	23,87	30,26
20	24,49	20,45	21,84	19,41	25,51
30	21,95	18,50	20,18	17,94	24,33
60	20,74	18,31	20,32	18,18	24,90
120	21,28	18,82	21,04	18,77	25,59
300	21,60	19,24	21,78	19,18	25,98
600	21,75	19,38	22,00	19,21	26,15

Table G2 : Grade Data for Leached Ore and Calcium Nitrate

TIME	GRADE				
	0 meq/l	25 meq/l	50 meq/l	75 meq/l	100 meq/l
5	33,06	48,15	45,94	50,14	48,74
10	26,84	47,50	45,72	49,46	47,41
20	22,35	45,39	45,33	48,46	45,88
30	20,22	44,52	45,59	48,42	45,72
60	19,13	43,07	45,68	47,38	45,32
120	19,56	42,06	44,57	46,26	45,21
300	19,77	41,55	43,50	45,06	43,40
600	19,94	41,34	42,83	44,61	42,77

Table G3 : Grade Data for Leached Ore and Magnesium Nitrate

TIME	GRADE				
	0 meq/l	25 meq/l	50 meq/l	75 meq/l	100 meq/l
5	23,85	50,67	49,38		
10	22,14	49,15	48,48	48,63	
20	18,46	46,99	47,28	47,74	45,76
30	16,62	46,71	47,33	48,06	47,13
60	15,63	45,58	46,93	47,46	48,32
120	16,06	44,57	45,54	47,61	48,54
300	16,17	43,48	43,86	46,03	46,73
600	16,26	42,93	43,03	45,40	46,06

Table G4 : Grade Data for Leached Ore and Sodium Chloride

TIME	GRADE				
	0 meq/l	25 meq/l	50 meq/l	75 meq/l	100 meq/l
5	33,06	22,28	25,48	30,79	37,22
10	26,84	18,92	21,69	25,82	31,94
20	22,35	16,99	18,26	22,14	27,85
30	20,22	15,21	17,85	21,47	27,29
60	19,13	14,98	18,34	22,37	28,12
120	19,56	15,45	18,81	22,92	28,73
300	19,77	15,91	19,05	23,25	29,04
600	19,94	16,08	19,17	23,33	29,09

Table G5 : Grade Data for Leached Ore and Sodium Sulphate

TIME	GRADE				
	0 meq/l	25 meq/l	50 meq/l	75 meq/l	100 meq/l
5	33,06	26,95	31,85	36,83	37,76
10	26,84	21,29	26,40	30,70	32,85
20	22,35	16,78	22,04	26,99	28,96
30	20,22	15,20	20,86	25,99	28,21
60	19,13	15,52	21,42	26,61	28,73
120	19,56	15,95	21,99	27,11	29,15
300	19,77	16,12	22,39	27,35	29,34
600	19,94	16,25	22,45	27,38	29,25

Table G6 : Graph Data for Leached Ore and Sodium Hydrogen Carbonate

TIME	GRADE				
	0 meq/l	25 meq/l	50 meq/l	75 meq/l	100 meq/l
5	33,06	41,45	36,90	37,43	39,49
10	26,84	34,29	30,90	31,29	33,85
20	22,35	26,70	24,70	26,09	27,92
30	20,22	23,46	22,77	24,86	26,47
60	19,13	22,53	23,11	25,39	26,77
120	19,56	22,98	23,72	25,96	27,13
300	19,77	23,33	24,47	26,36	27,28
600	19,94	23,48	24,49	26,34	27,26

APPENDIX H : FROTH STABILITY TESTS

Table H1 : Froth Stability Tests using De-ionised Water and Sodium Ions

CONCENTRATION ppm	CONCENTRATION mol/l	HEIGHT cm	BREAKDOWN RATE cm/sec
0	0	2,5	0,66
10	4E-4	3,0	0,50
100	4E-3	2,8	0,64
200	0,009	2,7	0,66
500	0,022	3,1	0,54
1000	0,044	3,5	0,42
1500	0,065	4,0	0,44
2000	0,087	3,9	0,37

Table H2 : Froth Stability Tests using Tap Water and Sodium Ions

CONCENTRATION ppm	CONCENTRATION mol/l	HEIGHT cm	BREAKDOWN RATE cm/sec
13	5E-4	1,9	0,31
24	0,001	2,5	0,31
119	0,005	2,5	0,26
214	0,009	2,3	0,29
499	0,022	3,0	0,28
970	0,042	3,7	0,35
1442	0,063	3,6	0,36
1970	0,086	3,6	0,41

Table H3 : Froth Stability Tests using De-ionised Water and Calcium Ions

CONCENTRATION				pH	HEIGHT cm	BREAK-DOWN RATE cm/sec
Total calcium ppm	mol/l	[$CaOH^+$] mol/l	[Ca^{++}] mol/l			
0	0	0	0	6,0	2,5	0,66
10	3E-4	1E-6	3E-4	10,2	2,0	0,25
108	0,003	7E-6	0,003	9,9	1,9	0,47
257	0,006	3E-5	0,006	10,2	1,4	0,28
498	0,013	6E-5	0,012	10,1	1,5	0,17
757	0,019	6E-5	0,019	10,0	1,5	0,25
1000	0,025	6E-5	0,025	9,9	1,4	0,27

Table H4 : Froth Stability Tests using Tap Water and Calcium Ions

CONCENTRATION				pH	HEIGHT cm	BREAK-DOWN RATE cm/sec
Total ppm	Calcium mol/l	[$CaOH^+$] mol/l	[Ca^{++}] mol/l			
16	4E-4	3E-8	4E-4	8,4	1,9	0,31
26	7E-4	1E-6	7E-4	9,8	2,5	0,34
126	0,003	8E-6	0,003	9,9	3,0	0,42
226	0,006	2E-5	0,006	9,9	1,7	0,49
526	0,013	4E-5	0,013	9,9	3,1	0,34
1026	0,026	9E-5	0,026	10,0	3,4	0,37
1526	0,038	1,4E-4	0,038	10,1	2,6	0,41
2126	0,053	1,5E-4	0,053	10,0	2,7	0,33

Table H5 : Froth Stability Tests using De-ionised Water and Magnesium Ions

CONCENTRATION					pH	HEIGHT cm	BREAK-DOWN RATE cm/sec
Total ppm	mol/l	[$MgOH^+$] mol/l	[Mg^{++}] mol/l	[$Mg(OH)_2$] mol/l			
0	0	0	0	0	6,7	2,5	0,66
25	0,001	2E-5	0,001	0	9,8	1,6	0,42
42	0,002	3E-5	4E-4	0,001	10,4	2,4	0,54
76	0,003	9E-5	0,003	0	9,9	2,9	0,51
171	0,007	9E-5	0,003	0,004	9,9	4,1	0,51
277	0,011	1,2E-4	0,006	0,006	9,8	3,6	0,35
530	0,022	1,1E-4	0,005	0,017	9,8	4,4	0,38
846	0,035	1,2E-4	0,006	0,030	9,8	5,0	0,34

Table H6 : Froth Stability Tests using Tap Water and Magnesium Ions

CONCENTRATION					pH	HEIGHT cm	BREAK-DOWN RATE cm/sec
Total ppm	mol/l	[$MgOH^+$] mol/l	[Mg^{++}] mol/l	[$Mg(OH)_2$ mol/l			
4	2E-4	1E-7	2E-4	0	8,4	1,9	0,31
185	0,008	1,3E-4	0,007	3,3E-4	9,7	3,6	0,24
471	0,020	2,0E-4	0,015	0,004	9,6	4,4	0,20
792	0,033	1,5E-4	0,008	0,025	9,7	4,7	0,31
1012	0,042	1,7E-4	0,011	0,031	9,6	5,0	0,27
1635	0,068	1,9E-4	0,013	0,055	9,6	5,5	0,33
2154	0,090	2,2E-4	0,018	0,071	9,5	5,8	0,34
2931	0,122	2,2E-4	0,019	0,103	9,5	6,0	0,36

Table H7 : Froth Stability Tests using De-ionised Water, Quartz and Sodium Ions

CONCENTRATION		HEIGHT cm
ppm	mol/l	
0	0	0,4
10	4E-4	0,5
100	0,004	0,5
200	0,009	0,3
500	0,022	0,3
778	0,034	0,4
1168	0,051	0,2
1552	0,068	0,4

Table H8 : Froth Stability Tests using Tap Water, Quartz and Sodium Ions

CONCENTRATION		HEIGHT cm
ppm	mol/l	
13	5E-4	0,3
39	0,002	0,4
128	0,006	0,5
204	0,009	0,6
482	0,021	0,7
924	0,040	0,7
1364	0,059	0,7
1886	0,082	0,7

Table H9 : Froth Stability Tests using De-ionised Water, Quartz and Calcium Ions

CONCENTRATION				pH	HEIGHT cm
Total calcium ppm	mol/l	[$CaOH^+$] mol/l	[Ca^{++}] mol/l		
0	0	0	0	6,7	0,4
88	0,002	7E-6	0,002	10,0	0,5
220	0,006	1E-5	0,006	9,8	0,5
305	0,008	1E-5	0,008	9,7	0,6
688	0,017	3E-5	0,017	9,8	0,6
1345	0,034	6E-5	0,034	9,8	0,5
1770	0,044	1E-4	0,044	9,9	0,5
2605	0,065	8E-5	0,065	9,6	0,5

Table H10 : Froth Stability Tests using Tap Water, Quartz and Calcium

CONCENTRATION				pH	HEIGHT cm
Total calcium ppm	mmol/l	[$CaOH^+$] mol/l	[Ca^{++}] mol/l		
16	4E-4	3E-8	4E-4	8,4	0,3
51	0,001	4E-6	0,001	10,0	0,6
151	0,004	9E-6	0,004	9,9	0,6
251	0,006	1E-5	0,006	9,8	0,5
578	0,015	3E-5	0,014	9,8	0,5
1091	0,027	6E-5	0,027	9,9	0,6
1823	0,046	2E-4	0,045	10,1	0,7
2347	0,059	1E-4	0,059	9,7	0,5

Table H11 : Froth Stability Tests using De-ionised Water, Quartz and Magnesium Ions

CONCENTRATION					pH	HEIGHT cm
Total ppm	Total mol/l	[$MgOH^+$] mol/l	[Mg^{++}] mol/l	[$Mg(OH)_2$] mol/l		
0	0	0	0	0	6,7	0,4
371	0,016	5E-5	0,001	0,014	10,1	0,7
656	0,027	1,0E-4	0,004	0,023	9,8	0,7
956	0,040	1,3E-4	0,006	0,033	9,7	0,7
1525	0,064	1,7E-4	0,012	0,058	9,6	0,6
2142	0,089	2,2E-4	0,019	0,070	9,5	0,6
3121	0,130	2,6E-4	0,026	0,104	9,4	0,5
3744	0,156	3,1E-4	0,036	0,119	9,4	0,6

Table H12 : Froth Stability Tests using Tap Water, Quartz and Magnesium Ions

CONCENTRATION					pH	HEIGHT cm
Total ppm	Total mol/l	[$MgOH^+$] mol/l	[Mg^{++}] mol/l	[$Mg(OH)_2$] mol/l		
4	2E-4	1E-7	2E-4	0	8,4	0,3
541	0,022	7E-5	0,002	0,021	10,0	0,8
574	0,024	1,2E-4	0,006	0,018	9,7	0,7
796	0,033	1,4E-4	0,008	0,025	9,7	0,8
1429	0,060	1,8E-4	0,013	0,047	9,6	0,8
2206	0,092	2,2E-4	0,019	0,073	9,5	0,7
2629	0,110	2,7E-4	0,028	0,082	9,4	0,6
3484	0,145	3,0E-4	0,033	0,112	9,4	0,7

Table H13 : Froth Stability Tests using De-ionised water, Quartz and Pyrite

CONCENTRATION				pH	HEIGHT cm	BREAKDOWN RATE cm/sec
$Ca(NO_3)\cdot 4H_2O$ meq/l	mmol/l	$[Ca^{++}]$ mmol/l	$[CaOH^{+}]$ mmol/l			
0	0	0	0	8,9	1,5	0,63
25	50	49,98	0,02	8,9	5,1	0,78
50	100	99,97	0,03	8,9	5,0	0,76
75	150	149,95	0,05	9,1	4,8	0,64
100	200	199,94	0,06	8,9	5,4	0,72
$NaNO_3$						
0 meq/l				8,9	1,5	0,63
25				9,0	3,9	0,65
50				9,0	4,5	0,57
75				9,0	4,5	0,89
100				8,8	6,0	0,80
NaCl						
0 meq/l				8,9	1,5	0,63
25				9,0	2,3	0,58
50				9,0	2,1	0,55
75				9,0	3,8	0,79
100				9,0	5,1	0,82
Standard Deviation					± 0,1	0,03